LALS 2023
Muğla, Turkey
October 15th-17th 2023

Book of Abstracts

17TH INTERNATIONAL CONFERENCE ON LASER APPLICATIONS IN LIFE SCIENCES

https://lals.sciencesconf.org

15-17 October 2023
Muğla, Turkey

Dear Participants,

On behalf of the Organizing Committee, we invite you to attend the "17th International Conference on Laser Applications in Life Science" (LALS-2023).

The conference is held from October 15-17, 2023, at the Convention Centre of the Liberty Hotels Lykia/Oludeniz in Muğla, Turkey.

The aim of LALS-2023 is to provide a global platform for researchers, engineers, and physicians to present and discuss recent optical techniques and innovations aimed at applications in life science. We hope to bring together professionals and scientists from various areas of life sciences to introduce novel biophotonics methods to healthcare professionals, encourage knowledge exchange, and promote the establishment of cooperation ventures. The scientific program will include plenary and invited talks.

We welcome you to the conference and wish a fruitful participation and enjoyment at the beautiful place.

Best regards,
Conference chair,
Prof., Dr. Kirill Larin (University of Houston, USA)

LALS 2023

LALS 2023 Muğla, Turkey October 15th-17th 2023

17th International conference on Laser Applications in Life Sciences
15-17 October 2023, Muğla (Turkey)

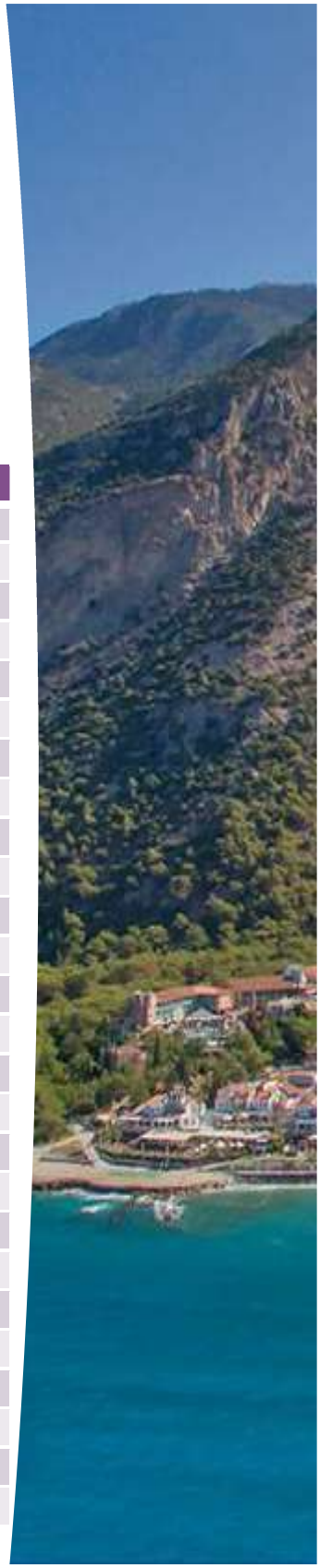

Conference Chair

Kirill Larin (University of Houston, USA)

International Advisory Board

Name	Affiliation	Country
R. Ansari	NASA Glenn Research Center, Cleveland	USA
W. Blondel	University of Lorraine / CRAN, Nancy	France
A. Bykov	University of Oulu	Finland
A. Chikishev	M.V. Lomonosov Moscow State University	Russia
O. Conde	Universidad de Cantabria	Spain
M. Darwin	Charité Universitätsmedizin, Berlin	Germany
H. Ma	Tsinghua University	China
H. Kano	University of Tsukuba	Japan
M. Kirillin	Institute of Applied Physics RAS, N. Novgorod	Russia
K. Koenig	Saarland University	Germany
K. Larin (chair)	University of Houston	USA
I. Larina	Baylor College of Medicine, Houston	USA
A. Lugovtsov	M.V. Lomonosov Moscow State University	Russia
I. Meglinski	Aston University	UK
T. Novikova	Ecole polytechnique / LPICM, Palaiseau	France
L. Oliveira	Polytechnico de Almeida, Porto	Portugal
C. Otto	University of Twente	Netherlands
A. Popov	VTT Technical Research Centre of Finland	Finland
J. Popp	Institute of Physical Chemistry	Germany
A. Priezzhev	M.V. Lomonosov Moscow State University	Russia
A. Rueck	Ulm University	Germany
H .Schneckenburger	Aalen University	Germany
E. Shirshin	M.V. Lomonosov Moscow State University	Russia
V. Tuchin	Saratov State University	Russia
Z. Zalevsky	Bar-Ilan University / Faculty of Engineering	Israel
D. Zhu	Huazhong Univ. of Science and Technology	China

Contents

Ultrafast optoacoustic imaging in biology and the clinics

Daniel RAZANSKY[1,2]

[1] *Institute for Biomedical Engineering and Institute of Pharmacology and Toxicology, Faculty of Medicine, University of Zurich, Switzerland*
[2] *Institute for Biomedical Engineering, Department of Information Technology and Electrical Engineering, ETH Zurich, Switzerland*

daniel.razansky@uzh.ch

ABSTRACT

Optoacoustic imaging is increasingly attracting the attention of the biomedical research community due to its excellent spatial and temporal resolution, centimeter scale penetration into living tissues, versatile endogenous and exogenous optical absorption contrast. State-of-the-art implementations of multi-spectral optoacoustic tomography (MSOT) are based on multi-wavelength excitation of tissues to visualize specific molecules within opaque tissues. As a result, the technology can noninvasively deliver structural, functional, metabolic, and molecular information from living tissues. The talk covers most recent advances pertaining ultrafast imaging instrumentation, multi-modal combinations with other ultrasound and optical imaging methods, intelligent reconstruction algorithms as well as smart optoacoustic contrast and sensing approaches. Our current efforts are also geared toward exploring potential of the technique in studying multi-scale dynamics of the brain and heart, monitoring of therapies, fast tracking of cells and targeted molecular imaging applications. MSOT further allows for a handheld operation thus offers new level of precision for clinical diagnostics of patients in a number of indications, such as breast and skin lesions, inflammatory diseases and cardiovascular diagnostics.

Stimulated Terahertz emission in molecular crystals and its application for the biomedical sensing

Valery KOVALEV[1], Anton SINKO[2] and Alexander SHKURINOV[3,4]
[1]*Lebedev Physical Institute, Russian Academy of Sciences, Russia*
[2]*ILIT RAS-Branch of the FSRC "Crystallography and Photonics RAS", Russia*
[3]*Faculty of Physics, Lomonosov Moscow State University, Russia*
[4]*Tomsk State University, Russia*
ashkurinov@physics.msu.ru

ABSTRACT

The generation of stimulated coherent electromagnetic radiation close to terahertz begins with the pioneering work of Nobel laureates N.Basov and A.Prokhorov [1]. The observed last years the growth of number of methods and devises for generation terahertz (THz) radiation and improvement of their performance are essential for the progress of THz science and technology [1]. In the recent years THz radiation below 3 THz realized with a reasonably high efficiency in the range of widegap solid crystals, including molecular based materials [3] under the irradiation of femtosecond near-IR laser pulses. Typical for such sources is a single-cycle THz splash at the very beginning of generated pulse, and the prolonged oscillation radiation, the frequency of which corresponds to the frequency of a Raman and IR active modes in the samples. While the splash accounted for in terms of the optical rectification of pump radiation, the prolonged oscillation attributed to the dipole emission by coherent phonons generated in an optically transparent solid medium when a sufficiently short laser pulse passes through the phenomenon was called the impulsive stimulated Raman scattering (ISRS)). Their THz radiation is possible because the correspondent phonon modes are both Raman and IR active.

THE DISCUSSION OF THE SUBJECT OF THE LECTURE

The present lecture studies narrow-band terahertz (THz) emission stimulated by femtosecond laser pulse in molecular crystal guanylurea hydrogen phosphite (GUHP). We demonstrate that this emission is closely connected with the excitement of high-quality phonon oscillations in the crystal, which is proved by the temperature dynamics of the spectra and DFT calculations. For the purposes of studying the origin of this stimulated THz emission and creation of the adequate model of the phenomenon, we analyzed the polarization sensitive spectra of spontaneous Raman scattering and THz transmission spectra while considering their polarization features in relation to crystallographic axes of GUHP crystal. In this paper we show that molecular crystals provide an effective means to convert vis-NIR laser light regardless of wavelength into the THz frequency range. This approach can lead to the creation of "laser-like" source with the desired THz frequency for a range of medical, scientific, and technological applications.

An important part of the present lecture is discussion of the possible application of the sources described above for the purposes of molecular sensory. Problems of detecting of molecules of biological importance, including pathogenic substances is well known. To increase the reliability and selectivity of the molecular detection, we use sensors based on metamaterials. A distinctive feature of the devices we are discussing in the lecture is that we are considering the possibility of frequency tuning of their selectivity through the use of phase-changing materials [4]. The phenomenon of phase change transition has been a fascinating research subject over decades due to a possibility of dynamically controlled materials properties, allowing the creation of optical devices with unique features. The present lecture unravels the optical characteristics and terahertz (THz) dielectric permittivity of a novel phase change material (PCM), $GeTe_2$, prepared by pulsed laser deposition (PLD) and their remarkable contrast in crystalline and amorphous states, in particular, a difference of 7 orders of magnitude in conductivity. The THz spectra were analyzed using the harmonic oscillator and Drude term. Using $GeTe_2$ PLD films, we designed and prepared a THz metasurface in the form of periodic structure and revealed a possibility of tuning the THz resonance either by a thermal control or light-induced crystallization response, thus achieving the dynamic and tunable functionality of the metastructure.

REFERENCES

[1] N. G. Basov and A.M. Prokhorov, Soviet Physics JETP, 3, 426-429,1956.
[2] X. Zhang, A. Shkurinov, Y. Zhang, Nature Photon **11**, 16–18, 2017.
[3] A. Sinko et all. Electronics, 11(17), 2731, 2022.
[4] M.R.Konnikova et all, ACS Appl. Mater. Interfaces, 15, 9638−9648, 2023.

Functional optical coherence tomography for investigation of cilia function in vivo

Irina Larina
Department of Integrative Physiology, Baylor College of Medicine, Houston, USA

larina@bcm.edu

ABSTRACT

Motile cilia are highly dynamic, hair-like structures that cover the epithelial surfaces in diverse organs. When the coordinated beating of cilia is disrupted, it leads to the emergence of motile ciliopathies, which are associated with severe clinical complications, including reproductive disorders. The coordinated ciliary beating generates metachronal waves, which propagate along the epithelial surface, facilitating the transport of fluids and mucus. Despite the well-recognized clinical significance of cilia, comprehensive investigations into their dynamics have been limited, impeding a thorough understanding of their functional intricacies and potential dysfunctions. Addressing this critical knowledge gap, we developed a quantitative imaging technique, leveraging dynamic optical coherence tomography (OCT) to volumetrically visualize cilia metachronal waves through tissue layers. Our methodology is based on precise spatiotemporal mapping of the frequency and the phase of intensity fluctuations in OCT images, arising from the rhythmic ciliary beating. This approach was validated across temperatures implemented in vivo resulting in captivating visualizations of cilia metachronal wave propagation within the mouse fallopian tube through the wall. This method can be extended to the assessments of physiological cilia function and ciliary dyskinesias across diverse organ systems.

Control of up-conversion nanoparticle luminescence intensity by optical clearing or heating

Irina YANINA[1,2], Anna DORONKINA[1], Daria TUCHINA[1,2,3] and Vyacheslav KOCHUBEY[1,2]

[1]*Institute of Physics, Saratov State University, Russia*
[2] *Laboratory of laser molecular imaging and machine learning, Tomsk State University, Russia*
[3] *Research Center of Biotechnology of the Russian Academy of Sciences, A.N. Bach Institute of Biochemistry, Russia*

irina-yanina@list.ru

ABSTRACT

The present work demonstrates the changes in luminescence intensity of upconversion nanoparticles (UCNPs) at different conditions. The luminescence spectra of the UCNPs were measured through 0.76±0.18 mm of skin (healthy and pathological tissue) at room and physiological temperatures. Heating and application of optical clearing agents significantly improved the intensity of UCNP fluorescence. UCNPs are promising alternatives to traditional fluorescent labels for cell imaging and have outstanding potential in biological and clinical applications.

Cancer is one of many diseases characterised by the development of abnormal cells that divide uncontrollably and have the ability to invade and destroy normal body tissue. It is therefore important to develop methods for diagnosing cancer at an early stage and then visualising the tumour.

The work was carried out on skin samples from control and experimental groups of laboratory animals. The experimental study was conducted at the Centre of Collective Use of the Saratov State Medical University (Russia). For the control group of 12 male and for the experimental group of 12 male white laboratory rats of the Wistar strain, weighing 300 ± 50 g, 0.5 ml of 25% tumour suspension in Hanks' solution of the RS-1 strain of alveolar liver cancer was implanted subcutaneously in the area of the scapula. In the experimental group of rats, the experiment was started when the tumours reached a volume of 1 cm^3.

The skin sample was placed in a cuvette filled with an agent. The cuvette was placed in a box that was kept at a fixed temperature. Spectral measurements were also made to avoid noise from lighting. The two groups of animals were divided into four subgroups of 3 animals each. The first and second groups: a glycerol solution was applied to skin samples at room temperature and physiological temperature, respectively. The third and fourth group: a propylene glycol solution was applied to skin samples at room temperature and physiological temperature, respectively.

We used the home-made synthesised UCNPs $NaYF_4$: Yb^{3+}, Er^{3+} (fluoride matrix doped with ytterbium and erbium ions) coated with SiO_2. The UCNPs (approximately 220 nm in size) were synthesised by hydrothermal method [1].

Skin samples were taken from two areas: healthy skin (normal) and skin overlying the tumour (pathology). Skin samples measuring 1x1 cm were placed in a Petri dish with the epidermis facing down. To prevent the sample from floating up, a metal disc with a hole diameter of 8 mm was placed on the surface. The luminescence was recorded through this hole. The luminescence was collected by a collimator with a diameter of 5 mm placed at an angle of 150 to the vertical at a distance of 20 cm from the sample. This allowed registration in the mode of collimated transmission of luminescence through the sample. The UCNPs were placed under a Petri dish. The collimated radiation that excited the luminescence was directed at the UCNPs from below along the vertical.

The luminescence was recorded at 2 minute intervals from the moment the clearing agent was poured into the Petri dish. The exponential approximation showed that the dynamics of the clearing depended only on the skin type (Table 1). The most likely mechanism of clearing at this stage is the diffusion of water from the skin, stimulated by the osmotic action of the clearing agent. The rate of water diffusion depends primarily on the structure of the skin, which is different in normal and pathological conditions, which explains its independence from the type of clearing agent.

Table 1: *Indicators of the exponent approximating the dynamics of rat skin clearing*

OCA	Norma	Pathology
Glycerol 100%	20±2 min^{-1}	39±8 min^{-1}
Propylene glycol 100%	19±3 min^{-1}	38±4 min^{-1}

The study was supported by a grant Russian Science Foundation No. 21-72-10057, https://rscf.ru/project/21-72-10057/.

REFERENCES

[1] Sagaydachnaya E A, et.al., Journal of Physics: Conf. Series, 917, 032006, 2017.

Raman spectroscopy for optical and liquid biopsy of non-communicable disease

Luydmila Bartchenko[1], Yulia Khrisoforova[1], Irina Matveeva[1], Sahar Al-Sammarrae[1], Elena Typikova[1], Peter Lebedev[2], Maria Skuratova[3] and Ivan Bratchenko[1]

1- Samara National Research University, Samara, Russia

2- Samara state medical university, Samara, Russia

3- Samara regional clinical hospital named after VD Seredavin

iabratchenko@gmail.com

ABSTRACT

In modern world practice, promising diagnostic methods are emerging, such as "optical biopsy" [1] and "liquid biopsy" [2], which are used for specific diseases biomarkers detection in biological tissues and fluids. Optical methods have the potential to overcome the limitations of traditional methods of clinical analysis. One of the most promising methods of optical analysis (and optical biopsy) is a Raman spectroscopy, which can contribute to understanding of molecular basis of diseases and creation of new bioanalytical tools for the diagnosis of diseases. Since each type of biological tissue and biofluid has an individual molecular composition and, thus, a unique spectral profile resulting from the transition of a molecule from one vibrational-rotational state to another, a set of such individual states of functional groups of nucleic acids, proteins, lipids and carbohydrates makes it possible to characterize component composition of tissues, which ultimately makes it possible to isolate disease markers [3]. Along with the use of optical biopsy methods, it is possible to apply a supersensitive technique for analyzing biofluids based on surface-enhanced Raman spectroscopy, which will be most effective for detecting low concentrations of disease markers in biological fluids. In the last decade, the development of nanotechnology has led to the creation of promising tools for solving new problems in the study of various human diseases, which is especially important for effective and targeted treatment and a deeper fundamental understanding of the biochemistry of diseases [2].

In this study we demonstrate application of conventional Raman spectroscopy for the analysis of skin tissues and application of SERS for serum analysis to determine the presence of non-communicable diseases. In this study, the in vitro analysis of human serum was performed for more than 400 subjects, and more than 300 skin samples were analyzed in vivo for the detection of chronic heart failure (CHF), chronic heart failure and other non-communicable diseases. Analyzed groups separation based on deep learning was implemented using a separate one-dimensional convolutional neural network (CNN). Application of Raman spectroscopy to investigate the forearm skin has yielded the accuracy of 0.96, sensitivity of 0.94 and specificity of 0.99 in terms of identifying the target subjects with kidney failure. When classifying subjects by the presence of kidney failure using the PLS-DA method, the most informative Raman spectral bands are 1315 to 1330, 1450 to 1460, 1700 to 1800 cm^{-1}. The performed study demonstrates that for in vivo skin analysis, the conventional Raman spectroscopy can provide the basis for cost-effective and accurate detection of CHF and associated metabolic changes in the skin.

The results of the SERS data for CHF demonstrates that CNN significantly outperforms standard methods of analysis as projection on latent structures and allows for detection of CHF with 95-100% accuracy. By means of multivariate analysis, the informative spectral bands associated with the CHF during disease progression were identified. In addition, the analysis of the correlation between the serum spectral characteristics and urea, creatinine has made it possible to determine the spectral bands correlated with levels of creatinine and urea into the complex spectral characteristics of serum. In general, the reported approach may form the basis for monitoring the health status of CHF patients and find application in studying other pathological conditions of the human body [3]. Raman-based optical and liquid biopsy may be promising in non-communicable diseases identification, as it provides fast and rapid diagnosis.

REFERENCES

[1] I. Bratchenko, et al. Optical biopsy of amelanotic melanoma with Raman and autofluorescence spectra stimulated by 785 nm laser excitation, Journal of Biomedical Photonics & Engineering, 7, 020308, 2021.

[2] L.A. Bratchenko, et al. Analyzing the serum of hemodialysis patients with end-stage chronic kidney disease by means of the combination of SERS and machine learning, Biomedical Optics Express, 13, 4926-4938, 2022.

[3] I.A. Bratchenko, et al. Classification of skin cancer using convolutional neural networks analysis of Raman spectra, Computer Methods and Programs in Biomedicine, 219, 106755, 2022.

Terahertz Spectroscopy in Glioma Diagnostics

Olga CHERKASOVA[1,2], Denis VRAZHNOV[3,4], Anastasia KNYAZKOVA[3,4], Maria KONNIKOVA[2,3,5], Nazar NIKOLAEV[1,6], Yury KISTENEV[3,4] and Alexander SHKURINOV[3,5]

[1]*Institute of Automation and Electrometry, Siberian Branch of the Russian Academy of Sciences, Russia*
[2]*Institute on Laser and Information Technologies, Branch of the Federal Scientific Research Centre "Crystallography and Photonics" of RAS, Russia*
[3]*Laboratory of Laser Molecular Imaging and Machine Learning, Tomsk State University, Russia*
[4]*V.E. Zuev Institute of Atmospheric Optics SB RAS, Russia*
[5]*Faculty of Physics, Lomonosov Moscow State University, Russia*
[6]*Institute of Laser Physics, Siberian Branch of the Russian Academy of Sciences, Russia*

o.p.cherkasova@gmail.com

ABSTRACT

The World Health Organization and the health departments of governments of all countries have listed tackling cancer as a top priority [1]. The main problem is late diagnosis, when the prognosis for a cure is unfavorable. Gliomas are one of the most grievous malignant central nervous system tumors, and have a high mortality rate with a low survival rate, with severe disability and increased risk of recurrence [2]. THz technologies are already being used in intraoperative diagnosis of brain tumors [3-5]. However, they cannot be used for non-invasive and early diagnosis. The molecular composition of body fluids changes significantly with the tumor appearance and development, which can be a good diagnostic criterion for early cancer diagnosis [6].

In this work, we performed a comparative study of the blood plasma of glioma patients and patients with skull craniectomy defects (SCD), as well as healthy donors, using terahertz time-domain spectroscopy (THz-TDS). The blood plasma samples of glioma patients before and after tumor removal surgery were also examined.

The human blood plasma was studied by THz time-domain spectrometer T-Spec 800 Teravil using the special cuvettes pre-printed on a 3D printer [7]. An analysis of experimental THz data was performed by machine learning (ML) methods detailed in [7-9].

It was shown that Random Forest, and Extreme Gradient Boosting provided a better differentiation of the group of patients with glioma from healthy donors and patients with SCD (AUC = 0.81–0.84). The major challenge is the non-invasive control of the effectiveness of the tumor removal surgery [10]. It was shown that THz spectroscopy combined with ML makes it possible to separate with high accuracy the blood plasma of glioma patients before and after tumor removal surgery (AUC = 0.92). The most informative frequencies were 0.56 and 1.2 THz. These THz frequencies coincided with informative frequencies obtained in an experimental mouse model of human glioblastoma [7]. Thus, the applicability of THz spectroscopy for the diagnosis of glioma and treatment monitoring has been shown.

This research was funded by the Ministry of Science and Higher Education of the Russian Federation: project No. 121032400052-6. This work was performed partly within the State Assignment of FSRC "Crystallography and Photonics" RAS. This work has been supported by the Interdisciplinary Scientific and Educational School of Moscow University «Photonic and Quantum Technologies. Digital Medicine» for part of the results analysis. The research was carried out with the support of a grant under the Decree of the Government of the Russian Federation No. 220 of 9 April 2010 (Agreement No. 075-15-2021-615 of 4 June 2021) for part of machine learning.

REFERENCES

[1] J. Ferlay et al, Cancer 2021. https://doi.org/10.1002/ijc.33588
[2] Q.T. Ostrom et al, Neuro-Oncology 24, v1–v95, 2022.
[3] K.I. Zaytsev et al, J. Opt. 22, 013001, 2020.
[4] A.A. Gavdush et al, J. Biomed. Opt. 24, 027001, 2019.
[5] N.V. Chernomyrdin et al, Opto-Electron Adv 6, 220071, 2023.
[6] O. Cherkasova et al, Photonics 8, 22, 2021.
[7] D. Vrazhnov et al, Appl. Sci. 12, 10533, 2022.
[8] D. Vrazhnov et al, Pharmaceutics 15, 203, 2023.
[9] O. Cherkasova et al, Appl. Sci. 13, 5434, 2023.
[10] M. Alieva et al, Clin. Exp. Metastasis 35, 319–331, 2018.

Making your Microscope more versatile for Life Sciences

Herbert SCHNECKENBURGER

Institute of Applied Research, Aalen University, Beethovenstr. 1, 73430 Aalen, Germany

E-Mail: herbert.schneckenburger@hs-aalen.de

ABSTRACT

In recent years many achievements have been made to adapt optical microscopy to the increasing demands in 3D resolution, super-resolution and low levels of phototoxicity. Some systems have been commercialized, e.g. modern confocal or light sheet systems for 3D microscopy or innovative setups for Stimulated Emission Depletion (STED) or Structured Illumination (SIM) microscopy. However, often those complex systems are not available or not appropriate, e.g. if various techniques have to be combined. Then specific microscope modules or add-ons – including our recent developments – are required:

- a light sheet module to add 3D resolution to conventional fluorescence microscopy under non-phototoxic conditions;[1]

- a setup for micro-axial tomography to observe specimens from various sides and to achieve an improved isotropic resolution;[2]

- a device for variable-angle Total Internal Reflection Fluorescence (TIRF) Microscopy to measure cell-substrate topology in the nanometer range to assess various cell metabolisms or the impact of pharmaceutic agents;[3]

- a structured illumination microscope (SIM), which is combined with TIRF Microscopy to achieve a combination of lateral and axial super-resolution;[4]

- adaptation of spectral as well as fluorescence lifetime equipment for Förster Resonance Energy Transfer (FRET) experiments;[5]

- components for laser micromanipulation, e.g. in optical tweezers or optoporation systems.[6]

Some technical solutions are explained and recent applications in live cell imaging are summarized.

REFERENCES

1. T. Bruns, M. Bauer, S. Bruns, H. Meyer, D. Kubin, H. Schneckenburger: “Miniaturized modules for light sheet microscopy with low chromatic aberration,” J. Microsc. 264(3), 261-267, 2016.

2. V. Richter, S. Bruns, T. Bruns, P. Weber, M. Wagner, C. Cremer, H. Schneckenburger: "Axial tomography in live cell laser microscopy," J. Biomed. Opt., 22(9), 091505, 2017.

3. A. Krecsir, V. Richter, M. Wagner, H. Schneckenburger: “Impact of doxorubicin on cell- substrate topology”, Int. J. Mol. Sci. 23, 6277, 2022

4. V. Richter, P. Lanzerstorfer, J. Weghuber, H. Schneckenburger: “Super-resolution live cell microscopy of membrane-proximal fluorophores”, Int. J. Mol. Sci., 21(19), 7099, 2020.

5. H. Schneckenburger: “Förster resonance energy transfer – what can we learn and how can we use it?" Methods Appl. Fluoresc. 8(1), 013001, 2019,.

6. H. Schneckenburger: “Laser-assisted optoporation of cells and tissues – a mini-review,” Biomed. Optics Express 10(6), 2833-2888, 2019.

Light propagation in biological tissue and its applications

Alwin Kienle[1], Andre Liemert[1], Florian Foschum[1]

[1]*Quantitative Imaging and Sensors, Institute of Laser Technologies in Medicine and Metrology at the University of Ulm, 89081 Ulm, Germany*

alwin.kienle@ilm-ulm.de

ABSTRACT

We studied the light propagation in biological tissue using analytical and numerical solutions of the radiative transfer equation (RTE). Analytical solutions of the RTE were derived for a series of geometries, e.g., for layered media. Both, solutions of elastically scattered light as well as luminescent light were found. Efficient numerical solutions of the RTE for, in principle, arbitrary complex geometries and polarized light were implemented using the Monte Carlo method. In order to perform realistic simulations, well characterized optical properties of the investigated tissues have to be determined.

Different devices for determination of the optical properties of scattering media were setup and validated with liquid and solid scattering phantoms applying the numerical and analytical solutions of the radiative transfer equation. The optical properties of a variety of biological tissue were determined ex vivo and in vivo spectrally resolved in the visible and near-infrared wavelength range.

For example, an integrating sphere setup was built using a halogen lamp as source and two spectrometers as detectors enabling the determination of the total reflected and total transmitted light from 400 nm to 1600 nm. The integrating sphere was fabricated using a 3D printer and coated with BaSO4 (Gigahertz-Optik GmbH, Germany). For the retrieval of the spectrally resolved effective scattering and absorption coefficients the Monte Carlo method was used considering the geometrical parameters of the illumination, the sphere including its apertures, the light propagation in the sphere and that in the scattering medium [1].

For in vivo measurements a multi-spectral setup in the spatially frequency domain using nine LEDs between 400 and 1000 nm as light source was built, compare figure 1. In addition, a hyperspectral device applying a halogen lamp as light source was setup, which in combination with a pushbroom imager allowed hyperspectral measurements again between 400 and 1000 nm, but now with a resolution of about 3 nm. The spatial frequency was changeable between 0.08 and 1 mm^{-1}. For evaluation analytical solutions of the RTE were used [2].

The determined optical properties and the implemented solutions of the RTE were used for a variety of applications.

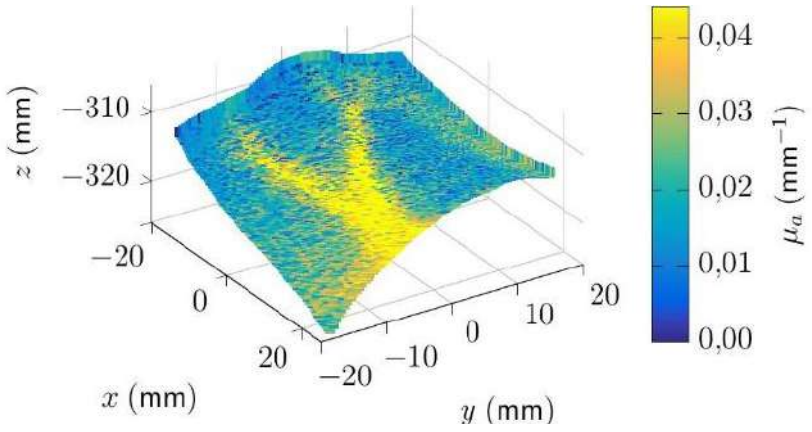

Figure 1: *Three-dimensional topography and absorption coefficient of a human wrist obtained by measurements in the spatial frequency domain and by applying analytical solutions of the RTE.*

REFERENCES

[1] F. Bergmann et al, Photonics 8, 365 (2021).
[2] S. Geiger et al, JOSA 40, 294-304 (2023).

Computer assisted reconstruction of the absorption spectra of human normal and pathological kidney

Luís OLIVEIRA[1,2], Maria PINHEIRO[2], Luís FERNANDES[2], Isa CARNEIRO[3,4], Sónia CARVALHO[5], Rui HENRIQUE[3,6], Valery TUCHIN[7,8] and Hélder OLIVEIRA[2]

[1]*Physics Department, Polytechnic of Porto – School of Engineering, Portugal*
[2]*Centre Telecommunications and Multimedia, Institute for Systems and Computer Engineering, Technology and Science, Portugal*
[3]*Department of Pathology and Cancer Biology and Epigenetics Group, Portuguese Oncology Institute of Porto, Portugal*
[4]*Department of Pathological, Cytological and Thanatological Anatomy, Polytechnic of Porto – School of Health, Portugal*
[5]*Department of Pathology, Santa Luzia Hospital, Portugal*
[6]*Department of Pathology and Molecular Immunology, Porto University – Institute of Biomedical Sciences Abel Salazar, Portugal*
[7]*Institute of Physics and Science Medical Center, Saratov State University, Russian Federation*
[8]*Laboratory of Laser Diagnostics of Technical and Living Systems, Institute of Precision Mechanics and Control of the FRC "Saratov Scientific Centre of the Russian Academy of Sciences", Russian Federation*

lmo@isep.ipp.pt

ABSTRACT

Biological tissues contain various chromophores, each of which presents a characteristic absorption spectrum. For a particular tissue, its absorption spectrum, as obtained from measurements, is a weighted sum of the individual absorption spectra of the chromophores in the tissue [1]. When the absorption spectra of the chromophores are available, such weighted sum can be made to reconstruct the spectral absorption coefficient of the tissue. The weights used in such reconstruction provide information about the concentrations of each chromophore in the tissue [2].

In the present work, and with the objective of acquiring diagnostic information, the experimental absorption spectra of human kidney tissues, both in normal and in chromophobe renal cell carcinoma (CRCC) states [3], were used to perform a reconstruction from the absorption spectra of various biological chromophores. Such reconstruction was made for both kidney tissues through the least-square method, using two approaches. In the first approach, a single weight was determined for each chromophore after optimizing the reconstructed spectra. In the second approach, wavelength-dependent weights were estimated for each chromophore in a way that the reconstructed spectra would match the experimental absorption coefficient spectra of both kidney tissues. The single weights obtained in the first approach show that the CRCC kidney contains less melanin, more blood, more water and more lipofuscin than the healthy kidney, as previously demonstrated by direct calculations [3]. The spectral weights that were estimated for each chromophore with the second approach were used in a further calculation where the spectra obtained for the CRCC kidney were subtracted by the corresponding spectra obtained for the healthy kidney. Such difference spectra did not produce concluding information regarding the contents of the pigments, such as melanin and lipofuscin, but it showed a higher content of water, DNA/RNA and blood in the diseased kidney, as described in literature [3,4].

The results obtained with both approaches seem to be complimentary and further studies with other tissues need to be performed to validate such approach for the retrieval of diagnostic information.

VVT was supported by the Ministry of Science and Higher Education of Russian Federation within the framework of a state assignment (project No. FSRR-2023-0007).

REFERENCES

[1] S. Jacques, Phys. Med. Biol. 58, R37–R61, 2013.
[2] B. Cox et al, J. Biomed. Opt. 17, 061202, 2012.
[3] A. Botelho et al, Spect. Acta Part A: Mol. And Biomol. Spectrosc. 286, 122002, 2023.
[4] S. Peña-Llopis & J. Brugarolas, Nat. Prot. 8, 2240-2255, 2013.

Optical spectroscopy in the assessment of the functional state of the liver

Elena POTAPOVA[1], Ksenia KANDUROVA[1], Vadim PRIZEMIN[1], Dmitrii SUMIN[1,2] and Andrian MAMOSHIN[1,2]

[1]*Research & Development Center of Biomedical Photonics, Orel State University, Russia*
[2]*Department of interventional radiology, Orel Regional Clinical Hospital, Russia*

potapova_ev_ogu@mail.ru

One of the current issues in emergency surgery is the assessment of the functional state of the liver at different stages of treatment of obstructive jaundice syndrome using simple and objective techniques. The primary goal in the treatment of patients with diseases complicated by obstructive jaundice is to decompress the biliary system. Minimally invasive procedures provide access to the liver tissue, allowing a single optical biopsy of the liver parenchyma when drainage systems are installed and subsequent study of bile in dynamics as a direct product of hepatocyte secretion. The methods used in this work included fluorescence spectroscopy, which is highly sensitive to metabolic changes in tissues [1], and Raman spectroscopy, which provides information on the chemical composition of biological tissues and fluids [2].

The aim of this work was to study the effect of the degree of liver failure on the optical properties of the parenchyma in vivo using the fluorescence spectroscopy and on the optical properties of the bile in vitro using the Raman spectroscopy.

The study included 20 patients with obstructive jaundice and 11 patients without obstructive jaundice as a comparison group. The latter group of patients has been previously studied in fine needle biopsy of liver neoplasms [1]. The fluorescence spectra were recorded with a fine needle probe and subjected to deconvolution analysis to assess the contribution of the major tissue fluorophores. In the first group of patients with obstructive jaundice, bile samples were collected through a drainage catheter to study Raman spectra dynamically (every 3-4 days). The typical spectral bands for bilirubin in the Raman spectra (1258-1264 cm^{-1} and 1615-1620 cm^{-1}) were analyzed after post-processing.

The results of fluorescence spectroscopy showed a statistically significant increase in the contribution of curves reflecting the fluorescence of NAD(P)H, bilirubin, flavins, and vitamin A in the group of patients with obstructive jaundice. These parameters may be used for further studies as promising diagnostic and prognostic markers for the development of liver failure. We also demonstrated that the detection of changes in bilirubin concentration in bile secreted through the drainage catheter by Raman spectral bands allows one to predict the dynamics of recovery in patients with obstructive jaundice syndrome after antegrade biliary decompression.

The studies conducted by fluorescence and Raman spectroscopy have shown that optical spectroscopy offers great opportunities for evaluating liver function in patients with obstructive jaundice syndrome. The results can be used by surgeons in clinical practice to adjust treatment algorithms.

The study was supported by the Russian Science Foundation grant № 23-25-00487, https://rscf.ru/project/23-25-00487/.

[1] V. Dremin et al, Sci. Rep. 10, 14200, 2020.
[2] K. Kong et al, Adv. Drug Deliv. Rev. 89, 121–134, 2015.

Optical Sensors Based on Hollow-Core Microstructured Optical Waveguides

Anastasiia MERDALIMOVA[1], Roman BARMIN[1],* Viktor VOROBEV[1], Daria TERENTYEVA[1], Tatiana ESTIFEEVA[1], Sergey GERMAN[1], Vasiliy CHERNYSHEV[2], Oleg MASLOV[3], Yulia SKIBINA[4], Polina RUDAKOVSKAYA[1] and Dmitry GORIN[1]

[1]*Center for Photonic Science and Engineering, Skolkovo Institute of Science and Technology,, Russia*
[2]*National Medical Research Center for Obstetrics, Gynecology and Perinatology named after Academician V.I. Kulakov,, Russia*
[3]*Department of Nanomaterials and Nanotechnology, Dmitry Mendeleev University of Chemical Technology of Russia, Russia*
[4]*SPE LLC Nanostructured Glass Technology, Russia*

anastasiia.merdalimova@skoltech.ru

ABSTRACT

Microstructured hollow-core optical waveguides (HC-MOW) have recently emerged among optical sensors[1]. Their applications include the detection and analysis of liquids and gases in industrial and clinical applications. Anti-resonant HC-MOW[2] have a quasi-sinusoidal transmission spectrum with minima positions affected by inner wall thickness and refractive indices of the cavity and walls, that allows the measurement of layer deposition on the inner walls or the refractive index of an introduced liquid analyte[3]. Furthermore, the long optical pathway of analyte-light interaction provided by HC-MOW leads to improved signal amplitude for Raman spectroscopy[4].

In this talk, we demonstrate different combinations of sensing modalities in HC-MOW: SERS sensing accompanied with layer deposition control while providing a SERS substrate[4]; 2-in-1 sensing of refractive index and Raman scattering for characterization of complex liquid analytes[5].

For implementation of SERS sensing with layer deposition control[4], we employed the layer-by-layer assembly technique for a straightforward functionalization of waveguide capillaries. Gold nanoparticles with an average diameter of 8 nm were introduced into the hollow core, followed by UV-induced reduction of chloroauric acid. A simple, swift analytical approach to monitor each phase of the SERS platform construction was realized by detecting spectral shifts in the optical transmission of HC-MOWs. The application of this SERS platform led to an enhanced Raman signal of Rhodamine 6G, that was used as a model analyte.

In the study about 2-in-1 sensing[5], we analyzed refractive index and Raman scattering of dispersive systems, namely nanosized copolymer protein complexes of bovine serum albumin (BSA) and a vinylpyrrolidone-acrylic acid (P(VP-AA)) polymer, and the corresponding air-filled microbubbles (MB) [6].

Thus, different ways of using HC-MOW for sensing in combinations of modalities are described, highlighting its perspectives for characterization of liquid analytes.

This work was supported by the Russian Science Foundation: Grant No. 21-73-10254 for synthesis of colloidal systems and Grant No. 23-79-00056 for microfluidics.

REFERENCES

[1] Wang XD, Wolfbeis OS. Waveguide-optic chemical sensors and biosensors (2015-2019). Anal Chem. 2020;92(1):397–430.
[2] Ni W, Yang C, Luo Y, Xia R, Lu P, Hu DJJ, et al. Recent advancement of anti-resonant hollow-core waveguides for sensing applications. Photonics. 2021;8(4).
[3] Ermatov T, Noskov RE, Machnev AA, Gnusov I, Atkin V, Lazareva EN, et al. Multispectral sensing of biological liquids with hollow-core microstructured optical fibres. Light Sci Appl. 2020;9(1):173.
[4] Merdalimova AA, Rudakovskaya PG, Ermatov TI, Smirnov AS, Kosolobov SS, Skibina JS, et al. SERS Platform Based on Hollow-Core Microstructured Optical Waveguide: Technology of UV-Mediated Gold Nanoparticle Growth. Biosensors. 2022;12(1).
[5] Merdalimova A, Vorobev V, Barmin R, Terentyeva D, Aleksandrov A, German S, Chernyshev V, et al. Two − in − One Sensor of Refractive Index and Raman Scattering using Hollow − Core Microstructured Optical Waveguides for Colloid Characterization. Phys Chem Chem Phys 2023 - *under submission*.
[6] Estifeeva TM, Barmin RA, Rudakovskaya PG, Nechaeva AM, Luss AL, Mezhuev YO, et al. Hybrid (Bovine Serum Albumin)/Poly(N-vinyl-2-pyrrolidone- co-acrylic acid)-Shelled Microbubbles as Advanced Ultrasound Contrast Agents. ACS Appl Bio Mater. 2022;5(7):3338–48.

Metasurface-enhanced mid-infrared spectral tissue imaging and biosensing

S. ROSAS[1], K. A. SCHOELLER[3,4], E. CHANG[3,4], H. MEI[2], M. A. KATS[2], K. W. ELICEIRI[1], X. ZHAO[3,4], AND F. YESILKOY[1]*

[1]*Department of Biomedical Engineering, University of Wisconsin-Madison, WI, USA*
[2]*Department of Electrical and Computer Engineering, University of Wisconsin-Madison, WI, USA*
[3]*Department of Neuroscience, University of Wisconsin-Madison, WI, USA*
[4]*Waisman Center, University of Wisconsin-Madison, WI, USA*

*filiz.yesilkoy@wisc.edu

ABSTRACT

Label-free and nondestructive mid-infrared (MIR) vibrational hyperspectral imaging has gained significance as a valuable tool for analyzing biomedical tissue. Several studies have demonstrated the potential of MIRSI in diagnosing various diseases [1,2]. However, the complex chemical composition and heterogeneous nature of tissue specimens along with the weak interaction of infrared light with biomolecules, pose limitations on the analytical performance of traditional MIR spectral histopathology. Here, we introduce an advanced MIR spectrochemical tissue imaging technique that utilizes plasmonic metasurfaces to enable the capture of quantitative molecular maps of large-area brain tissue sections. The proposed surface-enhanced chemical imaging method using plasmonic metasurfaces has great potential for translational biomedical research and diagnostic clinical histopathology.

In this research [3], a plasmonic metasurface-enhanced MIR spectral imaging (SE-MIRSI) method is introduced as an advanced label-free chemical tissue-imaging technique. The study demonstrates MIR spectroscopy of murine brain tissue sections by examining nanoscale thicknesses over large areas using engineered photonic substrates and a hyperspectral imaging microscope with illumination from four tunable quantum cascade lasers (QCLs) (Fig.1). To enable multiplexed molecular fingerprint analysis, polarization-tunable multi-resonant plasmonic metasurfaces are developed, enhancing light-matter interactions in sub-wavelength volumes within the target fingerprint spectral range of 950-1800 cm^{-1}. The research reveals the influence of tissue morphology on quantitative chemical analysis by comparing absorbance from various vibrational bands obtained from brain tissue sections of different thicknesses. It is shown that SE-MIRSI is not affected by the bulk morphological properties of complex tissue samples since the absorption occurs in plasmonic hotspots, which are nanoscale volumes with strong electric field intensity enhancement. Moreover, SE-MIRSI can detect fine spectral details corresponding to protein backbone structures and other important biomolecules such as glycogen, nucleic acids, proteins, and lipids. The study also demonstrates the capability of SE-MIRSI to analyze ultrathin brain tissue regions that are not detectable using standard substrates, highlighting the high analytical sensitivity of the approach. By decoupling chemical and morphological properties, this method addresses the quantitative analysis limitations of infrared absorption spectroscopy and enables highly sensitive and chemically selective analysis of complex and heterogeneous biosamples. The versatility of the proposed chemical imaging method makes it applicable to the study of various tissue types, with potential implications in fundamental research and clinical histopathology.

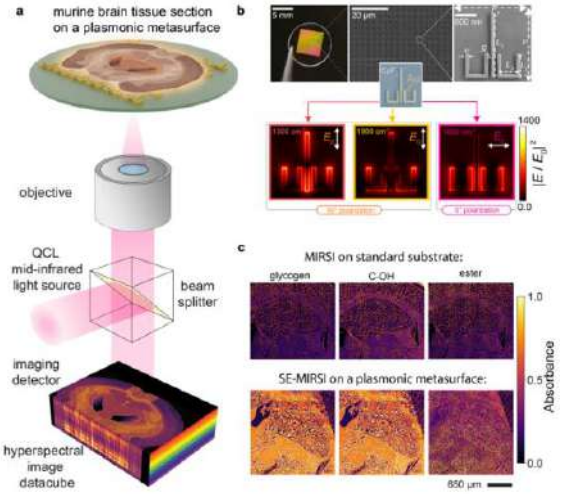

Figure 1: ***Surface-enhanced mid-infrared spectral imaging of tissues (SE-MIRSI). a****, Schematic of the tunable quantum cascade laser (QCL)-based mid-IR spectral imaging system. Hyperspectral datacubes are acquired using a microbolometer focal-plane detector array while sweeping the illumination wavenumber across the mid-IR fingerprint spectral range of 950 to 1,800 cm^{-1}.* ***b****, Photographs, SEM images show a fabricated plasmonic metasurface chip. Simulation generated images show the E-field enhancement pattern in a unit cell for orthogonal polarizations.* ***c****, MIRSI and SE-MIRSI of murine brain tissue section at different wavenumbers corresponding to absorption bands of functional groups present in endogenous biomolecules such as glycogens, nucleic acids, proteins, and lipids.*

REFERENCES

[1] Tiwari S, Kajdacsy-Balla A, Whiteley J, Cheng G, Jirstrom K, Birgisson H, et al. INFORM: INFrared-based ORganizational Measurements of tumor and its microenvironment to predict patient survival. Science Advances. 2021 Feb 3;7(6):eabb8292.
[2] Shi L, Liu X, Shi L, Stinson HT, Rowlette J, Kahl LJ, et al. Mid-infrared metabolic imaging with vibrational probes. Nat Methods. 2020 Aug;17(8):844–51.
[3] Rosas S, Schoeller KA, Chang E, Mei H, Kats MA, Eliceiri KW, et al. Metasurface-Enhanced Mid-Infrared Spectrochemical Imaging of Tissues. Advanced Materials. n/a(n/a):2301208.

Exploring the potential of multiphoton patterning

Peter T. C. So

The use of structured light for microscopic imaging has nearly a century long history. Recent important applications include attaining resolution beyond diffraction limit and imaging structures at a selective depth. We have recently developed De-scattering with Excitation Patterning or "DEEP," an extension of TRAFFIX approach developed by Dholakia group. DEEP allows high throughput depth selective wide-field multiphoton imaging in tissues without suffering from blurring due to the scattering of emission photons. Importantly, the combination of DEEP with modern computational approaches offers even faster imaging opportunities for specimens that can be sampled compressively. We are exploring extensions of this approach along several directions including to simultaneously reconstruct 3D volumes and to combine lifetime imaging to increase information content. In both cases, the extension to a higher dimensional measurement space allows better utilization of the inherent sparsity in many samples allowing for even higher efficiency. An application of these approaches is the in vivo mapping of neuronal connectivity.

New approaches to the laser plasmon resonance phototherapy of cancer

Elina GENINA[1,2,3], Vadim GENIN[1,2,3], Alla BUCHARSKAYA[2,3,4], Nikita NAVOLOKIN[4], Georgy TERENTYUK[4], Nikolai KHLEBTSOV[5], Valery TUCHIN[1,2,3,6]

[1]*Optics and Biophotonics Department, Saratov State University, Russia*
[2]*Laboratory of laser molecular imaging and machine learning, National Research Tomsk State University, Russia*
[3]*Science Medical Center, Saratov State University, Russia*
[4]*Department of Pathological Anatomy, Saratov State Medical University named after V.I. Razumovsky, Russia*
[5]*Institute of Biochemistry and Physiology of Plants and Microorganisms, FRC "Saratov Scientific Centre of the Russian Academy of Sciences" (IBPPM RAS), Russia*
[6]*Institute of Precision Mechanics and Control, FRC "Saratov Scientific Centre of the Russian Academy of Sciences", Russia*

eagenina@yandex.ru

ABSTRACT

The effect of laser plasmon resonance photothermal therapy (PPT) is based on the accumulation of plasmon resonance nanoparticles in tumor tissues and their local heating by laser irradiation with the appropriate wavelength [1]. However, the efficacy of the treatment can be not enough. Insufficient accumulation of nanoparticles in the tumor leads to a low heating temperature and continued tumor growth. At the same time, an overdose of nanoparticles leads to a strong attenuation of light in the upper layers of tissues and a decrease in the depth of light penetration. Overcoming the disadvantages and limitations of PPT monotherapy is possible by using a combined approach, including photodynamic therapy (PDT) and optical clearing (OC) [2,3].

In this study, a cholangiocarcinoma cell culture was transplanted subcutaneously to male albino rats Wistar. The rats were divided into three groups: PPT, PPT/PDT and PPT/OC. Gold nanorods (GNRs) were injected intratumorally. The dimensions of the GNRs were 41±8 nm (length) and 10±2 nm (diameter), so plasmon resonance was observed at the spectral range 800-820 nm. For PDT, a solution of indocyanine green in polyethylene glycol (MW=300 Da) with a maximum absorption wavelength of 790 nm was used as a photosensitizer. It was also injected intra-tumorically. For OC, a solution of glycerin (70%) and DMSO (5%) was applied to the skin before irradiation. The irradiation was carried out percutaneously using a diode laser at a wavelength of 808 nm. Skin heating was monitored using an IR visualizer. The temperature increase during the procedures was up to 60 ± 4.1°C. Diffusion reflection spectra were recorded before and after the procedures in the spectral range of 400-1000 nm.

The withdrawal of animals and sampling of tumor tissues for histological examination was performed 72 hours and 21 days after therapy. Morphological studies of tumor tissue were performed on tumor sections stained by standard methods and with immunohistochemical staining for the proliferation marker Ki-67 and the apoptosis marker Bax.

The most pronounced effect was observed in the PPT/PDT group. After 72 hours, necrotic changes were observed in the tumor tissue, and necrosis fields occupied up to 80% of the area. Preserved tumor cells were observed only at the periphery of the tumor; they showed a decrease in the expression of the proliferation marker and an increase in the expression of the apoptosis marker. After 3 weeks, a significant inhibition of tumor growth was noted; a decrease in tumor mass was 77.4%. A reduction in thermal damage of the skin was obtained during PPT/OC.

The work was supported by RSF grant 23-14-00287.

REFERENCES

[1] X. Huang, et al, Lasers Med. Sci. 23, 217-228, 2008.
[2] A. Bucharskaya, et al, Materials, 15, 1606, 2022.
[3] J.-I. Youn, Med. Laser, 10, 146-152, 2021.

Structural and functional imaging of the retina with UHR-OCT

Kostadinka BIZHEVA[1,2,3]

[1]*Department of Physics and Astronomy, University of Waterloo, Canada*
[2] *School of Optometry and Vision Sciences, University of Waterloo, Canada*
[3] *Systems Design Engineering Department, University of Waterloo, Canada*

kbizheva@uwaterloo.ca

ABSTRACT

Neurodegenerative ocular diseases such as diabetic retinopathy, glaucoma and age-related macular degeneration, can change the cellular structure of the retina and cause abnormalities in the retinal blood flow and blood perfusion, as well as alter the normal response of retinal neurons to visual stimulation. A number of optical imaging modalities such as scanning laser ophthalmoscopy (SLO), optical coherence tomography (OCT), Doppler flowmetry, Doppler OCT, OCT-based optical microangiography (OCTA), fluorescence-based angiography and two-photon microscopy, have been used in the past to investigate structural, vascular and functional changes in the human and animal retinal in health and disease. Here, we utilize a combined OCT+ERG system to investigate visually evoked physiological and blood flow changes in the healthy and glaucomatous retina.

For this study we used a fiber-optic based SD-OCT system that is powered by a superluminescent diode-based light source. The detection end of the system is comprised of a high-resolution spectrometer and a linear array camera with 250 kHz maximum readout rate. A telecentric pair of achromat lenses was used to generate a 2 mm wide optical beam incident on the cornea with optical power of 1.1 mW. A visual stimulator comprised of 4 LEDs (blue, red, green and white) and pair of achromat lenses was integrated into the OCT retinal imaging probe to deliver Maxwellian illumination of the retina. The visual stimulator was connected to a commercial electroretinography system (ERG), that allowed for precise control of the color, intensity, duration and pattern of the visual stimulus that was delivered to the human retina. Functional retinal OCT and ERG data were recorded synchronously from human subjects and rats (rodent model of glaucoma). The imaging studies have received full ethics clearance from the University of Waterloo Office of Research Ethics. OCT+ERG recordings were acquired over period of 10 seconds with 2s pre-stimulus period. The color, intensity, duration and pattern of the visual stimulus were varied to explore dependence of the recorded physiological and blood flow changes on these parameters. Custom Matlab-based algorithms were used to process and analyze the OCT data.

Figure 1 shows high resolution morphological images of the healthy human retina: (A) B-scan where all major retinal layers are resolved, enface images of the (B) retinal surface, (C) the outer plexiform layer showing capillary network, (D) inner – outer segment photoreceptors junction, (E and D) magnified views of the same layer showing reflections from individual cones. Note that all images are single-shots and no averaging or post-processing was applied. Figure 2 shows results from a functional blood flow test with the following stimulus parameters: color – blue (440 nm); pattern – flicker, duration – 1s, intensity – 0.8 Cd.s/m^2. An enface view of the retinal ONH, generated from a volumetric OCT image is shown in Fig. 2A. The red lines show the approximate location of the circular scans. A circular B-scan (Fig. 2B) shows cross-sections of major retinal blood vessels at the ONH. Fig. 2C shows stimulus-induced changes in the blood flow of a single retinal blood vessel over a period of 10s. The black and red lines correspond to the measured raw and filtered blood flow data respectively. The blue area in the graph marks the timing and duration of the visual stimulus. The blood flow shows ~ 500% peak increase relative to the baseline (dark recording). The latency of the peak response was ~2s relative to the onset of the visual stimulus.

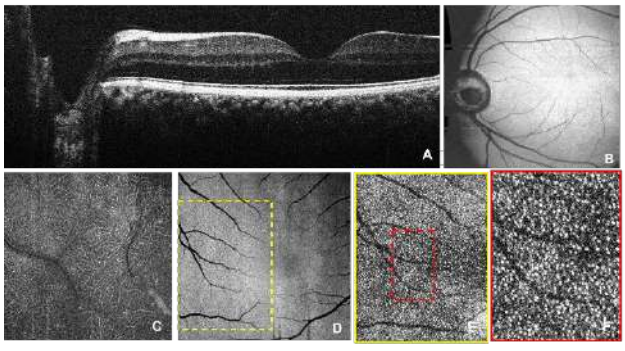

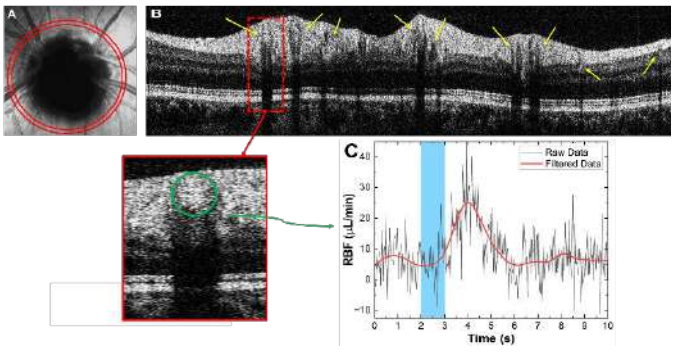

Figure 1: *(A)B-scan and (B) En-face view of the healthy human retina. En-face views of (C) the outer plexiform layer showing capillary network, (D) inner-outer segment junction, (E) magnified view of the ROI marked with yellow dashed line, (F) magnified view of the ROI marked with red dashed line where white dots correspond to reflections from cone photoreceptors.*

Figure 2: *(A) Enface view of the ONH with red circles marking the OCT scanning pattern. (B) Circular B-scan showing retinal blood vessels around the ONH (yellow arrows);(C) Transient changes in the blood flow measured from a blood vessel in response to blue flicker stimulation.*

Raman spectroscopy of UV doze-dependent conformational changes of human hair keratins

Elena TRAVKINA[1], Andrey CHIKISHEV[1], Elena MIKHALCHIK[2] and Nikolay BRANDT[1]

[1] *Faculty of Physics, Lomonosov Moscow State University, Russia*
[2] *Federal Scientific Clinical Centre of Physical Chemical Medicine, Russia*

brandt@physics.msu.ru

ABSTRACT

The problems of the study of human hair have been considered in the scientific literature for several decades. Raman spectroscopy remains to be extremely popular in this area due to its sensitivity to the conformational features of hair proteins and the ability to evaluate the effectiveness of cosmetic products both in vitro and in vivo. Multiple works have been devotes to the study of human hair with the aid of Raman spectroscopy. Alternative methods of vibrational spectroscopy (e.g., FTIR and CARS spectroscopy) have also been employed (see, for example, [1, 2]).

A hair consists of a core (medulla), a cylindrical surrounding layer (cortex), and a relatively thin (with a thickness of 1–4 μm) cylindrical outer shell (cuticle). Each part has individual molecular composition, but the main components are fibrillar water-insoluble protein macromolecules (keratins). A hair also contains low-molecular-weight proteins with a high content of sulfur-containing amino acids. Disulfide bonds in the hair structure provide its mechanical strength and, in addition, support the secondary structure of keratins. As for the secondary structure, the α-helix dominates in the cortex, while the β-structure dominates in the cuticle. Thus, the rigid cylindrical shell of the cuticle with a large number of the S-S bonds isolates bundle-like molecular complexes, which form elongated cortex cells, from the external environment.

The efficiency of Raman spectroscopy in the analysis of the structural features of such a system is determined by two main factors. First, the use of confocal Raman microspectroscopy makes it possible to obtain a spatial resolution (of up to 1 μm) sufficient for separation of the spectral contributions from different functional parts of the hair. Second, the conformation-sensitive bands in the Raman spectra of proteins make it possible to determine the ratio of secondary structure elements, the conformation of disulfide bridges, the relative concentration of C-S and S-H bonds, and the state of the hydroxyl groups of tyrosine side chains.

Different layers of a hair have experimentally been detected in the study of its cross section, obtained with the aid of microtomes. A large number of works have been devoted to the determination of hair changes under the influence of various chemical, in particular, cosmetic agents. It has been shown that cosmetic products can be incorporated in the hair structure. Thus, the desired effect (in particular, coloring or rejuvenation) is achieved.

Interestingly, the molecular structure of hair keratins changes not only under chemical exposure, but also under mechanical stress, temperature changes, and irradiation in the UV range. The results of [3] show that the UV irradiation leads to breaking of disulfide bonds in the structure of keratins, formation of thiols, and changes in the secondary structure of proteins.

In this work, we use confocal Raman microspectroscopy to determine the sequence in which conformational changes in human hair keratins occur with increasing UV dose in a wavelength interval of 200–400 nm. The Raman spectra are analyzed in spectral intervals of 500–550 cm^{-1} (S–S stretching vibrations), 600–750 cm^{-1} (C–S stretching vibrations), 820–860 cm^{-1} (tyrosine doublet), 1220–1260 cm^{-1} (amide III band), 1650–1690 cm^{-1} (amide I band), and 2520-2590 cm^{-1} (S–H stretching vibrations).

It is shown that the measurements of Raman spectra of a single region at different positions of a hair relative to the excitation radiation yield significantly different results. This is due to the polarization sensitivity of several bands in the Raman spectra of a hair, and the effect is manifested even when depolarized radiation is used for excitation. The results are analyzed with allowance for the orientation of a hair sample relative to the wave vector of the excitation radiation. The polarization sensitivity of Raman spectra must be taken into account in the study of biological objects containing fibrillar molecules even when depolarized radiation is used in experiments.

An irradiation dose of 10 mJ in a wavelength interval of 200–400 nm leads to the breaking of disulfide bonds in the proteins of the hair cortex. The secondary structure of keratins significantly changes under irradiation at a dose of 50 mJ. With a further increase in the irradiation dose (to a level of greater than 120 mJ), unbroken disulfide bonds are transformed from the gauche-gauche-gauche conformation to the trans-gauche-gauche conformation, and α-helices are transformed into β-structural fragments. The results will be used for monitoring and comparison of the structure of hair keratins in experiments with various cosmetic agents.

REFERENCES

[1] K.L.A. Chan et al, Appl. Spec. 62, 1041–44, 2008.
[2] S. Ogawa et al, J. Cosmet. Sci. 51, 379–399, 2000.
[3] M.V. Fedorkova et al., J. Photochem. Photobiol., B: Biol. 164, 43–48, 2016.

Optical Monitoring of Intradermal Delivery of Drug-Loaded Vaterite Carriers

Yulia SVENSKAYA[1], Valery TUCHIN[1]

[1]*Scientific Medical Center, Saratov State University, Russia*

svenskaya@info.sgu.ru

ABSTRACT

Administration of pharmacologically active molecules via skin appendages is gaining tremendous scientific interest, especially with regard to delivery to specific targeted regions and the reduction of systemic toxicity. However, the design of an appropriate effective method for clinical use remains challenging. We report on a novel non-invasive approach for topical delivery based on accommodation of drug-loaded submicron particles in hair follicles followed by sustained release of active molecules into the skin [1, 2]. The proposed delivery system is represented by submicron porous biodegradable vaterite carriers, which provide the degradation-driven *in situ* release of the loaded substance. By means of scanning electron microscopy, optical coherent tomography and confocal laser scanning microscopy, we demonstrated a deep and plentiful filling of hair follicles with the topically applied carriers *in vivo* under the sonophoresis. This group of optical methods was also utilized to monitor degradation of the delivered carriers in rats and mice *in vivo* [1-4].
The described method provides intra- and transdermal drug administration for the purposes of localized and systemic adsorption and was adopted for delivery of photosensitizers [5-7], antifungal drugs [4, 8-10], vaccines [11] and glucocorticoids. The use of vaterite particles allowed us to enhance dermal bioavailability of the applied drugs while targeting to specific areas in skin. In such a manner, by means of various optical methods we demonstrated that our protocol in non-invasive and easily practicable protocol for transdermal and topical drug administration.

The study is supported by Russian Science Foundation (project № 22-73-10194).

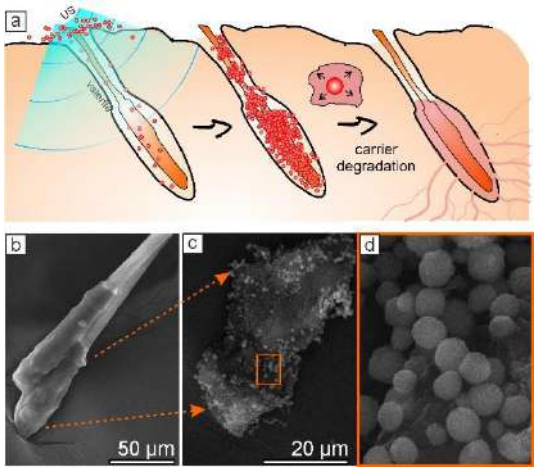

Figures: *(a) Schematics of intrafollicular drug delivery by means of biodegradable vaterite carriers. Adopted with permission from [1]. Copyright ©, 2019 American Chemical Society. (b)-(c) SEM images of the plucked follicle sac filled with the carriers performed at different magnifications. Adopted with permission from [5]. Copyright © 2020 British Association of Dermatologists*

REFERENCES

[1] Yu. Svenskaya et al, ACS Appl Mater Int 11 (19), 17270-17282, 2019.
[2] Yu. Svenskaya et al, Patent RU2698871C1, 2018.
[3] Yu. Svenskaya et al, Izv. Sarat. Univ. Physics 21(1), 80–85, 2021.
[4] O. Gusliakova et al, Mater. Sci. Eng. C. 119, 111428, 2021.
[5] Y. Svenskaya et al, Brit J Dermatol, 182(6), 1479-1481, 2020.
[6] Y. Svenskaya et al, Patent RU2698871C1, 2018.
[7] S. Utz et al, Vestn Dermatol Venerol., 95(1), 21-29, 2019.
[8] E. Lengert et al. Mater. Lett. 248, 211-213, 2019.
[9] M. Saveleva et al, Biomat. Sci. 10, 3323, 2022.
[10] R. Verkhovskii et al, ACS Infect. Dis. 9(5), 1137-1149, 2023.
[11] Yu. Svenskaya et al, J Mat. Chem. B,11(17), 3860-3870, 2023.

Wearable multimodal analyzers in the study of the microcirculatory bed and oxidative metabolism of biotissue

Andrey DUNAEV[1], Elena ZHARKIKH[1], Yulia LOKTIONOVA[1] and Victor SIDOROV[2]

[1]Research & Development Center of Biomedical Photonics, Orel State University, Russia
[2]SPE "LAZMA" Ltd., Russia

dunaev@bmecenter.ru

Currently, there is a surge of interest in wearable diagnostic devices with the possibility of daily monitoring of the functional state of the human body, for example, microcirculatory-tissue systems. The first such development is the «LAZMA PF» analyzer ((LAZMA Ltd, Russia; in EU/UK this device is produced by Aston Medical Technology Ltd., UK as «FED-1b»), which makes it possible to study the microvasculature and oxidative metabolism of biological tissues [1]. The design features of these devices make it possible to record index of microcirculation (perfusion) and NADH fluorescence intensity with less sensitivity to motion artifacts and with a larger diagnostic volume compared to stationary devices [2, 3]. The purpose of this work is to demonstrate the successful experience of using these devices in clinical practice.

Analyzers with wireless data transmission implement the methods of laser Doppler flowmetry (LDF) and fluorescence spectroscopy (FS), which allows for complex diagnostics of microcirculatory-tissue systems of the human body. The analyzers were used in the form of their distributed system (of 2 or 4 devices) in various parts of the upper and lower extremities of a human body [1, 4] without the use of functional tests in various fields of medicine – endocrinology (type 1 and 2 diabetes), cardiology (arterial hypertension), rehabilitation (post-covid rehabilitation), physiotherapy (hatha yoga breathing exercises), sports and space [1] medicine. The time of registration of the microcirculatory-tissue system parameters (I_m – index of microcirculation, A_{NADH} – normalized amplitude of the biotissue coenzyme NADH) averaged for 10 min.

Studies in patients with diabetes mellitus have shown a decrease in I_m and nutritive blood flow in the lower extremities and an increase in the upper extremities. The results indicate the body's attempts to compensate for microcirculation disorders in the upper extremities. Studies of women with pregestational diabetes revealed a decrease in the oscillatory activity of microcirculatory-tissue systems in patients and an increase in A_{NADH}. Patients with post-COVID syndrome had reduced values of I_m and nutritive blood flow, as well as increased oscillatory activity of blood flow. In the study of the effect of hypo- and hyperventilation yoga breathing exercises on the parameters of peripheral blood flow, a correlation was found between the parameters of blood microcirculation and gas analysis during free breathing and hypoventilation. Also, for the first time, a technique has been developed for measuring the microcirculatory bed and oxidative metabolism of biotissues of cosmonauts limbs during the period of acute adaptation to microgravity conditions and readaptation after the completion of a space flight. The results obtained in this study confirmed the redistribution of circulating blood volume to the upper part of the body during the first few days of space flight and the normalization of blood flow on the 6th day of flight.

Thus, data on the state of the microcirculatory bed and oxidative metabolism of biotissue, recorded using wearable multimodal analyzers when solving various diagnostic problems in clinical conditions, make it possible to more comprehensively and reliably assess the relationship and dynamics of oxygen utilization by tissues.

The study was supported by the Russian Science Foundation grant № 23-25-00522.

[1] A. Dunaev, J of Biomedical Photonics & Eng 9(2), 020201, 2023.
[2] E. Zharkikh et al, J. Biophotonics, e202300139, 2023.
[3] V.V. Sidorov, Biomedical Engineering 55(6), 379-382, 2022.
[4] E. Zherebtsov et al, IEEE Trans Biomed Eng, 2023.
[5] A. Dunaev et al, Proc. of Int. Conf. Laser Optics (ICLO), 2022.

OCT mapping of tympanic membrane mobility

Grigory Gelikonov

Department of Nonlinear Dynamics and Optics, Institute of Applied Physics RAS, Russia
grgel@ipfran.ru

ABSTRACT

Recently, the direction of optical coherence tomography for the study of the middle ear has begun to develop quite actively. OCT demonstrates the ability to obtain additional information to the structural image. This paper demonstrates the ability of OCT not only to visualize the tympanic membrane, but also to build a map of its mobility.

Optical coherence tomography has long been the gold standard in ophthalmology. At the same time, OST continues to develop new areas of diagnostics in medicine. A relatively new direction is the study of the human middle ear. In this direction, OCT is able to visualize the tympanic membrane and the area behind it. This is important in the diagnosis of exudative otitis [1], as it allows visualization of the exudate. Such a study allows you to evaluate the viscosity of the exudate and thus the tactics of treatment and increase its success. Recently, works have appeared on additional functional diagnostics of the middle ear using OCT [2][3]. In this work, we develop a method for determining the mobility of the tympanic membrane under the influence of sound vibrations and constructing a two-dimensional map of such mobility. In this paper, we present a method for extracting information about tympanic membrane mobility from an OCT signal. The method provides for the calculation of the signal over the entire range of depths (while overcoming the complex uncertainty), the suppression of the residual specular component, the suppression of object movements, and the isolation of movements at the frequency of the probing sound.

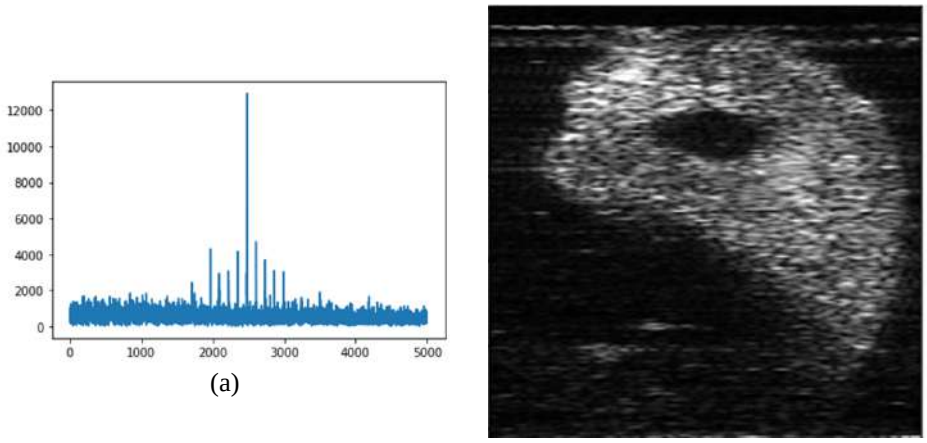

(a) (b)

Figure: *(a) Part of spectrum of tympanic membrane mobility, (b) 2D map of tympanic membrane mobility*

REFERENCES

[1] P. A Shilyagin, et al. Quantum Electronics 51, 371-376, 2021
[2] M. Hamra, et al. Hearing Research 431, 2023
[3] L.Kirsten, et al. Journal of Biomedical Optics 24, 031017 2018

VIS-NIR diffuse reflectance spectroscopy system with self-calibrating probe: pilot in vivo studies

Ilya TURCHIN[1], Vladimir BESCHASTNOV[2], Valeriya PEREKATOVA[1], Alexey KOSTYUK[1], Anna ORLOVA[1], Aleksander KHILOV[1], Ekaterina SERGEEVA[1], Mikhail KIRILLIN[1], Maksim RYABKOV[2]

[1]*Department for Radiophysical methods in medicine, Federal Research Center A.V. Gaponov-Grekhov Institute of Applied Physics of the Russian Academy of Sciences, Russia*
[2]*University Clinic, Privolzhsky Research Medical University, Russia*

ilya@ipfran.ru

ABSTRACT

Diffuse reflectance spectroscopy (DRS) is based on illuminating biological tissue with broadband light in the visible (VIS) and/or near infrared (NIR) spectrum region and detecting backscattered light at a given distance from the source. The recorded spectrum contains information on the absorption of various tissue chromophores (oxy- and deoxyhemoglobin, melanin, water, lipids), the concentration of which can be reconstructed by solving an inverse problem. One of the key points of successful reconstruction of tissue chromophores is taking into account the instrumental characteristics of the DRS system. Traditional ratiometric approach based on the measurements with two source-detector distances (one source and two detectors or two sources and a single detector) allows for compensation of detector spectral sensitivity and the source brightness variations [1], but it does not allow compensating all transient functions of the source and detector. The self-calibrating approach proposed in [2] is based on symmetrical multi-distance measurements (at least four measurements with two sources and two detectors) and makes it possible to compensate for the instrumental contributions of the source and detector channels. Additionally, it is less sensitive to changes in the optical coupling between the optical sensor and tissue [3] in comparison to single-distance and single-slope approaches. In this paper, we present an experimental setup for VIS-NIR DRS with a fiber optic probe using a self-calibrating approach. The stability of the self-calibrating and traditional single-slope approaches to instrumental perturbations were compared in phantom and in vivo studies on human palm, including attenuations in individual channels, fiber curving, and introducing optical inhomogeneities in the probe–tissue interface [4] . The self-calibrating approach demonstrated high resistance to instrumental perturbations introduced into the source and detection channels, while the single-slope approach showed resistance only to perturbations introduced into the source channels. The developed experimental setup has been employed successfully in the in vivo studies on rats to reveal the differences in dynamics of allo- and autografts physiological parameters - blood and water content, and oxygenation (Figure 1) [5].

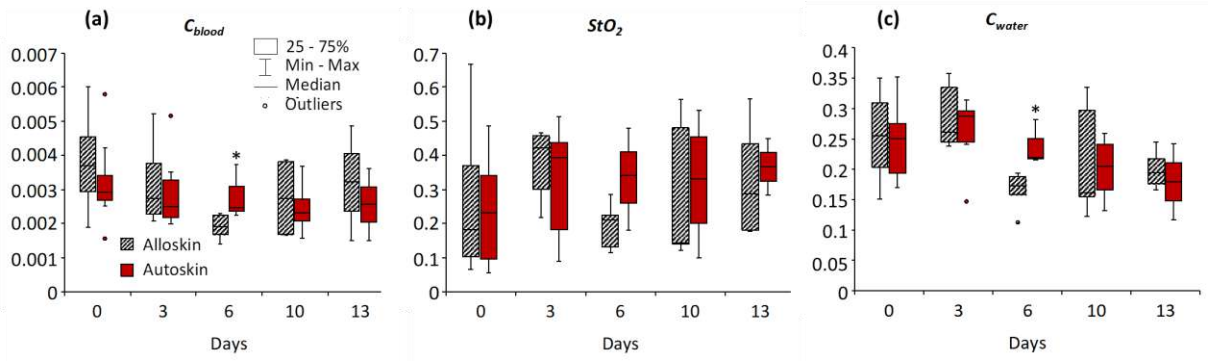

Figure 1: *The dynamics of saturation, blood content, C_{blood} $(a.u.)$ (a), StO_2, (b) and water content, C_{water}, (c), reconstructed from the DRS measurements. * - statistically significant differences between groups ($p \leq 0.05$, Mann–Whitney test)*

The study was supported by Center of Excellence «Center of Photonics» funded by The Ministry of Science and Higher Education of the Russian Federation, Contract No. 075-15-2022-316.

REFERENCES

[1] F. Scholkmann, A. J. Metz, and M. Wolf, Physiological measurement 35, 717 2014.
[2] D. M. Hueber, S. Fantini, A. E. Cerussi, and B. B. Barbieri in Optical tomography and spectroscopy of tissue III, (SPIE), 618-631 1999.
[3] A. Sassaroli, G. Blaney, and S. Fantiniб JOSA A 36, 1743-1761 2019.
[4] V. Perekatova, et.al. Diagnostics, 13, 457 2023.
[5] I. Turchin, et. al. Biomedicines, 11, 351 2023.

Polarization-Sensitive OCT Guided Catheter Ablation of Atrial Fibrillation

Andrew ROLLINS

Departments of Biomedical Engineering and Medicine, Case Western Reserve University, USA

andrew.rollins@case.edu

ABSTRACT

Atrial fibrillation (AF) is the most common arrhythmia worldwide. Clinical trials have shown that catheter ablation is superior to antiarrhythmic drugs in regard to freedom from recurrent AF. During this procedure, the electrophysiologist steers a catheter into the left atrium and ablates a lesion fence around common sources of ectopic signals, blocking arrhythmogenic tissue from initiating an erroneous heartbeat. Technological advancements in this maturing technique have made catheter ablations more widespread and effective for patients, but there is still a need to improve long term efficacy of the procedure. The rate of recurrent AF after an ablation is 20% to 40% in the USA, and this is predominantly due to reconnection because of poor lesion quality. With current catheter technology available to clinicians, it is difficult to assess whether a lesion line will remain durable, or heal to allow recurrent AF.

We have developed and validated a polarization-sensitive optical coherence tomography (PSOCT)-integrated radiofrequency ablation catheter. We have shown in large animals that PSOCT can confirm the quality of catheter contact with the atrial wall and monitor lesion formation *in vivo* during an ablation procedure. Results further indicate that PSOCT guidance may provide clinicians with critical feedback including wall thickness, confirmation of lesion transmurality, and prediction of overtreatment. This technology has the potential to improve catheter ablation by reducing procedure time, reducing recurrence, and improving safety.

Discovery of new structures in the *stratum corneum* of glabrous skin with optical methods: crystallized urea dendriform structures are affect the hydration levels

Maxim DARVIN[1], Roland BENNEWITZ[2,3], Marius KRÖGER[1], Martina MEINKE[1], and Victor INFANTE[1,2]

[1]*Department of Dermatology, Charité-Universitätsmedizin Berlin, Germany*
[2]*INM – Leibniz Institute for New Materials, Germany*
[3]*Department of Physics, Saarland University, Germany*

maxim.darvin@protonmail.com

ABSTRACT

Glabrous skin is found on the palms and soles of humans and is characterized with the absence of hair, a high density of sweat glands and the largest stratum corneum (SC) thickness. Here we report the discovery of new structures in the SC of glabrous skin, visualized non-invasively with reflectance confocal laser scanning microscopy (RCLSM) on the palms, fingers and soles of healthy individuals. The observed structures are remarkable and characterized by strong light reflection in RLSM images and were observed in ≈70% of individuals (Fig. A–D). The size and shape of these structures vary by organization and exhibit an elongated shape with attached small arms 2–15 µm in length (Fig. A). Longer arms are often attached to each other, forming a chain that is most pronounced in the superficial SC region and decreases towards the bottom of the SC. We hypothesized that the observed structures originate from crystallized urea. Urea crystals are known to yield a second harmonic generation (SHG) signal. Using *in vivo* two-photon tomography, we confirmed the presence of SHG structures in the SC of glabrous skin (Fig. E), which have a similar appearance to the RCLSM images. The chemical composition of the discovered structures was assessed *in vivo* by confocal Raman micro-spectroscopy measuring a shift of a Raman band at 1004 cm^{-1} associated with dissolved urea towards higher wavenumbers, as occurs during urea cristallization. The strong shift observed as a shoulder in the Raman spectrum at 1010 cm^{-1} confirms that the discovered structures are urea crystals, confirming our hypothesis (Fig. G). Therefore, we have named the discovered structures as crystallized urea dendriform (CUD) structures. The thick SC seems to be crucial for the crystallization process, where urea, mainly released with sweat, is deposited in the superficial SC region where it crystallizes under certain physiological circumstances. It was found with confocal Raman micro-spectroscopy and confirmed with corneometry that the individuals with a higher volume fraction of CUD structures had lower skin hydration (R^2=0.55, p<0.001, Fig. F). In addition, confocal Raman micro-spectroscopy reveals the lower concentration of natural moisturizing factor molecules in the SC with CUD than without CUD structures. Thus, the presence of CUD structures in the glabrous skin seems to indicate a reduced water binding capacity. Further studies should aim to understand whether CUD structures are a signature or cause of dry skin. These findings provide a new direction in dermatology and cosmetology to understand the mechanisms that lead to dry hands and open up possibilities for the development of better moisturizers and for the diagnostic of dry skin.

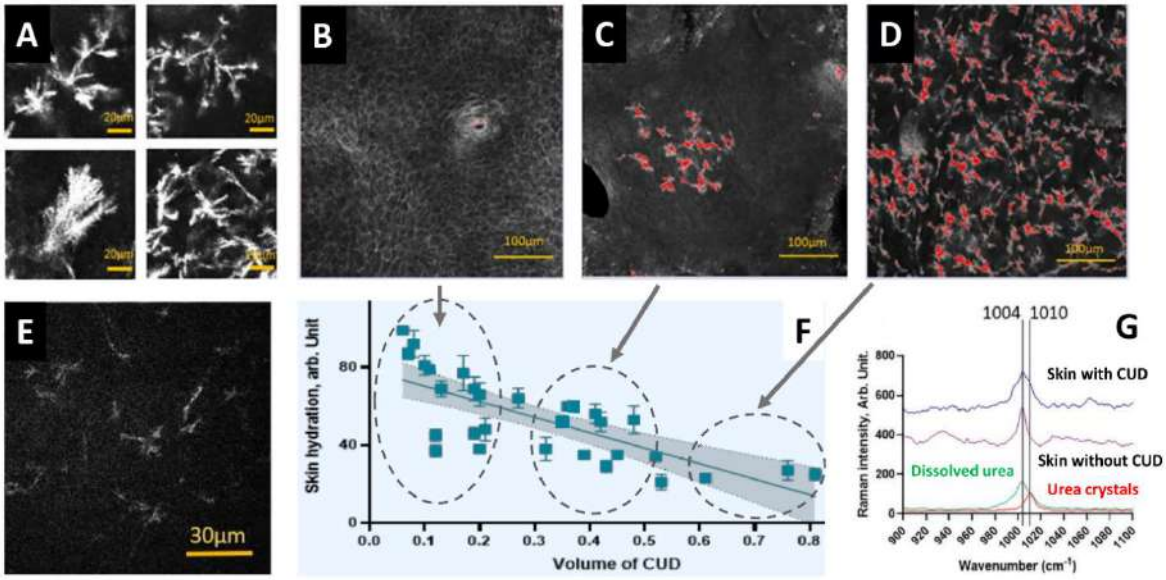

Figures: *In vivo images of SC from human glabrous skin with CUD structures measured with RCLSM (A –white areas, B-D – red areas), SHG (E – white areas); negative correlation between skin hydration and volume of CUD structures (F); in vivo Raman spectra for SC with/without CUD structures, in vitro dissolved and crystallized urea with the bands at 1004 and 1010 cm^{-1} (G).*

REFERENCES

[1] V. Infante et al, Exp. Dermatol. 32, 986–995, 2023.

Automatic temperature controlled retinal laser therapies – method and first clinical results

Ralf BRINKMANN[1,2], Claus VON DER BURCHARD[3], Christopher KREN[1], Veit DANICKE[1], Hossam ABBAS[4], Dirk THEISEN-KUNDE[1] and Johann ROIDER[3]

[1] *Medical Laser Center Lübeck, Germany*
[2] *Institute of Biomedical Optics, University of Lübeck, Germany*
[3] *Department of Ophthalmology, University Medical Center Schleswig-Holstein Campus Kiel, Germany*
[4] *Institute for Electrical Engineering in Medicine, University of Lübeck, Germany*

ralf.brinkmann@uni-luebeck.de

ABSTRACT

Recently, retinal laser treatments for some diseases like diabetic macular oedema (DME) and central serous chorioretinopathy (CSR) are performed towards thermally stimulating the fundus tissue without adverse damage as in standard photocoagulation. Due to the invisibility of this irradiation strategy proper dosing is a challenge. Therefore typically test lesions near the vascular arcades are applied to achieve barely visible coagulations. Based on this power a reduced power for the macular target area is calculated, typically 30 - 50 % is used. However, due to the strong intraocular variations of light scattering and fundus pigmentation (20 – 80 %), this strategy is highly error-prone. Moreover, cellular response to a transient temperature rise is very crucial with respect to the temperature.

Since objective real-time optoacoustic (OA) temperature measurements have already been demonstrated clinically [1], this method was now extended towards an automatic closed-loop feedback power control in order to automatically obtain a desired target temperature preselected by the ophthalmologist [2]. The power control modul consists of a low pulse energy Q-switched laser (QSL, Crystalaser, 75 ns pulse duration) which excites temperature dependent thermoelastic expansion at the retina with a repetition rate of 3 kHz. The excited ultrasound waves at the target area are measured with an appropriate transducer embedded in a Mainster contact lens. The control module was optically coupled between a standard continuous wave clinical laser (Zeiss Visulas 532s) and a laser slitlamp. The modul controls the output power with a repetition rate of 3 kHz by means of an acoustoptic modulator to reach the desired target temperature within the total irradiation time of 100 ms (Figure). For safety and regulatory reasons, it can only downregulate the preset power of the treatment laser.

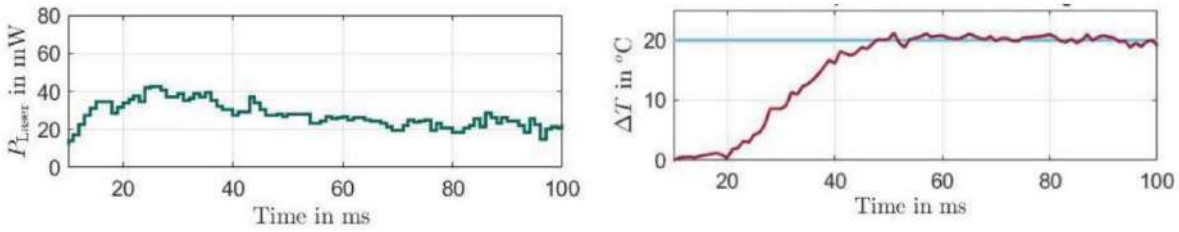

Figures: *Left side shows the power variations (here in steps of 1 ms) in order to achieve the shown temperature profile and temperature rise (right side) of 20 °C on a RPE-choroidal porcine explant in a cuvette*

Patients suffering from central serous chorioretinopathy (CSR) with subretinal fluid and a single leakage point in angiography were included in the study. Titration lesions at the arcades were performed to correlate visibility and temperature rise. Therefore target temperatures of 55 °C, with steps of 5 °C increase were applied until immediate funduscopic visibility. In all patients so far, the direct funduscopic visibility threshold was found at 65°C, in good accordance with data in rabbits [3]. For treatment six central treatment spots 200 µm in diameter were then performed around the leakage point with a target temperature of 51°C. After irradiation, color fundus photography (CFP) and optical coherence tomography (OCT) were performed to assess potential damage. So far 7 patients have been treated. The laser power during the irradiation varied between 35 and 94 mW, demonstrating the need for a dosing control system. All laser spots stayed invisible in CFP and OCT. The results and clinical outcome will be discussed in the presentation.

REFERENCES

[1] Brinkmann, R., Koinzer, S., Schlott, K., Ptaszynski, L., Bever, M., Baade, A., Luft, S., Miura, Y., Roider, J., and Birngruber, R., Real-time temperature determination during retinal photocoagulation on patients, *J of Biomed Optics* 22(11), 118001–1–11, 2012.
[2] Herzog, C., Thomsen, O., Schmarbeck, B., Siebert, M., and Brinkmann, R., "Temperature-controlled laser therapy of the retina via robust adaptive H1-control," at-*Automatisierungstechnik* 66(12), 1051–1063, 2018.
[3] Baade, A., von der Burchard, C., Lawin, M., Koinzer, S., Schmarbeck, B., Schlott, K., Miura, Y., Roider, J. Birngruber, R., and Brinkmann, R., "Power-controlled temperature guided retinal laser therapy," *J of Biomedical Optics* 22(11), 118001–1–11, 2017.

Advanced Approaches to Optical Imaging Data Processing

Viktor DREMIN[1,2]

[1]*Research & Development Center of Biomedical Photonics, Orel State University, Russia*
[2]*College of Engineering and Physical Sciences, Aston University, UK*

viktor.dremin@bmecenter.ru

ABSTRACT

The development of optical imaging methods is inextricably linked with the development of new image processing methods. Image analysis is a powerful tool in biology and medicine to collect qualitative and quantitative information in time and space. Because different optical imaging techniques can easily produce gigabytes of research data, accurate and automated analysis methods are the key to the successful interpretation of the information registered. Also, some methods, such as hyperspectral imaging (HSI), contain hundreds of spectral bands, and these data cannot be analysed by visual inspection, instead special algorithms must be developed to extract meaningful information from images. Other methods relate to the registration of dynamic processes, and time-frequency analysis of such signals can provide valuable additional information.

An artificial neural network (ANN) approach for analysing HSI data and continuous wavelet transform (CWT) for decomposing laser speckle contrast imaging (LSCI) signals will be presented here.

A compact, hand-held hyperspectral imaging system utilizing ANN-based processing for the reconstruction of 2D maps of blood volume fraction and skin blood oxygenation in the skin was developed [1]. For the training of ANN, the diffuse reflectance spectra of the skin for all possible combinations of the considered parameters were simulated by GPU-accelerated Monte Carlo technique. Examples of the system and algorithm capabilities are shown in Fig. 1. The developed approach was tested in clinical conditions and showed high sensitivity in detecting vascular complications of diabetes mellitus [2].

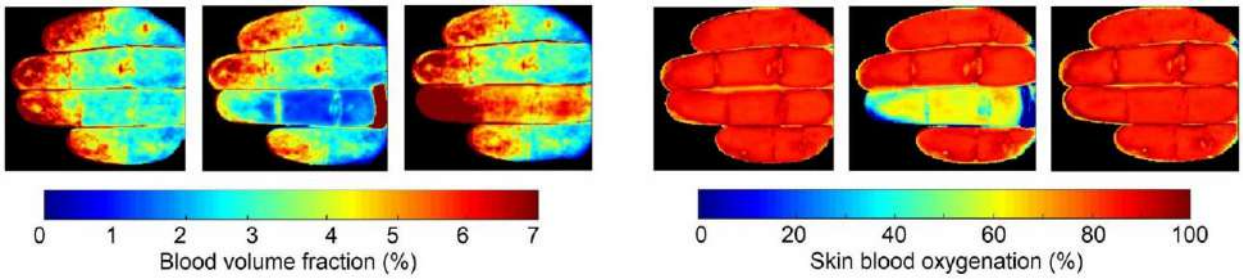

Figure 1: *Retrieved maps of blood volume fraction and skin blood oxygenation before, during, and 1 min after finger occlusion test.*

CWT expands the capabilities of the existing dynamic light scattering methods and can provide spatial mapping of blood flow oscillations (cardiac, respiratory, myogenic, etc.) [3]. Fig. 2 shows the application of LSCI for mapping the cerebral vessels of a laboratory animal, and presents the time-frequency processing of the registered signals. The proposed technology makes it possible not only to measure the relative cerebral blood flow of the cerebral cortex, but also to expand diagnostic capabilities for detailed analysis of the physiological mechanisms of changes in cerebral blood flow.

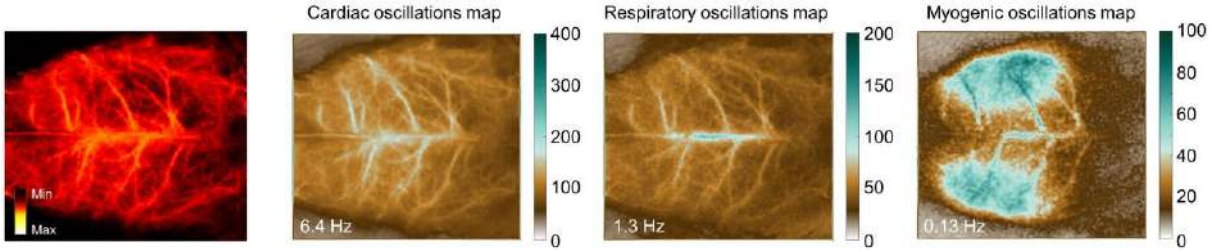

Figure 2: *LSCI image of the rat brain obtained transcranially and spatial variations in cardiac (6.4 Hz), respiratory (1.3 Hz), and myogenic (0.13 Hz) activity.*

REFERENCES

[1] E. Zherebtsov et al, Biomed. Opt. Express 10(7), 3545–3559, 2019.
[2] V. Dremin et al, IEEE Trans. Med. Imaging 40(4), 1207–1216, 2021.
[3] N. Golubova et al, Biomed. Signal Process. Control 85, 104969, 2023.

AI-Based approaches for cardiovascular diagnosis and tumor margin delineation

Olga M. CONDE[1,2,3], José A. GUTIERREZ[1,2], Verónica MIEITES[1,2], Arturo PARDO[1], Eusebio REAL[1], and José M. LOPEZ-HIGUERA[1,2,3]

[1]*Photonics Engineering Group, University of Cantabria, Spain*
[2]*IDIVAL - Valdecilla Biomedical Research Institute, Spain*
[3]*CIBER-BBN – Instituto de Salud Carlos III, Spain*

olga.conde@unican.es

ABSTRACT

Optical imaging technologies such as Hyperspectral Imaging (HSI) or Optical Coherence Tomography (OCT), both in their intensity or polarization modalities, allow to assessment of tissue composition and morphology both for non-invasive diagnosis and for tissue development, degradation, and improvement under the application of specific therapeutic treatments. Understanding the physics of light-tissue interaction mechanisms helps to obtain accurate optical properties (absorption and scattering coefficients, birefringence, anisotropy, etc.) that can be used for diagnosis. In general, and due to the heterogeneity of tissues, this problem is affected by a multiparametric scenario that cannot be addressed by deterministic or empirical approaches.

In this sense, within the workflow that guides the processing and analysis path from optical measurements to automated diagnosis (Figure 1), AI-based technologies are applied at different stages: (1) directly on raw optical measurements to provide signal denoising or feature extraction capabilities [1]-[3]; (2) to estimate tissue optical parameters from optical measurements [4], [5], or also (3) to provide discrimination and classification of tissue pathologies both, from raw measurements [6], [7] or from optical properties mapping [8]. Also, combination of different optical modalities or different AI-based approaches [9], [10] allows to reduce the problems related to classification uncertainty. The talk will describe the strategies attempted and the results obtained when applied to different biomedical fields.

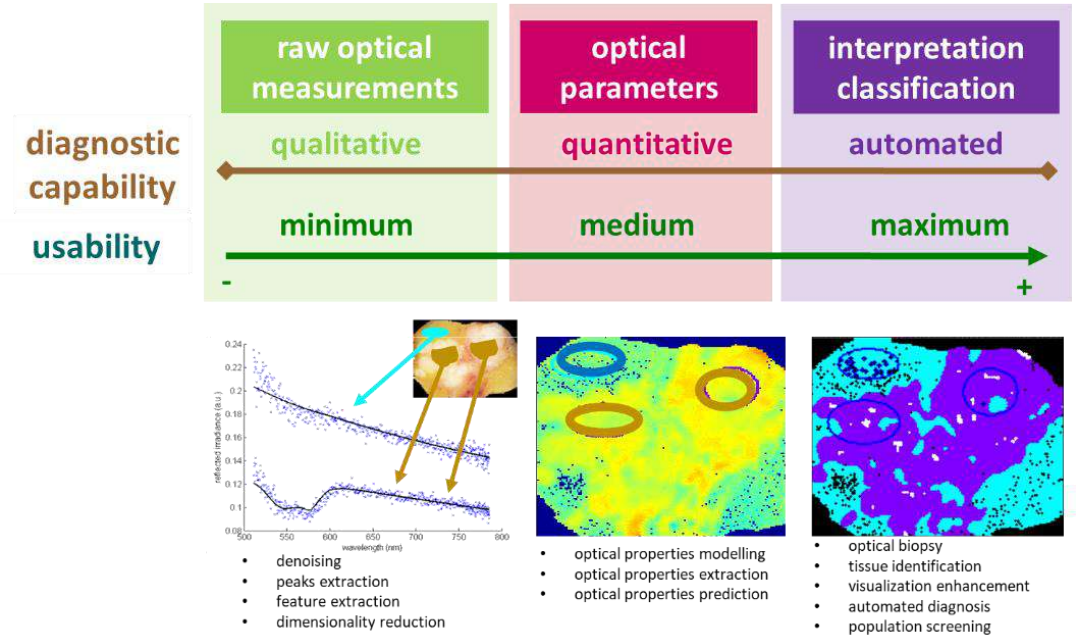

Figure 1: *Scenarios of AI-based approaches intended for tissue diagnosis.*

REFERENCES

[1] E. Real et al, Biomed. Opt. Express 5, 4089-4100, 2014.
[2] A. Eguizabal et al, Biomed. Opt. Express 4, 1104-1118, 2013.
[3] A. Pardo et al, Biomed. Opt. Express 11, 133-148, 2020.
[4] A. Pardo et al, IEEE Trans Med Imaging 40, 1687-1701, 2021.
[5] A. Eguizabal et al, ECBO, 2013.
[6] A. Pardo et al, IEEE Transactions on Medical Imaging 36, 64-73, 2017.
[7] P.B. Garcia-Allende et al, Biomed Opt. 14, 034034, 2009.
[8] P.B. Garcia-Allende et al, Proceedings of SPIE-OSA 7368, 7368_1C, 2009.
[9] P.B. García Allende et al, Proceedings of SPIE 7715, 77151B, 2010.
[10] A. Pardo et al, Proceeding of SPIE 11253, 112530K, 2020.

Biotissue-mimicking phantoms as an enabling technology in Biophotonics research

Alexey Popov

VTT Technical Research Centre of Finland

alexey.popov@vtt.fi

ABSTRACT

The field of Biophotonics focuses on studying light interaction with biological matter on different levels, starting from molecular through cellular up to the organism, both *in vivo* and *in vitro*. In addition to purely research interest, it has a practical aim to develop new methods, theoretical and experimental models and technologies for diagnostics and therapy and to improve existing ones, with the ultimate goal of translating the research from laboratory to clinical settings.

During this development, it is essential to test validity of the models, methods and instrument prototypes. However, real-time testing on humans is laborious, time-consuming, costly and can even raise ethical concerns (e.g. due to difficulty of inclusion a variety of individual features). Moreover, properties of living organisms and their body parts deviate over time, becoming an essential drawback in the case of R&D. Along with this, controlled change of different parameters of the body *in vivo* upon request is hardly possible. Accuracy of measurements due to different skin types, motion artefacts, improper mechanical contact with body, low sensitivity or concentration of target analytes, to name a few, contribute to the set of challenges.

This calls for development of stable physical models of target organs and biotissues (called 'phantoms') with controlled properties. In other domains of science and research 'phantoms' are called calibration samples, simulators, decoys, alternatives, substitutes, surrogates, models, equivalents, replicas, and artificial/synthetics objects. In everyday life, a commonly used term is 'fake objects'. Examples of such objects are plastic indoor plants, shop human dummies, dolls, swimming pools, 'fake food' in Japan, digital twins, even a Finnish sauna. All these objects feature some properties the most important in the relevant context.

In the case of Biophotonics research, these properties are optical (wavelength-dependent scattering and absorption coefficients, scattering anisotropy factor, refractive index) and geometrical (shape, size) but mechanical also play an important role. Microfluidics and liquid optical and rheological properties in case of perfusion phantoms are essential to account for as well.

This paper provides a (non-exhaustive) overview of phantoms, fabrication procedures and materials used in the phantom development for development of such technologies as diffuse optical tomography, hyperspectral imaging, optical coherence tomography, fluorescent imaging, photoacoustic imaging.

(a) (b) (c)

Figure 1: *Phantoms of (a) a hand, (b) brain and (c) female breasts.*

REFERENCES

[1] L. Hacker et al, Nat. Biomed. Eng. 6, 541-558, 2022.
[2] S. Schädel-Ebner et al, J. Biomed. Opt. 27, 074702, 2022.
[3] A.K. Dabrowska et al, Skin Res. Technol. 22, 3-14, 2016.
[4] J. Hwang et al, Biomed. Opt. Express, 3, 1399-1403, 2012.
[5] B. Pogue and M. Patterson, J. Biomed. Opt. 11, 041102, 2006.

The quest for novel endogenous fluorophores in the human organism

Evgeny SHIRSHIN[1], Boris YAKIMOV[1]

[1]*Department of Physics, M.V. Lomonosov Moscow State University, Russia*

eshirshin@gmail.com

ABSTRACT

Possessing a number of fundamental advantages, optical methods are widely used in the study of living systems. Using the methods of optical spectroscopy and microscopy, intermolecular interactions, processes in cells and biological tissues are studied, and various sensory systems are created. At the same time, the use of optical diagnostics in solving problems in clinical practice is difficult for two reasons. First, the depth of optical probing of biological tissues is relatively small and varies from tenths to several millimeters, in exceptional cases reaching several centimeters. However, this factor is not limiting in solving a wide range of problems: studies of intermolecular interactions and structural dynamics of molecules in solutions, analysis of biofluids, intraoperative diagnostics, non-invasive diagnostics of a number of physiological parameters.

Secondly, the use of external (exogenous) labels, which are often used in scientific research to increase the sensitivity and specificity of optical methods, is difficult when measured on humans in vivo and, moreover, can affect the process under study, despite the fact that it is the creation of new types labels led to a breakthrough in the study of living systems using optics. Thus, the use of endogenous contrast, an optical signal from molecules and systems of molecules already present in the sample (cell, biofluid, tissue), is of interest.

Despite the fact that the optics of biomolecules, cells, and tissues has been the subject of many years of research, a paradox attracts attention: in the literature, a list of only about ten molecules is considered as endogenous chromophores and fluorophores in the human body. At the same time, each “classical” fluorophore or chromophore molecule has its own niche of applications in biomedicine. Thus, the optical response of hemoglobin is used in wearable devices, cancer diagnostics, and neuroimaging. Using the fluorescence signal of the NADH (nicotinamide adenine dinucleotide) molecule, optical metabolic imaging was built, which is used in personalized oncology for the selection of chemotherapy.

The discovery of new endogenous fluorophore molecules in the body and the study of their photophysical properties is the central task of biomedical photonics. Here we present the machine-learning based model capable of predicting optical properties of molecules from its structure. The model is applied to the human metabolome data aimed at discovering novel endogenous fluorophores prospective for biomedical diagnostics.

Partial Mueller Polarimetry: an Avenue for *In Vivo* Tissue Diagnosis

Tatiana NOVIKOVA[1], Jessica RAMELLA-ROMAN[2,3]

[1]*LPICM, CNRS, Ecole polytechnique, IP Paris, France*
[2]*Department of Biomedical Engineering, College of Engineering and Computing, Florida International University, Miami, USA*
[3]*Department of Ophthalmology, Herbert Wertheim College of Medicine, Florida International University, Miami, USA*

tatiana.novikova@polytechnique.edu

ABSTRACT

Complete Mueller polarimetry has already shown its potential for biomedical applications, e.g. early detection of cancer, digital histology, etc. [1]. The most common approach consists of performing at least 16 measurements to get all elements of Mueller matrix of a sample and then applying a non-linear algorithm of data compression for the physical interpretation of tissue optical properties. However, the completeness of this approach comes along with the polarimetric instrument complexity and does not allow the video-rate acquisition that is often required in clinical settings.

We present the theoretical framework and experimental studies on calculating the diagnostic polarimetric parameters (linear retardance, orientation of optical axis and linear depolarization) for optical phantoms and biological tissues using only first three rows of Mueller matrix [2] and validate the results versus the corresponding parameters obtained from the Lu-Chipman decomposition [3] of the complete Mueller matrices .

We showed that when a sample is measured at near-normal incidence either in transmission or in reflection configuration, its depolarization and birefringence properties can be calculated from the partial 3 x 4 Mueller matrix with the same accuracy as from the complete Mueller matrix. When the linear depolarization of a sample is anisotropic (i. e. its value varies with the rotation of the polarization plane) one should account for this effect in order to get the correct value of the orientation angle of the optical axis (see Fig.1). In case of the isotropic linear depolarization one can measure 4 elements of the last column of Mueller matrix with left- and right-circularly polarized probing light beam and calculate the exact value of the azimuth of the optical axis of uniaxial linear birefringent medium (an equivalent of the angle of polarization in Stokes polarimetry) as well as the product of linear depolarization and sine of scalar linear retardance (an equivalent of the degree of polarization in Stokes polarimetry).

With the advent of polarization sensitive cameras our findings open an avenue for the development of simple and compact imaging partial Mueller polarimetric systems that can operate at video rate and provide the required accuracy for tissue monitoring and diagnosis in clinical settings.

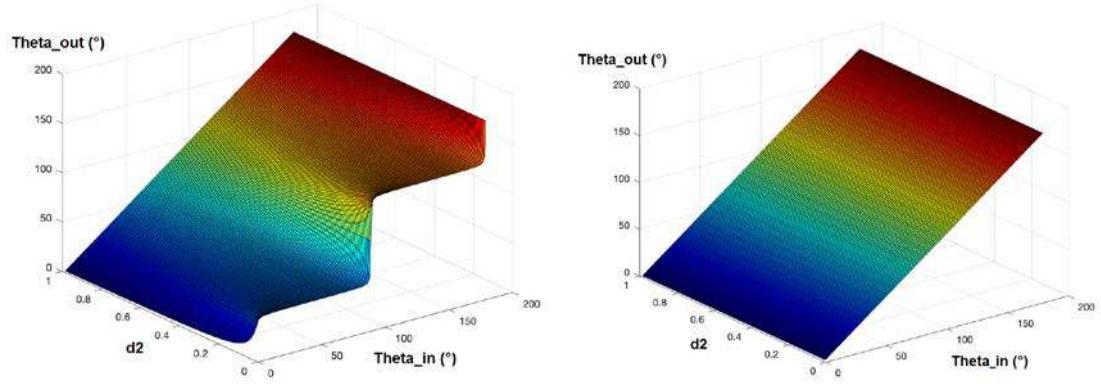

(a) (b)

Figures: *Reconstructed values of the orientation of the optical axis of linear retarder from the 3 x 4 Mueller matrix of optical phantom representing the linear diattenuator, linear retarder and canonical depolarizer (linear depolarization coefficients $d_1 = 0.99$, $0.01 < d_2 < 0.99$, the anisotropy of linear depolarization ($d_1 \neq d_2$)): (a) is neglected (b) is taken into account*

REFERENCES

[1] M. D. Singh, N. Ghosh, and A. Vitkin "Mueller Matrix Polarimetry in Biomedicine: Enabling Technology, Biomedical Applications, and Future Prospects" in *Polarized Light in Biomedical Imaging and Sensing*, J. C. Ramella-Roman, T. Novikova (Eds), Springer, Cham (2023).

[2] T. Novikova, J. C. Ramella-Roman "Is a complete Mueller matrix necessary in biomedical imaging?" Opt. Lett. 47(21) 5549-5552 (2022).

[3] S.-Y. Lu and R. A. Chipman, "Interpretation of Mueller matrices based on polar decomposition," J. Opt. Soc. Am. A 13(5), 1106–1113 (1996).

Quantitative Blood Flowmetry Imaging Using Laser Speckle and High-Density Optical Flow Tracing

Jiachi HONG[1], Liangwei MENG[1], Jinling LU[1] and Pengcheng LI[1,2*]

[1] *Britton Chance Center for Biomedical Photonics and MoE Key Laboratory for Biomedical Photonics, Wuhan National Laboratory for Optoelectronics, Huazhong University of Science and Technology, China*
[2] *Department of Biomedical Engineering, Hainan University, China*

pengchengli@mail.hust.edu.cn

ABSTRACT

Quantitative measurements of microvascular blood flow velocity are critical for the diagnosis and therapy of microvascular dysfunction. As a non-contact wide-field imaging technique for mapping the blood flow, laser speckle techniques are attracting increasing attempts to explore their potential in the clinical applications. However, several challenges affect the accuracy of laser speckle detection of blood flow, such as coherence loss and noise associated with the imaging system, the form of the auto-correlation function of the electric field related to the optical properties of biological tissue, non-ergodic components associated with static scattering, and finite statistical sample size. To improve the quantitative measurement of blood flow speed using speckle and improve the robust of the measurement in the practical clinic conditions. The influence of the statistical sample size on the mean of the speckle contrast was deduced by the probabilistic and statistical methods [1]. A method for unbiased estimation of flow velocity in the range of 0.1~30 mm/s was proposed [2]. The influence of the properties of biological tissue and the imaging system on laser speckle auto-inverse covariance was discussed. The quantitative laser speckle auto-inverse covariance model for imaging blood flow velocity was established and validated in phantom and animal experiments [3]. Moreover, since multiple speckle images are usually required to reconstruct a high-resolution and high SNR blood flow map, LSCI is highly sensitive to the motion artifacts. The blood flow perfusion obtained by LSCI during tissue motion is a mixture of the artifacts due to inter-frame im-age misalignment and intra-frame image blurring. It is of urgent importance to minimize the impact of motion when LSCI is put into practical use. Previous studies have mainly focused on correcting either the inter-frame or intra-frame arti-fact of global rigid motion. However, in practical biomedical applications, owing to the flexibility of biological tissues, the subjects often produce many non-rigid, spatially non-uniform movements. We proposed a dual-wavelength imaging system to solve the problem that laser speckle images with graininess are difficult to be directly registered[4]. To further address the problem of overestimation of blood flow due to non-rigid tissue motion during the exposure of a single frame, we proposed a method that combines the strategy of heterogeneous regression analysis with the above dual-wavelength imaging, enabling the extraction of the true blood flow signal from the measured mixture LSCI signal. Optical flow analysis allows for the quantitative imaging of absolute blood flow velocity with high spatial resolution by using the variation in pixel brightness between consecutive frames to trace the motion of red blood cells. However, traditional optical flow algorithm usually suffers from a strong noise in background tissue and significant underestimation of blood flow speed in blood vessels, due to the errors in detecting the feature points of optical images. Here, we proposed a temporal direction filtering and peaks interpolation optical flow method (TPIOF) to suppress the background noise and improve the accuracy of blood flow velocity estimation.

REFERENCES [HEADING 1 STYLE]

[1] J. Hong et al, Opt. Lett., 43(21): 5214-5217, 2018
[2] J. Hong et al, Opt. Lett., 44(23):5812-5815, 2019
[3] J. Hong et al, Opt. Lett., 46(10): 2505-2508, 2021
[4] X. Liu et al, Opt. Lasers Eng., 140:06526, 2021

Towards OCT on a chip

Wolfgang DREXLER[1], OCTChip consortium, HandheldOCT consortium

[1]*Center for Medical Physics and Biomedicla Engineering, Medical University Vienna, Austria*

Wolfgang.Drexler@meduniwie.ac.at

ABSTRACT

Optical coherence tomography (OCT) is an extremely successful non-invasive interferometric imaging technique. Thanks to the use of coherence gating for axial feature resolution, OCT does not rely on the use of tightly focused beams and is able to deliver tomograms with good lateral (10-15 µm) as well as axial (1-10 µm) resolution in a depth range of 1-2mm. Recently there has been a strong need for cost-effective OCT systems enabling point-of-care screening. Current technology does not allow the required advancements of OCT for their widespread use. Silicon nitride waveguide based photonic integrated circuit (PIC) technology and suitable packaging methods will enable realization of reliable low-cost and miniaturized OCT systems.

Progress in the field of photonic methods and techniques for health and life sciences are expected to significantly contribute to solve main socio-economic challenges of our time. The required disruptive innovations will, to a large extent, be triggered by the emergence of new fabrication technologies. For a widespread adoption in point-of-care screening an OCT system in developed and emerging markets should have a target price in the range of 15-25k€, > 3x cheaper than momentary OCT systems. Further prerequisites are a small footprint, ease-of-use, and high reliability making the system virtually maintenance-free - maintaining necessary diagnostic imaging performance (>4x faster). First accomplishments in PIC based 1300nm dermatologic OCT and 800 nm as well as 1060nm ophthalmic OCT on a chip systems will be presented.

A toolbox for personalized plasmonic photothermal cancer therapy

Clara VILCHES[1]

[1]*Medical Optics, Institut de Ciències Fotòniques ICFO, Spain*

clara.vilches@icfo.eu

ABSTRACT

Plasmonic photothermal therapy (PPTT) has emerged as a complementary technique for the treatment of malignant solid tumors. It involves the use of gold nanoparticles that can efficiently convert light into heat inducing cell death around where the nanoparticles are concentrated, eventually reducing tumor volume or impairing its further growth. However, and as most other cancer therapies, the broad tumour and patient heterogeneity affects treatment outcomes, varying between individuals even under the same regime. This has greatly compromised PPTT development and hindered its clinical use. Hence, there is a need of methods that allow for personalization and optimization of therapy based on individual's physiology.

In PPTT, the dose of nanoparticles injected and the amount of light delivered are parameters that can be adjusted to personalize the treatment and improve its efficacy. In this talk, I will present our multimodal platform that provides an integrative approach for plasmonic photothermal therapy in pre-clinical mouse models of renal and breast cancer, as it allows the *in vivo* and *ex vivo* study of all variables involved in PPTT and their potential role in outcome. We have shown how diffuse optical techniques, namely diffuse correlation spectroscopy and diffuse reflectance spectroscopy, can be used to non-invasively gather physiological properties and hemodynamics of the tumor –as blood flow, water content, tissue oxygenation and nanoparticle concentration, and relate the optical and hemodynamic parameters to the crucial variables in PPTT, as nanoparticle and light dosages. The platform also includes a set of tools to extend the knowledge on PPTT and its underlying molecular mechanisms. Furthermore, experimental data has been used in simulations using light transport and heat diffusion equations to design personalized protocols to optimize PPTT treatment. Altogether, our platform offers a comprehensive toolbox that will pave the way to PPTT optimization and personalization, ultimately bringing this therapy closer to clinics.

Nonlinear distortion operator for coherent imaging in tissues using second harmonic and third harmonic nonlinear holography

Randy Bartels[1], Gabe Murray[2], Yusef Farah[1], Olivier Pinaud[4]

[1]*Morgridge Institute for Research and Biomedical Engineering at the University of Wisconsin, Madison, USA*
[2]*Department of Physics, Colorado State University, USA*
[3]*Department of Electrical and Computer Engineering, Colorado State University, USA*
[4]*Department of Mathematics, Colorado State University, USA*

rbartels@morgridge.org

ABSTRACT

Non-invasive imaging with high resolution deep within biological materials without the use of harmful ionizing radiation is of great interest in the field of medical imaging. Second- and third- harmonic generation are excellent mechanisms to circumvent this issue by providing outstanding contrast and optical sectioning [1]. In general, these signals are weak and prone to scattering which introduce great challenges when imaging deep within turbid media. We will discuss recently demonstrated nonlinear distortion, which can detect very weak backscattered SHG optical fields in a widefield holography configuration, from which distortion from aberrations and scattering can be estimated and corrected. This approach uses field phase information to allow diffraction limited imaging within deep tissue.

REFERENCES

[1] P. J. Campagnola and C.-Y. Dong, Laser & Photonics Reviews 5, 13–26 (2011).
[2] D. R. Smith, D. G. Winters, and R. A. Bartels, Proceedings of the National Academy of Sciences 110, 18391 (2013).
[3] C. Hu, J. J. Field, V. Kelkar, B. Chiang, K. Wernsing, K. C. Toussaint, R. A. Bartels, and G. Popescu, Nature Photonics 14, 564–569 (2020).
[4] G. Murray, J. Field, M. Xiu, Y. Farah, L Wang, O. Pinaud, and R.A. Bartels, arXiv preprint arXiv:2305.12012 (2023).

Multimodal optical spectroscopy for human skin cancer *in vivo* diagnosis

Walter BLONDEL[1], Valentin KUPRIYANOV[1,2], Christian DAUL[1], Grégoire KHAIRALLAH[1,3], Yuri KISTENEV[2,4] and Marine AMOUROUX[1]

[1]*Université de Lorraine, CNRS, CRAN UMR 7039, Nancy, France*
[2]*Laboratory of Laser Molecular Imaging and Machine Learning, Tomsk State University, Tomsk, Russia*
[3]*Department of plastic, aesthetic and reconstructive surgery, Regional Hospital Metz-Thionville, France*
[4]*Laboratory for Remote Sensing of the Environment, V.E. Zuev Institute of Atmospheric Optics SB RAS, Tomsk, Russia*

walter.blondel@univ-lorraine.fr

ABSTRACT

The present contribution concerns the investigation of multimodal tissue spectroscopy as an *in vivo* optical biopsy method combining several complementary techniques for the non-invasive characterization and analysis of human skin conditions applied to skin cancer diagnosis and more specifically to carcinoma surgical margin delineation guiding.

First, the main technical features of the *Spectrolive* spatially-resolved bimodal spectroscopy medical device developed [1,2] will be described including a four source-detector separation multiple optic fiber probe (D_1=400µm, D_2=600µm, D_3=800µm and D_4=1mm), a diffuse reflectance spectroscopy modality in the [340-785]nm range and an autofluorescence spectroscopy modality allowing to collect sequentially five autofluorescence emission spectra at five excitation peaks (365, 385, 395, 405 and 415nm), respectively. These features are to be linked to known skin carcinogenesis modulation factors targeted such as epidermis hyperplasia, collagen enzymatic degradation, overactive cell metabolism, cell pleomorphism, neovascularization etc. [3].

Second, the clinical protocol involving 140 patients with skin carcinomas will be presented, including the spectroscopic acquisition methodology, the histological classification of all the excised samples and the final data base built from all the data collected [4].

The third part of this presentation will be dedicated to the exploitation of the multidimensional spectroscopic data set collected, in order to build efficient Machine Learning-based models for automatic supervised classification. Several methods and combinations of methods were tested such as principal component analysis, non-negative matrix factorization, support vector machine, linear discriminant analysis, multilayer perceptron and random forest classifiers. In order to optimize the combination of the results of analysis provided by each of the modalities, data fusion methods (stacking, begging, boosting, majority voting) were also implemented [5].

Finally, the confusion matrices resulting from multi-class classification of cancerous, precancerous and healthy states of human skin, based on the spatially resolved autofluorescence and diffuse reflectance spectra obtained *in vivo* will be presented as well as a comparison of the performance of the aforementioned machine learning and data fusion methods.

ACKNOWLEDGEMENTS

The research was carried out with the financial support of the French embassy in Russia under a Vernadski international joint PhD grant (2021-2024) completed by the Université de Lorraine. Authors also acknowledge the financial support from the Government of the Russian Federation under the Decree No. 220 of 09 April 2010 (Agreement No. 075-15-2021-615 of 04 June 2021) and the French National Research Agency (ANR) under the grant ANR-21-CE19-0056 for the Spec-LCOCT project and the PhotoVivo platform, a member of France Life Imaging network, by CPER IT2MP (Contrat Plan Etat Région «Innovations Technologiques, Modélisation et Médecine Personnalisée»), the Ligue Contre le Cancer and the FEDER (Fonds Européen de Développement Régional).

REFERENCES

[1] W. Blondel et al, Br. J. Cancer 74, 1302–1307, 1996.
[2] M. Amouroux et al, World patent WO2017093316 (A1), filed November 30th 2015, and issued June 8th 2017.
[3] E. Borisova et al, IEEE J. of Select. Topics in Quantum Electronics, 20(2), 211-222, 2013.
[4] T. Elsen et al, SpectroLive Database, DOREL repository, Université de Lorraine, July 10, 2023. https://doi.org/10.12763/EYVX3P
[5] V. Kupriyanov et al, J. Biophotonics, e2023000, 2023.

Photobiomodulation improves restoration of functions of the meningeal lymphatics: the perspectives for therapy of Alzheimer's disease

Dubrovsky Alexander[1], Fedosov Ivan[1], Shirokov Alexander[2,3], Blokhina Inna[2], Terskov Andrey[2], Tsoy Maria[1], Zlatogosrskaya Daria[2], Adushkina Viktoria[2], Telnova Valeria[2], Tzven Anna[2], Krupnova Valeria[2], Manzhaeva Maria[2], Dmitrenko Alexander[2], Evsukova Arina[2], Semyachkina-Glushkovskaya Oxana[2,4]

[1]*Institute of Physics, Saratov State University, Russia*
[2]*Department of Biology, Saratov State University, Russia*
[3]*Institute of Biochemistry and Physiology of Plants and Microorganisms, Russian Academy of Sciences, Russia*
[4]*Institute of Physics, Humboldt University, Germany*

paskalkamal@mail.ru

ABSTRACT

Photobiomodulation (PBM) is a perspective non-pharmacological approach for Alzheimer's disease (AD) treatment. Since the mechanisms and the effects of PBM are not fully explored, we investigate its effect on the clearance of fluorescent beta-amyloid (FAβ) from the ventricular system of the brain in mice as well as on the restoration of clearing function of the meningeal lymphatics vessels (MLVs) after photo-ablation.

Male mice (25-28 g, 3 months age) were used in all experiments. The photo-ablation of MLVs in each mouse was achieved with 5 μL injections of 5-aminolevulinic acid (5-ALA) excited 15 minutes afterwards by a 635 nm laser (15 J/cm^2). The cisterna magna, the left and right transverse sinuses, the superior sagittal sinus, and the junction of all sinuses were subjected to laser irradiation. 7 days after photo-injury of MLVs, The PBM was performed daily with an LED (central wavelength 1050 nm) for 1 week. 1 μL of FAβ at a final concentration of 1 μg was injected into the hippocampus of the mice on the 4th day for further study of PBM effects. The cumulative dose of 7-day PBM therapy was 3.5 kJ/cm^2. The confocal images of full brain samples and brain slices of mice for further quantitative analysis were obtained using a confocal laser scanning microscope (Nikon A1R MP, Nikon Instruments Inc., Tokyo, Japan). We analyzed distribution of FAβ in the mouse brain samples in the five groups: 1) 5-ALA injection only; 2) 635 nm laser irradiation only; 3) 5-ALA + 635 nm laser irradiation; 4) PBM treatment during wakefulnessl; 5) PBM treatment during sleep.

Photo-ablation of MLVs negatively affected the FAβ drainage from the hippocampus. Indeed, the FAβ fluorescence in the hippocampus was higher in mice with the damaged MLVs compared to the control groups "5-ALA only" and "Laser only", i.e. removal of FAβ was suppressed in mice after photo-injury of MLVs. The 7 days-course of PBM had a positive effect on clearance of FAβ that was more pronounced in the "PBM during sleep" vs. "PBM during wakefulness", based on relative FAβ fluorescence intensity.

In this pilot study, we demonstrate that the brain lymphatic functions after the MLVs injury can be improved with the PBM treatment. We also show that PBM during sleep has a better restorative effect in comparison with PBM during wakefulness. Our results provide more insight into the field of PBM, as well as demonstrate the PBM stimulation of the brain lymphatic drainage that transports FAβ via the lymphatic pathway. The improved restoration of the brain lymphatics after PBM during sleep opens a new niche in the studies sleep functions and AD therapy technologies. PBM as a non-invasive and safe approach has the high prospects for implementation in clinical practice for the treatment of brain diseases associated with lymphatic disorders.

This study was supported by grant (No. 23-75-30001) (No. 21-75-10088) from the Russian Science Foundation and by Grant from the Russian Ministry of Science and High Education (No. 075-15-2022-1094).

Progress towards improved sensitivity and specificity of detection of early-stage bladder cancer

Audrey BOWDEN[1], Shuang CHANG[1], Haoli YIN[2], Greyson WINTERGERST[2], Soheil KOLOURI[2], Giovanna GIANNICO[3] and Sam CHANG[4]

[1]*Department of Biomedical Engineering, Vanderbilt University, USA*
[2]*Department of Computer Science, Vanderbilt University, USA*
[3]*Department of Pathology, Vanderbilt University Medical Center, USA*
[4]*Department of Urology, Vanderbilt University Medical Center, USA*

a.bowden@vanderbilt.edu

ABSTRACT

Bladder cancer (BC) — the 4th most common cancer in men and the most expensive cancer to treat over a patient's lifetime — is a lifelong burden to BC patients and a significant economic burden to the U.S. healthcare system [1,2]. The high cost of BC stems largely from its high recurrence rate (>50%); hence, BC management involves frequent surveillance. Unfortunately, the current in-office standard-of-care tool for BC surveillance, white light cystoscopy (WLC), is limited by low sensitivity and specificity for carcinoma in situ (CIS), a high-grade carcinoma with high potential to metastasize. Early detection and complete eradication of CIS are critical to improve treatment outcomes and to minimize recurrence. The most promising macroscopic technique to improve sensitivity to CIS detection, blue light cystoscopy (BLC), is costly, time-intensive, has low availability and has a high false-positive rate. Given the limitations of WLC, we aim to change the paradigm around how BC surveillance is performed by validating new tools with high sensitivity and specificity for CIS that are appropriate for in-office use.

We have introduced several new tools to improve mapping of the bladder for longitudinal tracking of suspicious lesions and to perform in-office surveillance with improved sensitivity and specificity over the standard of care. To improve the sensitivity of detection, we have developed a new strategy for image-to-image translation of white light cystoscopy into blue light cystoscopy images. This technology can reduce the cost, time and administrative burden of current BLC systems, increasing availability for use in the clinic. To improve the specificity of detection, we introduce multiparametric interference-based polarization-enhanced imaging (Multi-PIPE) as a strategy to identify biomarkers of early-stage bladder cancer that are distinct from its visually confounding relative, inflammation.

Our results suggest that we are able to: 1) successfully create large-area maps of the bladder from cystoscopy videos **(Fig. 1a)**, 2) successfully perform image-to-image translation of white light cystoscopy videos into blue-light look-alikes with high correlation with ground truth images **(Fig. 1b,c)**; 3) use Multi-PIPE parameters to differentiate CIS from inflammation with 18.5% improved specificity over the standard of care and a four-fold reduction in the false-positive rate **(Fig 1d)**. The success of the results represents a critical first step towards integration of these tools into clinical practice to potentially change and better inform the management of patient care.

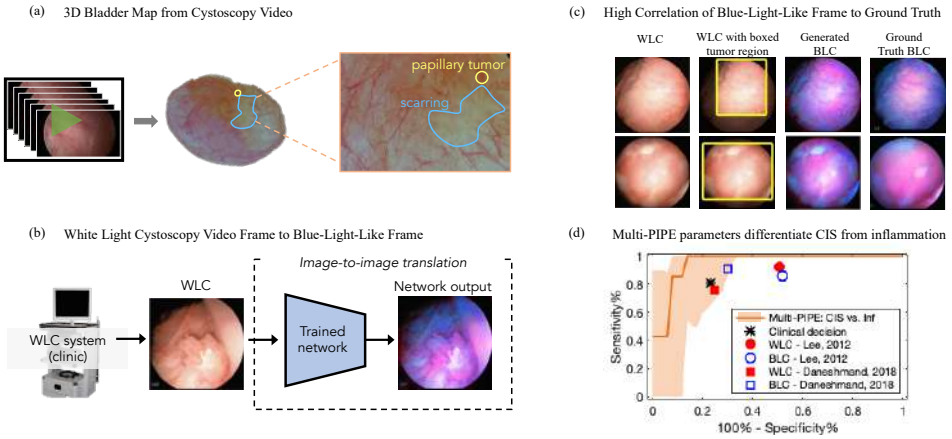

Figure 1: *(a) 3D bladder reconstruction from cystoscopy video; (b) BLC-like frames generated from WLC frames via image-to-image translation; (c) Digitally generated BLC-like frames show high correlation with ground truth; (d) Multi-PIPE parameters (orange line, shaded region shows 95% confidence interval) differentiates CIS tumors from inflammation.*

REFERENCES [HEADING 1 STYLE]

[1] O. Sanli et al, Nat. Rev. Dis. Prim. 3**,** 17022, 2017.
[2] E.BC. Avritscher et al, Urology 68**,** 549–553, 2006.

Biophotonics For Stem Cell Research

Elena ZAGAYNOVA[1,2], Alexandra MELESHINA [1], Daria KUZNETSOVA[1], Svetlana RODIMOVA [1], Alena KASHIRINA[1], Polina ERMAKOVA[1], Vladimir ZAGAINOV[1,3], Vladislav SHCHESLAVSKIY [1,4]

[1]*Institute of Biomedical Technologies, Privolzhskiy Medical Research University, Russia*
[2] *Lopukhin FRCC PCM, Russia*
[3]*Nizhny Novgorod Regiona Clinicall Oncological Dispanceyr, Nizhny Novgorod, Russia*
[4] *Becker&Hickl GmbH, Germany*

ezagaynova@gmail.com

ABSTRACT

In regenerative medicine, it is necessary to solve the following problems: label free estimation of differentiation state and quality of stem cells, label-free assessment both of the organ quality before isolation of cell product and isolated cell product before transplantation, in vivo diagnose of regenerative potential of organ before cell therapy or surgery, testing 3D-models based on stem cells (spheroids, organoids) for disease phenotypes identification, stem cell niche metabolic demands and screening of new drugs. This applies to both cell therapy and tissue engineering Modern imaging methods using time-resolved fluorescence (FLIM microscopy, FLIM in vivo imaging systems) provide information on the co-factors of NADH and FAD, the ratio of their free and bound forms, which reflects the type of energetic metabolism: Glycolysis or Oxidative phosphorylation. Metabolic imaging does not require additional contrasts, which brings it closer to the clinic. Cells with changing proliferation activity are of particular interest for monitoring metabolic changes both in the process of differentiation / regeneration and in the treatment process.

Using FLIM and multiphoton fluorescence microscopy of stem cell we have made investigation of metabolic status in mesenchymal stem cell during adipogenic, osteogenic and chondrogenic differentiation, metabolic activity and intracellular pH in induced pluripotent stem cells differentiating in dermal and epidermal directions **[1]**, label-free sorting of iPS cells during neuronal differentiation, analysis of the metabolic and oxygen status of 3D neurospheres from iPSCs , energy Metabolism and Intracellular pH Alteration in Neural Spheroids Carrying Down Syndrome **[2]**, contrast-free revealing Metabolic Changes in living Pathological Islets of Langerhans **[3]**. Also we try to define new optical criteria of liver regenerative potential for intraoperative use. We have already studied the metabolic state of hepatocytes, the content of collagen in animal liver during normal regeneration and modeling of pathologies.
We found a significant correlation between the percentage of liver recovery and the contribution of the NADPH (before the induction of regeneration), as well as with an increase in the contribution of the bound form of NADH (in the early stages of liver regeneration) [4].

REFERENCES

[1]. Kashirina, A et al Cells **2022**, 11, 2730
[2]. Kashirina A et al. Biomedicines. **2021** Nov 22;9(11):1741
[3]. Ermakova, Pet al Int. J. Mol. Sci. **2022**, 23, 13728.
[4]. Rodimova S, et al. Cells. **2023**; 12(3):479.

Breath air analysis using laser IR and THz spectroscopy and machine learning

Yu.V.Kistenev[1,2], A.V.Borisov [1], D.A. Vrazhnov [1,2], V.E Skiba[1], V.V. Prischepa[1]

1- Laboratory of Biophotonics, Tomsk State University, 634050 Tomsk, Russia

2- V.E. Zuev Institute of Atmospheric Optics of Siberian Branch of the Russian Academy of Sciences, Academician Zuev Square, 1, 634055 Tomsk, Russia
email: yuk@iao.ru

The report is devoted to the discussion of the benefits of machine learning application in the development on new methods of medical diagnostics using breath air analysis by IR and THz laser spectroscopy. This problem is connected with useful experimental spectral data preprocessing, and after that, the informative features extraction and finding effective classification methods. Artificial neural networks will be demonstrated to allow conducting effective noise reduction in breath air spectra. The informative features can be associated with two ways of a breath air sample analysis: (i) the sample absorption spectrum profile, (ii) contained in the sample volatile molecular compounds concentration profile. The latter approach requires effective methods of the spectroscopy inverse problem solution when the breath air sample molecular composition is not a priori known. A choice of acceptable classification methods is defined by the ability to work well with small-volume datasets.

We will demonstrate examples of above-mentioned problems' solution.

The research was carried out with the support of a grant under the Decree of the Government of the Russian Federation No. 220 of 09 April 2010 (Agreement No. 075-15-2021-615 of 04 June 2021).

Speckle Rheological Microscopy (SHEAR) to explore tumor mechanopathology

SEEMANTINI K. NADKARNI[1]

[1]*Wellman Center for Photomedicine, Massachusetts General Hospital, Harvard Medical School, USA*
snadkarni@mgh.harvard.edu

ABSTRACT

Tumor pathogenesis is frequently associated with anomalous changes in the mechanical properties of the extracellular matrix (ECM). Biological tissues are viscoelastic, exhibiting both solid-like (elastic) and liquid-like (viscous) behaviors, under different loading conditions. The mechanical behavior of the extracellular matrix (ECM) is a powerful regulator of many oncogenic processes including proliferation, invasion, differentiation, and metastasis. Increased stiffening, due to collagen deposition drives malignant transformation of cells. Macrophage infiltration on the other hand degrades and liquidizes the ECM, resulting in 'liquid-like' stromal properties that aid cancer cells in squeezing through stromal boundaries. Thus, elastic, and viscous behaviors of the ECM co-exist and act concurrently to drive cancer metastasis. Comprehensively profiling of the mechanical landscape of cancers is therefore a crucial need.

Tissue mechanical behavior is often defined by the frequency-dependent viscoelastic modulus that is a measure of both, the elastic or solid-like behavior, and viscous energy dissipation of the sample. Speckle Rheological Microscopy (SHEAR) is a new tool that maps the frequency-dependent viscous and elastic properties of biological tissues and biomaterials from dynamic intensity fluctuations of laser speckle without applying an external force, physically contacting the specimen, or using exogenous particles (Fig. 1). This talk will provide an overview of recent advances in the SHEAR technology to access both, the viscous and elastic contributions of the tumor ECM to enable us to investigate key mechanopathological drivers of oncogenesis in patients. I will discuss results of our recent studies on breast tumors in patients to simultaneously quantify mechanical parameters that define tumor viscoelasticity and micromechanical heterogeneity, which together serve as co-conspirators in oncogenic signaling. Thus, by enabling comprehensive viscoelastic profiling, the SHEAR innovation yields new diagnostic and prognostic insights based on tumor mechanopathology to augment standard histopathologic profiling and open new avenues for advanced therapeutic strategies to target the aberrant mechanical landscape of cancer.

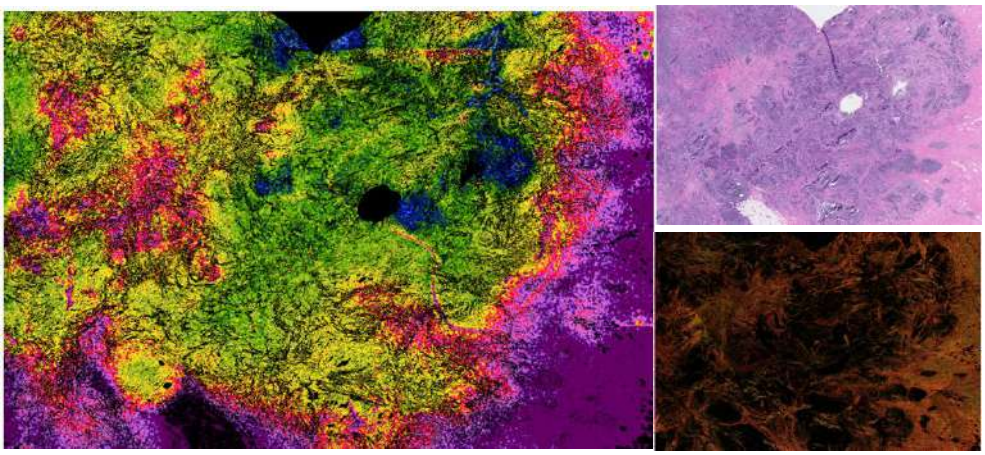

Figure 1: (L) *SHEAR map of, G*, of an invasive ductal carcinoma of the breast. The stiff tumor stroma (red to magenta to purple) in striking contrast with the soft tumor epithelium (blue to green to yellow). In breast tumors, micromechanical metrics including heterogeneity and gradients of G* measured by SHEAR are associated with histological subtype, grade, molecular expressions, and nodal status.* ***(R)*** *H&E (top) and Picrosirius Red (bottom) stained sections show the corresponding tumor histopathological features, including the presence of collagen stroma.*

New Trends in Megahertz-OCT

Sazgar Burhan[1], Madita Göb[1], Simon Lotz[1], Wolfgang Draxinger[1], Marie Klufts[1], Muhammad Asim Bashir[1], Nicolas Detrez[2], Paul Strenge[2], Sven Böttger[3], Floris Ernst[3], Linh Ha-Wissel[4,5], Jennifer Hundt[5], Berenice Schulte[6], Mark Ellrichmann[6], Awanish Pratap Singh[1], Mike Rahlves[1], Matteo Mario Bonsanto[7], Ralf Brinkmann[1,2], Robert Huber[1,2,*]

[1]*Institut für Biomedizinische Optik, Universität zu Lübeck, Peter-Monnik-Weg 4, 23562 Lübeck, Germany*
[2]*Medizinisches Laserzentrum Lübeck GmbH, Peter-Monnik-Weg 4, 23562 Lübeck, Germany*
[3]*Institut für Robotik und Kognitive Systeme, Universität zu Lübeck, Ratzeburger Allee 160, 23562 Lübeck, Germany*
[4]*Klinik für Dermatologie, Allergologie, Venerologie, Universitätsklinikum Schleswig-Holstein,*
[5]*Lübecker Institut für Experimentelle Dermatologie, Universität zu Lübeck, Ratzeburger Allee 160, 23562 Lübeck, Germany*
[6]*Klinik für Innere Medizin I, Universitätsklinikum Schleswig-Holstein, Ratzeburger Allee 160, 23562 Lübeck, Germany*
[7]*Klinik für Neurochirurgie, Universitätsklinikum Schleswig-Holstein, Ratzeburger Allee 160, 23562 Lübeck, Germany*
*robert.huber@uni-luebeck.de

ABSTRACT

Optical coherence tomography (OCT) is one of the most important techniques in biomedical optics research and is increasingly being used in various clinical applications. Current clinical OCT systems achieve imaging speeds of approximately 100,000 depth scans per second, which corresponds to frame rates of about 100 frames per second. The introduction of Fourier domain mode locking (FDML) revolutionized OCT lasers and enabled systems to achieve speeds of many million depth scans per second. This breakthrough, known as Megahertz OCT (MHz-OCT), enables imaging rates of many thousands of frames per second at high quality [1, 2].

The significant increase in imaging speed by a factor of 10 to 100 enables the acquisition of ***very large volumes*** in a short period of time, which can be particularly important in dermatological applications with large-area lesions. Furthermore, the high imaging speed allows for the acquisition of complete three-dimensional ***volumes in rapid succession*** at speeds beyond video rate. This is essential for applications where OCT is intended to be used as live feedback, such as in surgical microscopes or medical robots. The rapid acquisition of volumes is also beneficial for applications that utilize temporal changes as image contrast, such as dynamic OCT or OCT elastography. Moreover, the ability to acquire sequential volumes in quick succession with the MHz-OCT system facilitates the implementation of more efficient numerical motion correction algorithms for *in vivo* applications.

The paper discusses results of our MHz-OCT applied for elastography measurements and we present data from an ongoing clinical study using MHz-OCT in a neurosurgery operating microscope. Additionally, large-area scanning of human skin in vivo using OCT-guided robots for dermatology is presented. We describe the path to future endoscopic large area OCT. Finally, we will present our newest FDML lasers at wavelength ranges centered around 850nm and 1180nm for ophthalmic, microscopic and spectroscopic applications.

Figures: *(a) MHz-OCT elastography image, phase-based displacement map [3] (b) MHz-OCT on robot [4] (c) OCT-scan of entire hand with MHz-OCT robot [4] (d) Home built MHz-OCT in neuro surgical microscope [5] (e) Image of human brain [5]*

REFERENCES

[1] Huber et al, *Optics Express*, vol. 14, no. 8, pp. 3225 - 3237, 04 2006.
[2] Göb et al., *Biomed. Opt. Express*, vol. 13, no. 2, pp. 713--727, 02 2022
[3] Burhan et al., Proc. SPIE 12367, 123670Q (8 March 2023)
[4] Göb et al., Proc. SPIE 12367, 123670C (8 March 2023)
[5] Draxinger et al., Proc. SPIE 12390, 123900D (16 March 2023)

Funding. The presented results have been generated in projects funded by the German Research Foundation (EXC 2167-390884018), the German Federal Ministry of Education and Research (BMBF no. 13GW0227B: “Neuro-OCT”, 13N14663, “UltraLas”), the European Union H2020 Marie Curie-Innovative Training Network, H2020-MSCA-ITN-2019, 860807 “NETLAS” and the State of Schleswig-Holstein, Germany (Excellence Chair Program by the universities of Kiel and Luebeck).

Progress on assessment of retinal physiology with light.

Robert ZAWADZKI[1,2,3], Pengfei ZHANG[4], Sarah KARLEN[5], Ewelina PIJEWSKA[1,3], Ratheesh MELEPPAT[1,2] , Ravi JONNAL[2,3]and Edward PUGH JR.[1,2,5]

[1] *UC Davis Eye-Pod Small Animal Ocular Imaging Laboratory, Department of Cell Biology and Human Anatomy, University of California Davis, USA*
[2] *UC Davis Eye Center, Dept. of Ophthalmology & Vision Science, University of California Davis, USA*
[3] *Center for Human Ocular Imaging Research (CHOIR), Dept. of Ophthalmology & Vision Science, UC Davis, USA*
[4] *School of Optoelectronic Engineering and Instrumentation Science, Dallan University of Technology, China*
[5]*Department of Cell Biology and Human Anatomy, University of California Davis, USA*

rjzawadzki@ucdavis.edu

ABSTRACT

The development of noninvasive, objective methods to assess retinal function in connection with simultaneously measured retinal structure is of great interest to clinical and experimental ophthalmology. If successful, it would revolutionize current clinical practice that relies on an independent evaluation of disease-related changes in retinal morphology and its function. This presentation will review our recent progress in developing Optical Coherence Tomography (OCT) - based retinal imaging methods allowing direct measurements of retinal morphology and its underlying function using optoretinography (ORG). The ORG comprises light-dependent changes in retinal layer thickness and scattering measured *in vivo* with submicrometer resolution by OCT. Several examples of ORG-OCT instruments developed to study retinal physiology at different spatiotemporal resolutions and in diverse species will be presented. Our recent data confirm that the mechanism underlying the "slow" ORG response is that extreme phototransduction increases osmotic pressure in the outer segment, driving water entry and swelling to restore osmotic balance. Overall, the results and modeling provide a new experimental and theoretical toolkit that allows insights into retinal physiology using imaging and stimulation with light only.

Optical coherence tomography (OCT) is a gold standard for clinical retinal imaging [1-2]. OCT applications in ophthalmology have been recently extended to probing light-evoked transient changes in cellular and tissue morphology in response to light stimulation. These visible light-driven retinal signals measured with OCT have been collectively called the optoretinogram (ORG) [3-8], in parallel to the well-known electroretinogram (ERG). Understanding of underlying retinal physiology of the ORG signals is of broad interest to both basic visual science and clinical ophthalmology because, like the ERG, it provides a means of investigating photoreceptor function in vivo and provides single-cell resolution biomarkers for diagnosis of retinal diseases and evaluation of therapeutic interventions. Two major biophysical mechanisms underlying rod and cone ORG signals have been attributed to charge-dependent changes in disc-membrane forces [9] for "fast" response and water movement into rod outer segments driven by osmolytes produced by phototransduction [10] for "slow" response. A critical question linked with the latter is whether the water permeabilities of the choriocapillaris (CC) and retinal pigment epithelium (RPE) are sufficient to provide water movement of the magnitude and time scale to explain swelling during the ORG. To extract the permeabilities of barriers to water movement in the posterior eye, a model was developed based on the modern Starling theory of fluid filtration through vascular capillaries. Application of the model enabled estimation of the osmotic pressure differential across key water barriers and the barrier water permeabilities for the ORG. We used this paradigm to quantify water movement between different retinal layers in a mouse model, allowing estimates of the water permeability of key barriers between the choriocapillaris (CC) and photoreceptors, viz., of the CC cell membrane, Bruch's membrane (BrM), the RPE layer, and the rod plasma membrane. Additionally, a retinal tissue reflectance model proposed to link the changes in refractive index caused by the osmotically driven water movement between the CC lumen and the outer segment during the ORG predicts the observed BrM scattering changes.

REFERENCES [HEADING 1 STYLE]

[1] D. Huang et al, Science 254, 1178, 1991.
[2] W. Drexler et al, Progress in retinal and eye research 27, 45, 2008.
[3] M. Azimipour et al, Optics Letters, 45, 4658, 2020.
[4] R.F. Cooper et al., Opt. Ex. 28, 39326, 2020.
[5] J.B. Mulligan et al., In Vision Science and Its Appl. Topical Meeting, 1994.
[6] R.S. Jonnal Ann Transl Med 9, 1270, 2021.
[7] V.P. Pandiyan et al. Science Advances 6, eabc1124, 2020.
[8] P. Zhang et al, Investigative Ophthalmology & Visual Science 61, 9, 2020.
[9] K.C. Boyle, et al, Biophysical Journal 119, 1481, 2020.
[10] P. Zhang et al, Proceedings of the National Academy of Sciences 114, E2937, 2017.

Effect of Endothelium on RBC Interaction and Adhesion in Microfluidic Channels Studied by Laser-Optic Techniques

Alexander PRIEZZHEV[1], Matvey MAKSIMOV[1], Petr ERMOLINSKIY[1], Olga SHCHEGLOVITOVA[2] and Andrei LUGOVTSOV[1]

[1] *Faculty of Physics, M.V. Lomonosov Moscow State Universioty, Russia*
[2] *N.F. Gamaleya National Research Institute of Epidemiology and Microbiology, Russia*

avp@biomedphotonics.ru

ABSTRACT

Vascular endothelial cells (ECs) make up the inner surface of arteries, veins, and capillaries and therefore interact directly with various components of the blood. The interaction between ECs and red blood cells (RBCs) is important because many hemorheological disorders are accompanied by increased adhesion of RBCs to vascular ECs. To date, the mechanisms of this pathology are not fully understood. This work was aimed at studying *in vitro* the effect of ECs on the microrheological properties of RBCs, in particular on spontaneous aggregation and shear deformation of the latter, using laser methods. The study of the mechanisms of adhesion and its quantitative characterization without damaging mechanical contact with the blood cells is of particular interest and novelty.

We performed experiments with fresh blood samples drawn from the cubital vein of healthy volunteers. Human umbilical vein endothelial cells (HUVEC) were cultured and grown at the N.F. Gamaleya National Research Center for Epidemiology and Microbiology. Cells were placed inside microfluidic chips under flow or stopped flow conditions. Subsequently, tumor necrosis factor alpha (TNF) and adenosine diphosphate (ADP) activators were used to activate EC. In our experiments, we used laser aggregometry based on diffuse light scattering from whole blood samples, which makes it possible to obtain the critical shear stress (CSS) parameter characterizing the hydrodynamic strength of RBC aggregates. Analyzing the dependencies of the intensity of laser light scattered by the RBCs suspension at various shear stresses, we measured the CSS of the RBC aggregates in a microchannel coated with an EC layer. To assess the effect of the endothelium on the deformability of RBC, we used the laser ektacytometry method, which makes it possible to measure the elongation index of RBCs at different shear stresses. All measurements were taken with blood samples at 37°C. Similar microchannels without EC were used as controls. Experiments carried out using laser aggregometry showed a decrease in the CSS parameter in the presence of EC by 40 ± 12% compared with the control. In the case of EC preactivation, the CSS parameter increased by approximately by 16 ± 4% (TNF) and 50 ± 7% (ADP) compared with non-activated cells. It is worth mentioning that in the case of preactivation using TNF, the CSS was below the control value, and in the case of preactivation with ADP, the CSS was above the control value. Experiments performed using laser ectacytometry showed that the ability of erythrocytes to deform under shear stress somewhat decreases in the presence of EC (13 ± 5% lower than in control). We believe that this process is due to the adhesion of RBCs to the endothelial layer.

Also, by trapping and manipulating single cells with laser tweezers in a microcuvette, we measured the strength of interaction between RBC and EC in a monolayer culture in various media using laser tweezers. In the first series of experiments, a solution of bovine fibrinogen in serum at various concentrations was used as a medium; in the second series of experiments, plasma (lithium heparin anticoagulant) was used with the addition of the amino acid L-arginine at various concentrations. The force of interaction between an RBC and EC is defined as the minimum force necessary for the free movement of an RBC along the surface of a monolayer of EC. Data were obtained indicating an increase in the force of interaction between RBC and endothelium with an increase in the concentration of fibrinogen in the medium and the subsequent release of this force to saturation. With an increase in the concentration of L-arginine in the medium, a slight decrease in the strength of interaction was found. Numerically, the interaction forces ranged from 1 to 4 pN.
The work was supported by the RSF grant № 22-15-00120.

Application of laser techniques for investigating the effect of vital blood plasma proteins on erythrocytes and platelets aggregation

Andrei LUGOVTSOV[1], Petr ERMOLINSKIY[1], Matvey MAKSIMOV[1], Danila UMERENKOV[1], Alexey SEMENOV[2] and Alexander PRIEZZHEV[1]

[1]Faculty of Physics and [2]Faculty of Biology, M.V. Lomonosov Moscow State University, Russia

anlug@biomedphotonics.ru

ABSTRACT

Aggregation of red blood cells (RBC) and platelets is one of key factors, which determines the blood flow and thereby affects the blood rheology and microcirculation. Alterations in these properties lead to changing the blood viscosity and, as a consequence, to changes in blood flow through vessels and capillaries. This can lead to significant impairment of blood function. Aggregation of RBCs and platelets are commonly known to be dependent on the concentration of vital plasma proteins. The exact role of each plasma protein in platelets aggregation and especially in RBC aggregation is still not well understood. Sometimes the experiments conducted using different techniques with whole blood samples or RBC/platelets suspensions containing mixtures of different plasma proteins yield somewhat controversial results [1]. We assumed that there might be an unaccounted synergetic effect of proteins (e.g. interference between proteins) on cells aggregation [2]. The aim of this work was to assess the kinetics of RBC interaction *in vitro* in samples with varying plasma proteins (fibrinogen, albumin, gamma globulin, C-reactive protein) and their concentrations by direct measurement of cells interaction forces on cellular level as well as to obtain RBC and platelets aggregation properties in whole blood and plasma samples on large ensembles of the cells.

In this work for measurements on ensembles of RBC and platelets we used diffuse elastic light scattering and turbidimetry technique accordingly. To measure pair aggregation of RBC we performed the experiment with optical tweezers. These methods are widely used to measure several parameters that characterize the RBC and platelets aggregation properties in blood. In the paper, we demonstrate the physical foundations of these methods [3] and the results of *in vitro* measurements of the indices and rate of RBC and platelets aggregation, hydrodynamic strength, characteristic time of formation of RBC aggregates, forces, and aggregation in environment with different plasma proteins.

We found that albumin in plasma changes its role from agonist to inhibitor of RBC aggregation with increasing the concentration of fibrinogen. When the concentration of fibrinogen is relatively high, an increase in albumin concentration does not increase the aggregation force but weakens the binding force between the RBCs. Furthermore, a model solution including five major aggregation-inducing proteins yields a weak aggregation force that can hardly be measured. These results indicate that there is an apparent interference among various plasma proteins involved in RBC aggregation and that the synergetic effect of plasma proteins determines the degree of RBC aggregation as well as the aggregation and disaggregation forces. Possible underlying mechanisms of the observed synergetic effects could be due to a change in the RBC and platelets membrane potential or formation of albumin-fibrinogen complexes preventing strong RBC aggregation. These ideas require further studies.

To find possible ways of correction of an enhanced aggregation that may be observed in such pathologies as arterial hypertension and diabetes mellitus [3, 4] the studies of the effect of several commonly used inhibitors (RGDS, eptifibatide, tirofiban) on RBC aggregation were performed with blood samples. The hypothesis that cells aggregation can be corrected (reduced) in arterial hypertension by integrin IIb/IIIa glycoproteins (IGP) inhibition of fibrinogen adsorption on RBC membrane was verified experimentally. IGP reduces nonspecific binding of fibrinogen molecules to cell membranes, which results in decreasing molecular bridging between interacting cells.

This work was supported by the Russian Science Foundation (Grant No. 22-15-00120).

REFERENCES

[1] K. Lee, et al., J. Biomed. Opt. 21(3), 035001, 2016.
[2] K. Lee, et al., Clin. Hemorheol. Microcirc. 64 (4), 853-857, 2016.
[3] A. Lugovtsov, et al., Biomed. Opt. Express 10(8), 3974–3986, 2019.
[4] P. Ermolinskiy, et al., J. Biomed. Photonics Eng. 4(3), 030303, 2018.

OCT guided clinical Raman spectroscopy of the eye

Rainer Leitgeb[1], Ryan Sentosa[1], Milana Kendrisic[1], Clara Stiebing[2], Matthias Eibl[3], Matthias Salas[1], Arjen Amelink[4], Wim de Jong[4], Michael Schmitt[2], Jürgen Popp[2], Andreas Pollreisz[5], Michael Kempe[3], Wolfgang Drexler[1]

[1]*Center for Medical Physics and Biomedical Engineering, Medical University of Vienna, Austria*
[2] *Institute of Photonic Technology (Leibniz-IPHT), Germany*
[3] *Carl Zeiss Meditec AG, Germany*
[4] *TNO Delft, Netherlands*
[5] *University Clinics of Ophthalmology and Optometry, Medical University of Vienna, Austria*

rainer.leitgeb@meduniwien.ac.at

ABSTRACT

While optical coherence tomography (OCT) has found extensive application in visualizing the structure and vasculature of the human retina (1), it falls short in providing the essential molecular insights which is believed to be crucial for early-stage diagnosis. Especially when using the eye as window to the brain various studies indicated that information on structural changes alone as provided by OCT is missing diagnostic specificity. The presentation will review various approaches to assess the molecular biomarkers of disease through the human fundus spanning from resonance Raman spectroscopy to retinal fluorescence lifetime imaging and recent two photon imaging results. Multimodal imaging has specific benefits, as for example structural details obtained with fast widefield confocal scanning or by a quick OCT scan help to guide molecular specific methods that often need larger measurement times, or are limited to a small areas. The central part of the presentation is how to unleash the diagnostic capabilities of in vivo retinal Raman spectroscopy (RS) within a clinical setting. Raman spectroscopy has become widely renowned within the field of biomedical science, offering a molecular signature of biological tissues without the necessity for external markers (2). Nevertheless, the initial investigations into Raman spectroscopy in the field of ophthalmology predominantly lean on the resonant Raman technique, employing shorter visible wavelengths and consequently capturing solely macular pigment information(3). A comprehensive Raman fingerprint data set could potentially prove essential for thorough molecular assessment of retinal tissue. So far the strong pigmentation of the fundus and resulting autofluorescence has hindered successful application of spontaneous Raman spectroscopy to the eye. The pigmentation is however missing in the region of the optic nerve head, which is in fact directly linked to the human brain. The developed apparatus to assess the retinal molecular fingerprint consisted of three main components: infrared (IR) fundus imaging at 730 nm, swept-source optical coherence tomography (SS-OCT) at 1060 nm, and Raman spectroscopy (RS) at 785 nm. IR fundus imaging played a role in aligning the device with the subject's pupil, while OCT en face imaging rapidly generated images to pinpoint suitable positions for Raman spectroscopy readings. In a first study Raman spectra of patients with age-related macula degeneration (AMD) could be distinguished from healthy controls with an accuracy rate of 90% (Fig.1). The results highlighted the clinical potential of nonresonant Raman spectroscopy (RS) and ongoing clinical investigation aims to ascertain how the molecular insights derived from RS could facilitate the early detection also of brain disorders.

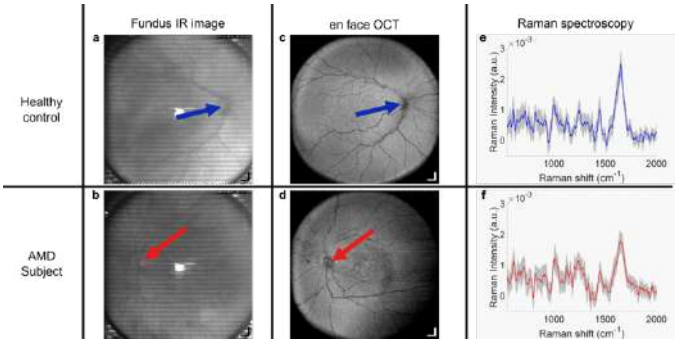

Figure 1: *In vivo measurement result: (a) and (b) representative fundus IR image results from each group, (c) and (d) en face OCT measurement results, (e) and (f) average Raman spectrum from each measurement group. Arrows indicate the position of the optic nerve head. Scale bar: 1 mm*

REFERENCES

[1] Everett, M., Magazzeni, S., Schmoll, T. & Kempe, M. Optical coherence tomography: From technology to applications in ophthalmology. *Transl. Biophotonics* **3**, (2021).

[2] Krafft, C. & Popp, J. The many facets of Raman spectroscopy for biomedical analysis. *Anal. Bioanal. Chem.* **407**, 699–717 (2015).

[3] Sharifzadeh, M., Zhao, D.-Y., Bernstein, P. S. & Gellermann, W. Resonance Raman imaging of macular pigment distributions in the human retina. *J. Opt. Soc. Am. A* **25**, 947 (2008).

Biomedical Imaging Reveals Optical Criteria For Violated Liver Regenerative Potential

Daria KUZNETSOVA[1], Svetlana RODIMOVA[1], Vadim ELAGIN[1], Artem MOZHEROV[1], Maria KARABUT[1], Nikolai BOBROV[1,2], Vladimir ZAGAINOV[1,3], Elena ZAGAYNOVA[1]

1 - Privolzhsky research medical university, Russia
2 - The Volga District Medical Centre of Federal Medical and Biological Agency, Russia
3 - Nizhny Novgorod Regional Clinical Oncologic Dispensary, Russia

daria.s.kuznetsova@gmail.com

Liver resection remains the most effective treatment of liver tumors [1]. However, in the presence of hepatic pathologies, the regenerative potential of the violated liver is significantly reduced [2]. Current clinical methods not efficient enough for predicting the function of the liver remnant. Modern label-free methods of multiphoton microscopy with fluorescence lifetime imaging microscopy (FLIM) and second harmonic generation (SHG) allow determining the criteria for reducing the regenerative potential of the liver with concomitant hepatic pathology.

A series of experiments were performed on Wistar rats. Liver fibrosis was induced by CCl4 injections and steatosis was induced by 60% high-fat diet. At different stages of the pathology, we induced liver regeneration by 70% partial hepatectomy (PH). Using multiphoton microscopy, we analysed the structure of the liver tissue on 3rd and 7th day after PH, and also determined the intensity of NAD(P)H autofluorescence in the zones of low and high signal. Using FLIM, we determined the fluorescence lifetime contributions of the free and bound forms of NADH and NADPH. Standard morphological analysis and a standard biochemical blood test were performed as controls.

As a result, we revealed the characteristic optical criteria of the structural and functional state at different stages of liver regeneration with steatosis and fibrosis. In case of steatosis, we identified zones with a reduced NADH autofluorescence intensity, corresponding to lipid infiltration or fibrosis. The area of zones with a reduced NAD(P)H autofluorescence intensity increased with the development of steatosis. We also showed a decrease in the contributions of the bound form of NADH and NADPH already in the early stages of steatosis. During regeneration with the presence of steatosis, there was no sharp increase in the contributions of the bound form of NADH and NADPH on the 3rd day of regeneration, due to mitochondrial dysfunction of hepatocytes. In case of fibrosis, we also identified zones with a reduced signal of NADH autofluorescence intensity, which corresponded to fibrosis. The area of zones with a reduced NAD(P)H autofluorescence intensity increased with the development of fibrosis. There was sharp a decrease in the contributions of the bound form of NADH and NADPH in the early stages of pathology, followed by an increase in these parameters in the later stages. Such result indicates mitochondrial dysfunction in the early stages and the progression of compensatory processes in the later stages of fibrosis. The work was supported by the Grant from the Russian Science Foundation №19-15-00263.

REFERENCES

[1] E. Ramos et al, Hpb 18, 389-396, 2016.
[2] V.E. De Meijer et al, Journal of British Surgery 97, 1331-1339, 2010.

Development of Antibacterial Photodynamic Therapy for Urology

Vadim ELAGIN[1], Nadezhda IGNATOVA[2], Artem ANTONYAN[3], Ivan BUDRUEV[4], Pavel BUREEV[4], Olga STRELTSOVA[3], and Vladislav KAMENSKY[1,5]

[1]*Institute of Experimental Oncology and Biomedical Technologies, Privolzhsky Research Medical University, Russia*
[2]*Department of Epidemiology, Microbiology and Evidence-Based Medicine, Privolzhsky Research Medical University, Russia*
[3]*Department of Urology Named after E.V. Shakhov, Privolzhsky Research Medical University, Russia*
[4]*Institute of Biology and Biomedicine, Lobachevsky State University of Nizhny Novgorod, Russia*
[5]*Federal Research Center Institute of Applied Physics of the Russian Academy of Sciences, Russia*

elagin.vadim@gmail.com

ABSTRACT

It is well known that from 30% to 51% of urinary calculi are infected or have a bacterial origin. Modern lithotripsy approaches are based on crushing stones into small fragments that can be removed/washed out through small diameter accesses. In the case of infected stones, large amount of toxins and bacteria are inevitably released during fragmentation. Antimicrobial photodynamic therapy is considered to be an alternative to the antibiotic treatment of localized infectious processes. The purpose of the study was to evaluate the antibacterial efficacy of photodynamic therapy against human antibiotic-resistant bacterial uropathogens and safety for recipients.

At first, the interaction between photosensitizer and urapothogenic microorganisms was analyzed. The bacteria were incubated with Photoditazine at various concentration and time. After washing samples from unbound photosensitizer, the fluorescence intensity was analyzed. The fluorescence intensity was found to be higher for Gram-negative strains than for the Gram-positive ones regardless of the photosensitizer concentration. The strains of *E. faecalis* and *S. aureus* demonstrated the enhancement of the fluorescence intensity in a time-dependent manner with the maximal value at 60 min. *E. coli* and *P. mirabilis* had the maximal value of fluorescence intensity after 30 min and that significantly decreased by 60 min. The optimal incubation time was found to be 30 minutes. After 15 minutes of incubation in the dark followed by 15 minutes of manipulation (dilution, inoculation) at ambient light, no colony of *S. aureus* and *E. faecalis* was detected on the plates. The treatment of either Gram-positive or Gram-negative bacteria by laser light only did not induce significant reduction of CFUs. The survival rate of *P. mirabilis* for photodynamic inactivation was power-dependent. The number of viable bacteria was decreasing from 65% to 10% with an increase in power from 50 mW to 150 mW. The maximal bactericidal effect was reached at 150 mW. Next, the antimicrobial photodynamic therapy was adapted for Gram-negative species. The efficacy of aPDT of *E. coli* washed from an unbound photosensitizer under continuous wave irradiation was only 5%. Tween 80 provided an insignificant enhancement of aPDT efficacy of up to 9%. The efficacy of aPDT of *E. coli* incubated with photosensitizer and Triton X-100 achieved 52.5%. It was found that washing of the extracellular photosensitizer led to loss of the aPDT efficacy. *K. pneumoniae* was not sensitive to aPDT without extracellular photosensitizer, while the efficacy of aPDT with the photosensitizer was 89%. *E. coli* had low sensitivity to aPDT without extracellular photosensitizer as well as with it. The high sensitivity of *P. aeruginosa* to aPDT with extracellular photosensitizer significantly reduced after washing of the photosensitizer. The efficacy of aPDT of *P. mirabilis* did not change after washing of the extracellular photosensitizer. It was demonstrated that the aPDT efficacy depended on laser power in all studied species, excluded *K. pneumoniae*. The efficacy of *K. pneumoniae* treatment did not exceed 93%. The irradiation of other bacteria species with a power of 450 mW provided an aPDT efficacy of 99.99%. To test the efficacy of the developed aPDT technique, urine cultures of the patients were incubated with a photosensitizer and Triton X-100 for 15 minutes in the dark. Then, the unwashed samples were illuminated by a continuous wave laser at 450 mW of output power. The efficacy of the aPDT of infected urine cultures was not less than 99.996%.

Safety of developed technique was study on pig kidney *in vivo*. Following by an incision of soft tissues, the kidney and the upper third of the ureter were separated retroperitoneal. The ureter was ligated and a catheter was inserted through the incision into the pelvis. Solution containing the 5 mg/ml of Photoditazine and 10% of Triton x-100 was injected into the renal pelvis and kept for 15 minutes. Illumination of pelvis was performed by diode laser coupled with optical fiber through the catheter. Either continuous wave or pulsed illumination was carried out with output laser power of 150 or 300 mW at wavelength of 662 nm. Illumination of a pelvis containing of Photoditazine solution by continuous wave laser at 150 mW led to the formation of a few foci of loosening and areas of desquamation of the cells surface layer. Illumination of a pelvis containing of Photoditazine solution by pulsing laser at 150 mW led to local expanding of intercellular spaces of the surface layer of the urothelium. Increase the continuous wave laser power up to 300 mW led to appearing of areas of pronounced cell loosening due to the destruction of intercellular contacts. . Moreover, confluent areas of destruction of the urothelium surface layers were also present. The thickness of the preserved epithelium was 2-3 rows of cells. Illumination by pulsing laser at 300 mW led to the formation of few small foci of desquamation, as well as to local erosion of the contours. Thus, the animal study confirmed the safety of this technique and the possibility of its use intraoperatively in the surgical treatment of urolithiasis.

This work was supported by the Russian Science Foundation, project №21-15-00371.

FLIM-assisted analysis of Radachlorin localization in living cells

Irina SEMENOVA[1], Andrey BELASHOV[1], Anna ZHIKHOREVA[1], Anna SALOVA[1,2], Tatyana BELYAEVA[2], Ilya LITVINOV[2], Elena KORNILOVA[2] and Oleg VASYUTINSKII[1]

[1]*Ioffe Institute, Russian Academy of Sciences, Russia*
[2]*Institute of Cytology, Russian Academy of Sciences, Russia*

irina.semenova@mail.ioffe.ru

ABSTRACT

Intracellular localization of photosensitizer molecules affects cell death pathway and dynamics at photodynamic treatment and is influential on the efficacy of photodynamic therapy. We report analysis of the accumulation and distribution of Radachlorin photosensitizer in three established cell lines: HeLa, A549, and 3T3. Experiments were performed using fluorescence lifetime imaging microscopy (FLIM) and confocal fluorescence microscopy. The FLIM-based experiments demonstrated significant variations of Radachlorin fluorescence lifetimes in different cell compartments and among cell lines. The analysis of lifetime images recorded in living cells and corresponding phasor plots allowed us to establish a relationship between the quantified lifetime images, fluorescence quantum yield, and Radachlorin localizations.

The pronounced dependence of Radachlorin fluorescence quantum yield and lifetime on solution pH [1] was used for analysis of lifetime images of living cells and their phasor plot representations and allowed us to suggest that Radachlorin localizes predominantly in lysosomes, known to have acidic pH. The colocalization experiments of Radachlorin fluorescence intensity and lifetime and LysoTracker fluorescence intensity supported this suggestion. Radachlorin fluorescence lifetimes determined in lysosomes were on average about 1 ns shorter than those in other parts of the cytoplasm. Equalization of intracellular pH achieved by treatment with Bafilomycin A1 resulted in more narrow range and more homogeneous distributions of Radachlorin fluorescence lifetime in cells. Bafilomycin A1 washout provided slow recovery of the initial parameters. The approximation of FLIM phasor plots with two 2D Gaussian distributions allowed for automatic segmentation of cells into intracellular compartments with short and long fluorescence lifetimes, corresponding to acidic and close to neutral microenvironments. The relative quantum yield of Radachlorin fluorescence in solutions was shown to be several times lower in acidic microenvironment as compared to that in the normal one [1]. This finding suggests that the actual amount of Radachlorin accumulated in lysosomes as compared to other intracellular compartments can be underestimated if being evaluated solely by comparison of fluorescence intensities.

The previously performed colocalization analysis of intracellular distributions of Radachlorin fluorescence intensity and refractive index distributions obtained by holographic tomography demonstrated coincidence of the areas of predominant accumulation of Radachlorin molecules with the areas of high values of refractive index and refractive index gradient [2]. It also evidences Radachlorin accumulation in lysosomes, that are intracellular structures with highest refractive index and high concentration of dry mass [3].

The financial support from Russian Science Foundation under the grant #21–72-10044 is gratefully acknowledged.

REFERENCES

[1] A. Belashov et al, Journal of Photochemistry and Photobiology B: Biology 243, 112699, 2023.
[2] A. Zhikhoreva et al, Photodiagnosis and Photodynamic Therapy 39, 102973, 2022.
[3] P. Liu et al, Lab on a Chip 16, 4, 634-644, 2016.

A Personalized Approach to Evaluate the Effectiveness of Immunotherapy Using FLIM of NAD(P)H in T-cells

Diana YUZHAKOVA[1], Anna IZOSIMOVA[1,2], Darya SACHKOVA[1,2], Olesya VANTSEVA[2], Konstantin YASHIN[3], Elena KISELEVA[1], Anna ZOLOTOVA[3], Artem MOZHEROV[1] and Marina SHIRMANOVA[1]

[1]*Institute of Experimental Oncology and Biomedical Technologies, Privolzhsky Research Medical University, Russia*
[2]*Institute of Biology and Biomedicine, Lobachevsky State University of Nizhny Novgorod, Russia*
[3]*Department of Neurosurgery, Privolzsky Research Medical University, Russia*

yuzhakova-diana@mail.ru

ABSTRACT

A main problem in the field of cancer immunotherapy is the lack of reliable biomarkers to determine the susceptibility of individual patients to treatment. Metabolic status of T-cells plays a key role in early response to tumor and therapy [1] and has a great potential as a predictive biomarker, while fluorescence lifetime imaging (FLIM) of metabolic coenzymes can be a powerful non-destructive label-free tool to fully characterize reactivity of T-cells in their native state. FLIM has been extensively used for metabolic investigations of cancer and other diseases [2]; however, the studies of immune cells using metabolic autofluorescence imaging is a very recent trend [3,4], and within the framework of immunotherapy metabolic FLIM of T-cells was performed for the first time.

Our research consisted of two parts. First, we explored FLIM of NAD(P)H to assess the sensitivity of immune cells to the immune checkpoint inhibitor therapy on the most common tumor target – B16F0 mouse melanoma model. We visualized the lymphocytes from fresh sections of inguinal lymphatic nodes located near the tumor node. It was found that the most reliable marker is the relative contribution of the free fraction of NADH α_1. It is known that its rise is associated with a shift towards glycolysis and glutaminolysis to support the elevated demands of activated T cells. We found that α_1 NADH in activated T-cells gradually increased during the tumor development and reached 71.3% and 75% in "Small tumor" and "Large tumor" groups, respectively, compared to "Healthy mice" group (69.3%). After immunotherapy α_1 NADH was higher in "Responder" group which showed the inhibition of tumor growth (74.9%) compared to non-treated control "Small tumor" group (71.3%) and to "Non-responder" group with progressive tumor growth (71%). Therefore, evaluation of α_1 NADH in T-cells allows to: 1) identify the response of the immune system to the tumor development; 2) distinguish between early and late stages of tumorigenesis ($p<0.0001$); 3) distinguish groups of responders and non-responders to the therapy ($p<0.0001$).

Furthermore, a gradual increase in immune response to tumor was reflected by the appearance of relative contribution of protein-bound NADPH α_3, associated with biosynthetic processes, when the tumors reached a large size. Flow cytometry showed that the changes in the α_1 NADH fraction correlated with T-cell activation, while changes in α_3 NADPH correlated with cell proliferation. Our future work will be focused on validation of the metabolic FLIM on the material of patients with melanoma both to predict the efficiency checkpoint inhibitor therapy prior to treatment and monitor early response during the therapy.

Next step, we considered another type of aggressive tumor – human glioblastoma, which is the most common brain tumor with 100% mortality. Immunotherapy is not included in the standard-of-care for this tumor but recent studies have shown its potential as an alternative treatment [5]. We have developed an original *in vitro* patient-specific model based on the explant culture from a resected tumor specimen which was co-cultivated with the lymphocytes isolated from a blood sample of the same patient. Such model was created for 10 patients, treated with anti-CTLA-4 or anti-PD-1 inhibitors or combination and demonstrated a heterogeneous response among the patients and types of treatment. In some cases, a positive effect was achieved, expressed in an increase in α1 NADH (assessed by FLIM) and correlated with standard measurements – an increase in the number of immune cells and a decrease in the number of tumor cells (assessed by phase contrast microscopy), and activation of lymphocytes and a decrease in the proliferative index of tumor cells (according to flow cytometry).

Therefore, FLIM of NAD(P)H in T-cells provides a highly sensitive, label-free assay of immune response to treatment and can become an innovative platform for individual drug screening for patients.

This research was funded by the Russian Science Foundation, grant number 23-74-10109.

REFERENCES

[1] R.D. Leone et al, Nat. Rev. Cancer 20, 516–531, 2020.
[2] R. Datta et al, J. Biomed. Opt. 25, 071203, 2020.
[3] A.J. Walsh et al, Nat. Biomed. Eng. 5, 77-88, 2021.
[4] A.V. Izosimova et al, Int J Mol Sci. 23, 15829, 2022.
[5] M.W. Yu et al, Front Immunol. 12, 676301, 2021.

Development of Anti-Age technology based on ethosomes for transdermal delivery of methylene blue photosensitizer

Irina Nikitenko[1], Anna Loginova[2] and Victor Loschenov[3]

[1]*Clinic of Aesthetic Cosmetology and Dermatovenerology LLC "EsteMed", Russia*
[2]*Clinic of Aesthetic Cosmetology and Dermatovenerology LLC "EsteMed", Moscow, Russia; Kyrgyz-Russian Slavic University, Kyrgyzstan*
[3]*LLC BIOSPEC, Russia*

dermatolog_nikitenko@mail.ru

ABSTRACT

The advantages of topical drug administration are reduction of side effects, noninvasiveness, and prevention of elimination during passage through the liver and degradation in the intestine. The main barrier to transdermal delivery of drug is the impenetrability of the stratum corneum (SC). Cutaneous absorption may be increased by the use of ethosomes which affect the barrier properties of subcutaneous fat and/ or the properties of the penetrant and thus make it possible to achieve a therapeutic amount of the drug in the systemic bloodstream and in the deep layers of the skin (Fig. 1) [1]. This development is devoted to the creation of a transdermal cosmetical drug based on ethosomes containing methylene blue (MB). There are a number of publications confirming the use of MB as a drug mitochondrial action, brings an effective result in stimulating the proliferation of skin fibroblasts and slowing cellular aging [2]. For quality assessment of ethosomal complexes we use spectroscopic methods and methods for estimating the size of ethosomes using dynamic light scattering and scanning electron microscopy. The purpose of this study is to increase the penetration depth of the photosensitizer after its application to the skin. We developed a new method of transdermal delivery of methylene blue through the skin barrier with the use of ethosomes which consist of natural components. After applying the ethosomal complex to the treated (after removing the SC) and untreated pig skin, these areas were irradiated with an infrared light source. A confocal microscope was used in these areas to measure the penetration depth. The obtained results (Fig. 2, 3) showed that there was a sufficient concentration at a depth of more than 1.1 mm, which indicates penetration into the dermis. The rate of decrease in the concentration of MS is significantly less in comparison with the generally accepted value manifested by the diffuse mechanism of distribution of the drug substance. This means that stimulating with IR light significantly increases the depth of penetration by the ethosomes.

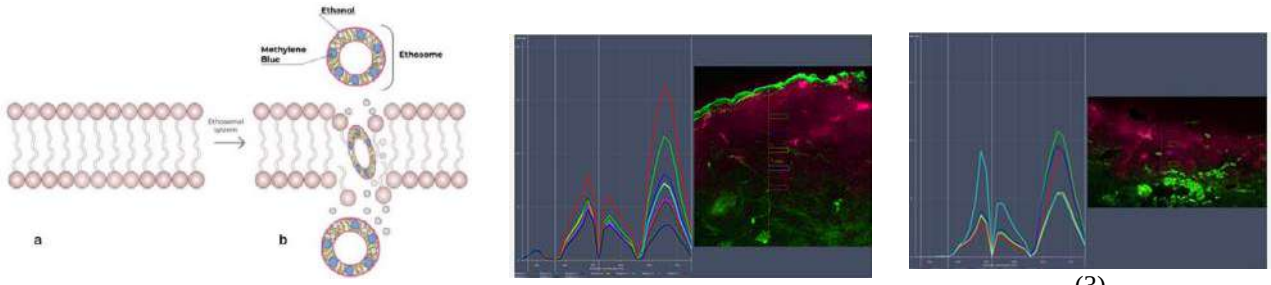

(1) (2) (3)

Figures: *(1) The proposed mechanism of penetration of the atosomal system through the membranes of the stratum corneum:*
a – ordered lipid bilayers
b – lipid bilayer, disturbed by ethanol and accumulated soft, malleable ethosomes [3]
(2) Confocal microscopy results in the area of untreated pig skin (3) Confocal microscopy results in the area of pig skin after removing the stratum corneum

REFERENCES

[1] Godin B., Touitou E. Ethosomes: New Prospects in Transdermal Delivery //Critical Reviewstrade; in Therapeutic Drug Carrier Systems. 2003. Vol. 20, no. 1.
[2] R. Santus, C. Kohen, E. Kohen et al. Permeation of lysosomal membranes in the course of photosensitization with methylene blue and hematoporphyrin: study by cellular microspectrofluorometry // Photochemistry and Photobiology. 1983. Vol. 38, no. 1. P. 71–77.
[3] Loginova A.G., Nikitenko I.S., Tikhonovsky G.V., Skobeltsin A.S., Voitova A.V., Loschenov V.B. Development of a method for assessing the depth of penetration of ethosomes with methylene blue into the skin during application and photodynamic exposure, Biomedical Photonics, 2022, vol. 11, no. 4, pp. 11–18. doi: 10.24931/2413–9432–2022–11-4-11–18.

Marker- independent pancreas and islets quality diagnostics with FLIM

Polina Ermakova[1], Alena Kashirina[1], Irina Kornilova[1], Alexandra Bogomolova [1,2], Ekaterina Vasilchikova [1,2], Nasipbek Naraliev[1], Denis Kuchin[1,3], Liya Lugovaya[1], Elena Zagaynova[4,1], Vladimir Zagainov [1,3,5], Alexandra Kashina [1]

[1] *Privolzhsky research medical university, Russia*
[2] Lobachevsky State University [Nizhni Novgorod], *Russia*
[3] *Nizhny Novgorod Regional Clinical Hospital named after Semashko, Russia*
[4] *Scientific Research Institute of Physical-Chemical Medicine, Russia*
[5] *Nizhny Novgorod Regional Clinical Oncological Dispensary, Russia*

bardina-polina@mail.ru

ABSTRACT

Insulin-deficient conditions are a significant public health challenge worldwide. Cell stress and dysfunction occur before the progressive loss of cell mass in various diseases such as type 1 and type 2 diabetes or pancreatitis. Cell dysfunction results from remodeled glucose metabolism as part of a conserved pro-survival signaling program. In healthy cells, an increase in glucose concentrations leads to a corresponding increase in adenosine triphosphate (ATP) generation from oxidative phosphorylation (OxPhos) [1]. This, in turn, acts on membrane channels, electrically coupling oxidative phosphorylation to insulin secretion. However, it has been suggested that in stressed cells, there is an increase in glycolysis that is largely unrelated to oxidative phosphorylation. This pattern is similar to the high survival-inducing Warburg effect characteristic of cancer cells. [2]. Most studies of cell metabolism rely on methods such as PCR, immunohistochemistry, and transcriptomic studies. However, these methods do not provide a complete picture of the islets and often provide contradictory results. Moreover, there is no single method that would allow quickly and without the use of staining to assess the quality of the islets both in the whole tissue and after their isolation. Metabolic FLIM is a powerful tool that has the potential to provide a non-invasive and label-free diagnostic method to assess the quality of pancreatic islets. To make FLIM more applicable in clinical settings, new FLIM criteria are necessary to identify islet quality and metabolism in various insulin-deficient conditions. FLIM can be applied to evaluate the quality of islets in whole tissue with various insulin deficiency diseases or to monitor the status of islets before and after transplantation in transplantation technologies. This study utilized FLIM and intracellular metabolite NAD(P)H to develop a non-invasive and label-free method for assessing the quality of isolated islet cells and pancreatic islets in tissue. The fluorescence lifetimes (t1, t2) and contributions of free and bound forms of NAD(P)H (a1, a2) were analyzed using LSM 880 (Carl Zeiss, Germany) equipped with a short-pulse femtosecond Ti:Sa laser Mai Tai HP and FLIM system for time-resolved microscopy (Becker&Hickle GmbH, Germany). FLIM was used to evaluate the quality of islet cells in both pathological (T1D, T2D/chronic pancreatitis) and normal pancreas. The FLIM parameters (a1 and a1/a2) of islet cells in the pathological and normal pancreas were found to differ, with a higher proportion of glycolytic phenotype islet cells observed in the pancreas with T1D and T2D/chronic pancreatitis. Metabolic FLIM imaging was also used to assess the metabolism and viability of isolated islet cells. The isolated islets exhibited typical fluorescence lifetimes for NAD(P)H, indicating their viability and metabolically active state after isolation. ELISA analysis confirmed that in isolated cells, when stimulated with glucose, the level of insulin increased. This correlates with the FLIM data, which show that upon stimulation with glucose, the level of the bound form of NAD(P)H and the predominance of oxidative phosphorylation over glycolysis. Thus, FLIM confirmed the viability and functional activity of the isolated islets. Non-contrast FLIM diagnostics can be used to develop new FLIM criteria for identifying islet cell quality and metabolism, and to develop a rapid technique for assessing islet viability to aid in islet transplantation in clinical settings. FLIM can be used not only to assess the quality of islets in whole tissue, but also during their isolation process, making it a valuable tool in transplantation technologies.

The work was carried out as part of the "Priority—2030"

REFFERENCES

[1] G. Aharon-Hananel et al, Cells, 11, 6, 929, 2022.
[2] M.E. Cerf et al, Frontiers in endocrinology 4, 37, 2013.

.

Changes in plasma membrane microviscosity of human colorectal cancer cells with different migration activity

Liubov SHIMOLINA[1], Nadezhda IGNATOVA[1], Irina DRUZHKOVA[1],
Marina KUIMOVA[2] and Marina SHIRMANOVA[1]

[1] *Institute of Experimental Oncology and Biomedical Technologies, Privolzhsky Research Medical University, Russia*
[2] *Department of Chemistry, Imperial College London, United Kingdom*

shimolina.l.e@gmail.com

ABSTRACT

Membrane microviscosity plays an important role in cell biophysics, controlling the rate of diffusion and transport, and the activity of many enzymes and receptors [1-4]. The cell membrane is a complex of proteins and lipids, which ensures the integrity of the cell and regulates many important processes of interaction between the cell and the environment. Mechanical properties of membrane play an important role in cell function, signaling various pathologies, including the transformation of a normal cell into a cancerous one. At the same time, chemotherapy remains one of the main types of treatment for cancer, treatment failure is a frequent occurrence, emphasizing the need for new approaches to the early assessment of tumor response. Understanding the role of membrane microviscosity in the response of tumor cells to chemotherapy is important, since the cell membrane is actively involved in drug transport [5–7]. But the study of the effect of chemotherapeutic drugs on the viscoelastic properties of living cells is important for a better understanding of the mechanisms of drug action and evaluation of the effectiveness of therapy. Previously, we developed methodologies that allows obtaining microscopic viscosity maps from individual cancer cells in vitro and from a mouse tumor model in vivo [2-4].

This work is aimed to study of membrane microviscosity using the BODIPY 2 fluorescent molecular rotor and FLIM lifetime fluorescence microscopy.

Cancer cell lines were used in the work - five colorectal cancer lines with different migratory ability: HT29, HCT116, Caco-2, SW480, SW837, as well as lines HT29 and HCT116 resistant to oxaliplatin or 5-fluorouracil. The cells were cultured in DMEM containing 100 µg/ml penicillin, 100 µg/ml streptomycin sulfate and 10% fetal bovine serum (FBS) at 37°C in a humidified atmosphere with 5% CO_2. The molecular rotor fluorescence lifetime was recorded using an LSM 880 confocal microscope (Carl Zeiss, Germany) equipped with a TCSPC-based FLIM module (Becker&Hickl Inc., Germany). Microviscosity was measured in the plasma membranes of individual cells using a BODIPY2 fluorescent molecular rotor (excitation 850 nm, reg. 500–550 nm). For microscopic imaging, the cells were seeded on glass-bottom FluoroDishes in complete DMEM medium without phenol red (Life Technologies). A laser scanning microscope LSM 880 (Carl Zeiss, Germany) equipped with a FLIM module SPC 150 TCSPC (Becker & Hickl GmbH, Germany) and a Mai Tai HP femtosecond laser, 80 MHz, 140 fs (Spectra Physics, USA) was used in the study. FLIM images were acquired at laser power 1%-2%, photons collection time 60 s to provide ≥5,000 photons per decay curve at binning factor 1. Fluorescence lifetime analysis was performed in the SPCImage software 8.3 (Becker&Hickl GmbH, Germany).

It was found that in the range of cell lines we selected, HT29 cells have the most fluid membranes, 427 ± 30 cP. Caco-2, HCT116, and SW837 cells have slightly more viscous membranes vs. HT29, with microviscosities 448±51 cP, 456±33 cP, and 457±27 cP, respectively. The highest values of microviscosity were observed in SW480 cell membranes – 457±27 cP.

To further determine whether drug-sensitive and drug-resistant cancer cells have different migratory activities in terms of the fluid properties of their membranes, we performed experiments on 5-FU and oxaliplatin-resistant cell lines. Thus, for HCT116-5-FUR cells, the membrane microviscosity was higher than in control cells and amounted to 579±37 cP. For HCT116-OXAR microviscosity was lower than in control cells - 407±22 cP. Cells of HT29 sublines have a similar trend. It was shown that the microviscosity of cell membranes HT29-5-FUR is higher than in the control HT29 - 521±30 cP versus 427±30 cP. A slight decrease was observed for HT29-OXAR up to 419±36 cP.

The obtained data open up the possibility of predicting changes in the membrane microviscosity, and will be useful for developing new diagnostic approaches in oncology.

This work was supported by the Russian Science Foundation (Project no. 23-74-00045).

REFERENCES

[1] M. Shirmanova et al, Advances in Experimental Medicine and Biology. 2017. 1035. 143-153.

[2] L.E. Shimolina et al, Scientific Reports. 2017. 7. 41097.

[3] L.E. Shimolina et al, Journal of Visualized Experiments. 2021. 173. 62708.

[4] L.E. Shimolina et al, Cancers. 2021. 13(24). 6165.

[5] L.E. Shimolina et al, Methods Appl Fluoresc. 2022. 10(4). 044008.

Classification of maxillary sinus pathologies in digital diaphanoscopy based on machine learning

Ekaterina BRYANSKAYA[1], Viktor DREMIN[1], Viacheslav ARTYUSHENKO[2] and Andrey DUNAEV[1]

[1]*Research and Development Center of Biomedical Photonics, Orel State University, Russia*
[2]*art photonics GmbH, Germany*

bryanskayae@mail.ru

ABSTRACT

The use of the digital diaphanoscopy method, based on the transmission of maxillary sinus tissues by low-intensity radiation, and subsequent registration of diaphanograms, is currently characterized by the absence of classification models to exclude the subjectivity of diagnosis. Thus, the purpose of this study is to use machine learning methods to identify the pathology of the maxillary sinuses by digital diaphanoscopy.

Experimental studies were conducted using the developed digital diaphanoscopy device in conditionally healthy volunteers and patients with confirmed diagnosis. The maxillary sinuses were probed with radiation of 650 nm and 850 nm using an LED applicator and the subsequent registration of diaphanograms was carried out using a CMOS camera (Fig. 1,a-b) [1]. The intensity parameter (*I*) and the asymmetry coefficient (*AC*) were calculated. To calculate the *I*, the average value of the light intensity on the registered diaphanogram was calculated. The calculation *AC* consisted in determination of the face central line (symmetry axis), diaphanograms rotation to ensure vertical position of the central line, and calculating the asymmetry coefficient between the left and right parts of the face.

Analysis of the data obtained by the Mann-Whitney criterion revealed a statistically significant difference ($p < 0.05$) for the calculated quantitative parameters in the studied groups. The application of linear discriminant analysis to construct a classification model is proposed. The best values of sensitivity and specificity (0.88 and 0.98, respectively) and an accuracy value of 0.93 were obtained for the sensing wavelength of 850 nm (Fig. 1,c) [2]. Thus, the proposed approach makes it possible to detect the presence of pathology in the maxillary sinuses with high accuracy, and reduces the probability of a false negative diagnostic result compared to traditional screening diagnosis methods [3,4].

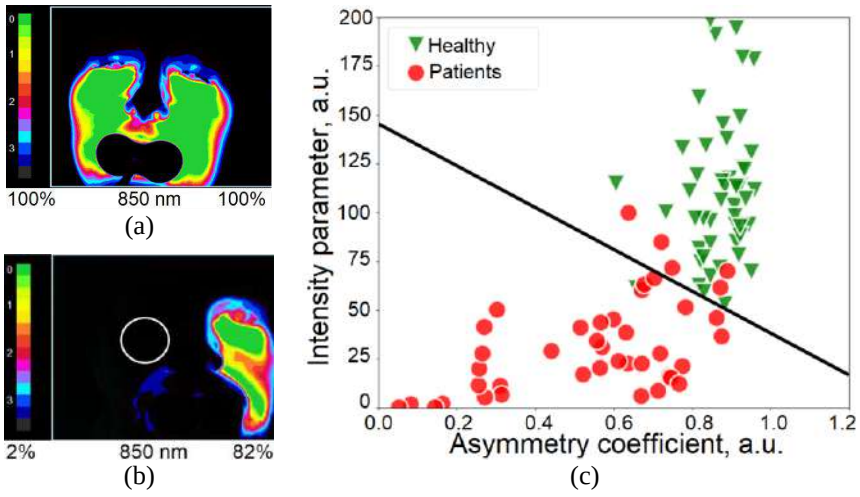

Figure 1: *(a) Typical diaphanoscopy examination results for healthy volunteer, (b) and patient with chronic right-sided maxillary sinusitis (white circle indicates the area of pathology), (c) the scatter plot with applied discriminant line obtained by linear discriminant analysis method.*

This study was funded by RFBR according to the research project No. 20-32-90147 and by FASIE according to the project No. 353ГС1ЦТС10-D5/80270. Thanks to the volunteers, patients and doctors of the University Clinic of the Yevdokimov A.I. Moscow State University of Medicine and Dentistry for assistance in conducting experimental studies.

REFERENCES

[1] E. Bryanskaya et al, Diagnostics 11, 77, 2021.
[2] E. Bryanskaya et al, J Biophotonics e202300138, 2023.
[3] A. Aysel et al, Eur J Rhinol Allergy 4, 77-80, 2021.
[4] A. Valkov et al, Int Bull Otorhinolaryngol 17, 40-41, 2021.

Reverberant Optical Coherence Elastography of Murine Embryos

Manmohan SINGH[1], Fernando ZVIETCOVICH[1,2], Christian ZEVALLOS-DELGADO[1], Yogeshwari AMBEKAR[1], Salavat AGLYAMOV[3] and Kirill LARIN[1]
[1]*Department of Biomedical Engineering, University of Houston, USA*
[2]*Department of Engineering, Pontificia Universidad Catolica del Peru, Peru*
[3]*Department of Mechanical Engineering, University of Houston, USA*
msingh@central.uh.edu

ABSTRACT

Many processes during embryogenesis, such as elongation [1], neural tube closure [2], and cardiogenesis [3], are fundamentally biomechanical processes [4]. Any disruption or failure of these events can lead to debilitating or even fatal pathologies, e.g., anencephaly [2]. While much is known about the genetic and molecular mechanisms underlying these processes, there remains a significant knowledge gap about the associated biomechanical parameters due to the lack of noninvasive high-resolution mechanical imaging techniques, particularly in live samples. In this work, we demonstrate completely noninvasive, label-free, high-resolution, and three-dimensional mapping of mouse embryo stiffness at several critical stages of embryogenesis based on reverberant shear wave optical coherence elastography (Rev-OCE)[5]. Mouse embryos at various developmental stages (embryonic day 9.5, 10.0, 10.5, 11.0, and 11.5) were dissected out and placed on an optical window during imaging. The samples were encompassed in embryo culture media to preserve the integrity of the delicate embryo tissues. The optical window was attached to a piezoelectric bender, which vibrated the optical window at 1 kHz. M-C-mode imaging was performed with a phase-sensitive spectral domain OCT system operating in the common-path configuration. Standard reverberant OCE processing steps were applied, and the local autocorrelation was fitted to the analytical solution of the reverberant shear field. The local shear wave speed was then mapped in 3D. The results in Figure 1 show that the stiffness of the spine, heart, and brain all increased as the embryo developed.

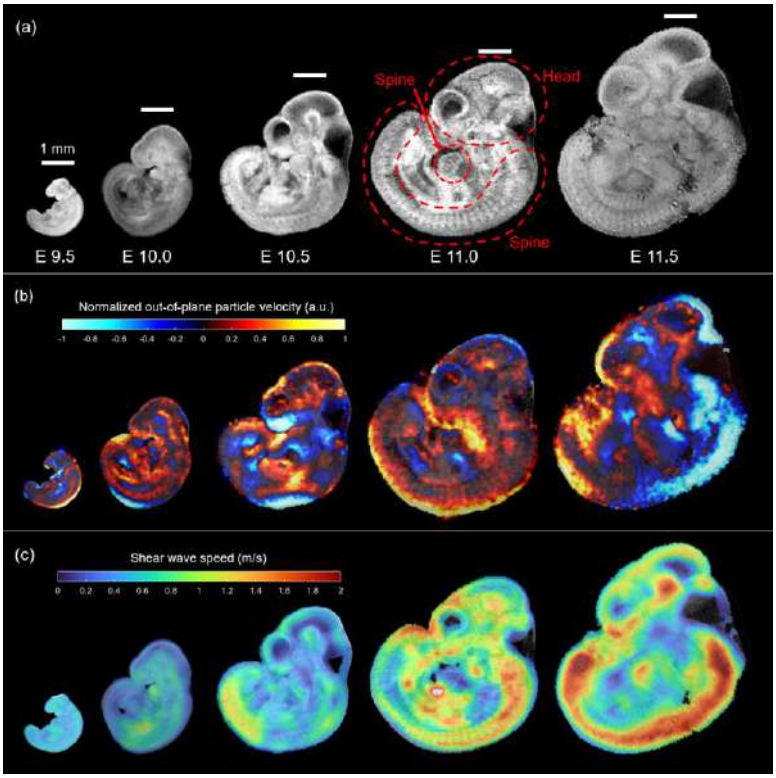

Figure 1. (a) Average intensity projections of 3D OCT images, (b) snapshots of the reverberant shear field, and (c) local shear wave speed of regions highlighted in (a) of murine embryos at various developmental stages.

REFERENCES

[1] T. T. Vuong-Brender, et al. Elife e23866, 2017.
[2] L. D. Moon, et al. Semin Cell Dev Biol 56-69, 2022.
[3] J. R. Hove, et al. Nature 6919, 172-7, 2003.
[4] J. Sutlive, et al. Small 6, e2103466, 2022.
[5] F. Zvietcovich, et al. Nat Commun 1, 4895, 2019.

Raman spectroscopy of proteins as a technique to reveal markers of tertiary structure

Anna MANKOVA[1], Anna NAGAEVA[1], Nikolay BRANDT[1], and Andrey CHIKISHEV[1]

[1]*Faculty of Physics, Lomonosov Moscow State University, Russia*

mankova@physics.msu.ru

ABSTRACT

Vibrational spectroscopy is a very helpful tool in the study of protein molecules. It gives information about secondary structure of protein molecules and can be efficient in the study of different function-related conformational changes that can occur in the molecule. For example, changes at higher (than the second) levels of the hierarchy of the protein structure can be manifested in vibrational spectra [1, 2].

Assignments of the spectral features to the vibrations that are correlated with the secondary structure elements are available in a lot of research databases. But the corresponding information on the tertiary structure of protein molecules is almost missing. Several approaches can be used to obtain such information. In this work, comparison of the spectra of proteins with similar secondary and different tertiary structures is used to detect spectral features that are related to the tertiary structure of a protein molecule. Comparative analysis of the spectra of native proteins and proteins that are thermally or chemically denatured is also carried out. Special attention is given to the tyrosine doublet (830 and 850 cm^{-1}), the bands assigned to three basic conformations of disulfide bridges (510, 525, and 540 cm^{-1}), and low-frequency spectral interval. Using agents that provide cleavage of disulfide bonds, we can detect spectral changes resulting from the changes at higher levels of the hierarchy of the protein structure. The experimental results show that spectral intervals of 140-470, 500-550, and 800-1000 cm^{-1} can be used in the study of changes of the tertiary structure of proteins.

REFERENCES [HEADING 1 STYLE]

[1] I.A. Balakhnina, et al, Vibrational Spectroscopy 114, 103250, 2021
[2] A.A. Mankova, et al, Vibrational Spectroscopy 120, 103375, 2022

Effects of intense 1-6 THz pulses irradiation on albumin

Teplyakov Valeriy[1,2], Konnikova Maria[3] Cherkasova Olga[4,5] and Nazarov Maxim[2]

[1] *Faculty of Physics, Lomonosov Moscow State University*
[2] *National Research Centre 'Kurchatov Institute'*
[3] *ILIT RAS – Branch of FSRC "Crystallography and Photonics" RAS*
[4] *Laboratory of Biophotonics, Tomsk State University*
[5] *Institute of Laser Physics of the Siberian Branch of the RAS*
tepliakov.vv17@physics.msu.ru

ABSTRACT

The objectives of this work were to diagnose and to analyze the results of the effects on dry albumin created by short powerful THz pulses. Also, the aim of the work was to experimentally determine the safe radiation dose in this range. The work is a logical extension of research in both laser physics [1] and biophysics [2].
The second task was to obtain and to describe from the point of view of nonlinear optics the generation of powerful homogeneous radiation in the THz range with a peak field value of at least 5MV/cm, as well as to assemble a setup for the characterization of THz pulses and for the subsequent biological experiment.
We determined the optimal $LiNbO_3$ crystal thickness =100 μm and the optimal pump radiation intensity - 1 GW/cm^2. An optical system for generation of THz pulses with the following parameters was designed and assembled: THz pulse energy - 10 μJ; duration - 5 ps; peak field strength - 3 MV/cm, spectrum - from 0.3 to 6 THz with a maximum at 2-3 THz. The time profile of the 5 ps pulse and its spectrum were also obtained (see Figures a and b). In the experiment, we irradiated the dry tablets for 15 minutes each, then examined the induced changes in the UV transmission spectrum of the aqueous solution of the tablets - Fig c and d). Importantly, this is the first time that a test biological subject has been exposed to powerful short pulses, where half of the energy is contained at frequencies above 3 THz.
The effect of THz radiation on albumin is confirmed by the systematic difference of the spectra for irradiated and non-irradiated samples. We studied the dependence of the UV transmittance coefficient of albumin 1mg/ml water solution on the influence of THz pulses. We obtained qualitative repeatability of results for several measurements (plots c and d). It can be seen from the graphs that the effect is manifested by an increase in the transmittance of the solution by 2-5% in the range of 250-300 nm. It is likely that the changes in the structure of BSA leading to these results are due to the influence of submillimetre waves on aromatic acids. The influence of heating is absent or negligible because of very long (100 ms) interval between short pulses, the heat has time to dissipate. Further, due to the presumed ability to self-organise for protective purposes the effect does not persist. As for the safe dose, we estimate it to be 0.1 μJ/sq.mm per pulse for 10 min of irradiation at 10 Hz pulse frequency.

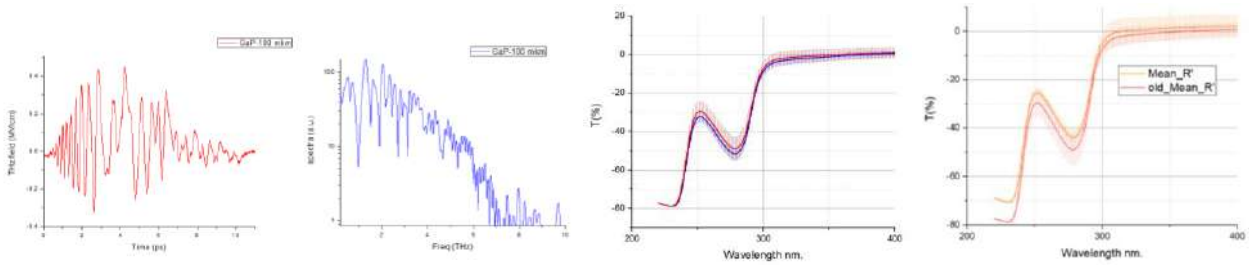

Figure 1: *(a) Time profile of THz pulse detected by 100 um GaP crystal (b) Spectrum of THz pulse (c) Transmittance dependence for irradiated (red curve) and unirradiated (blue curve) samples (d) Transmittance dependence for irradiated samples on the day of the experiment (red curve) and after 19 days (orange curve).*

We'd like to give thanks to Prof. Tverdislov V.A. for advisories during the research and to Prof. Shkurinov A.P. for provided hardware and facilities.

REFERENCES

[1] Broadband Terahertz Generation by Optical Rectification of Ultrashort Multiterawatt Laser Pulses near the Beam Breakup Threshold / Nazarov, M.M.; Shcheglov, P.A.; Teplyakov, V.V. et.al. // Optics Letters – 2021 – 46 – 5866-5869.
[2] Effects of Terahertz Radiation on Living Cells: a Review / Cherkasova, O.P., Serdyukov, D.S., Ratushnyak, A.S., et.al. // Biophotonics – 2020 – 128(6) – 855-866

Enhancing optogenetics: first demonstration of nonlinear properties of monomeric and dimeric *Deinococcus radiodurans* bacterial phytochrome

Diana GALIAKHMETOVA[1], Aleksandr KOVIAROV[1], Viktor DREMIN[1], Andrei GORODETSKY[2], Marios MAIMARIS[3], Dmitrii STOLIAROV[1], Mikhail BALOBAN[4], Vladislav VERKHUSHA[4,5], Sergei SOKOLOVSKI[1] and Edik RAFAILOV[1]

[1]*Aston Institute of Photonic Technologies, Aston University, United Kingdom*
[2]*School of Physics and Astronomy, University of Birmingham, United Kingdom*
[3]*Ultrafast Optoelectronics Group, Imperial College London, United Kingdom*
[4]*Department of Genetics and Gruss-Lipper Biophotonics Center, Albert Einstein College of Medicine, USA*
[5]*Medicum, Faculty of Medicine, University of Helsinki, Finland.*

galiakhmetova.di@gmail.com

ABSTRACT

Optogenetics has revolutionized the field of neuromodulation by enabling the monitoring and control of neural cell activity through the expression of light-sensitive proteins, such as opsins and phytochromes. However, the high absorption of visible light by the skin and skull presents a major obstacle for non-invasive *in vivo* modulation of neurons [1]. In this study, we demonstrate a significant advancement in overcoming this challenge by employing long wavelength light sources and exploiting the nonlinear photoconversion properties of bacterial phytochrome.

Our work shows the first two-photon photoconversion of new genetically engineered monomeric variants of phytochrome. Through a comprehensive analysis of the optical properties of monomeric and dimeric variants of *Dr*BphP bacterial phytochrome, we gained a deeper understanding of the structural characteristics underlying their nonlinear features. Our experimental findings provide compelling evidence that the monomeric variant exhibits a notably higher efficiency in two-photon Pr→Pfr conversion by 1.2 µm laser radiation compared to the original dimeric form of phytochrome [2]. Two-photon conversion is shown in Figure 1 (a,b). The utilization of this specific wavelength, located in the second biological window, represents a remarkable breakthrough in the field of optogenetics due to the enhanced penetration through the skin, skull, and brain tissues. This advancement enables the two-photon conversion of phytochromes expressed in neurons and, consequently, facilitates the non-invasive *in vivo* stimulation of neuronal activity.

Furthermore, we present the first-ever demonstration of two-photon fluorescence in both monomeric and dimeric variants using laser radiation at a wavelength range of 810-890 nm (Figure 1(c)). The excitation and fluorescence wavelengths utilized in this process are within the first biological windows, indicating the potential use of new monomeric *Deinococcus radiodurans* bacterial phytochrome as a sensitive biomarker for high-resolution imaging and early detection of neurological diseases.

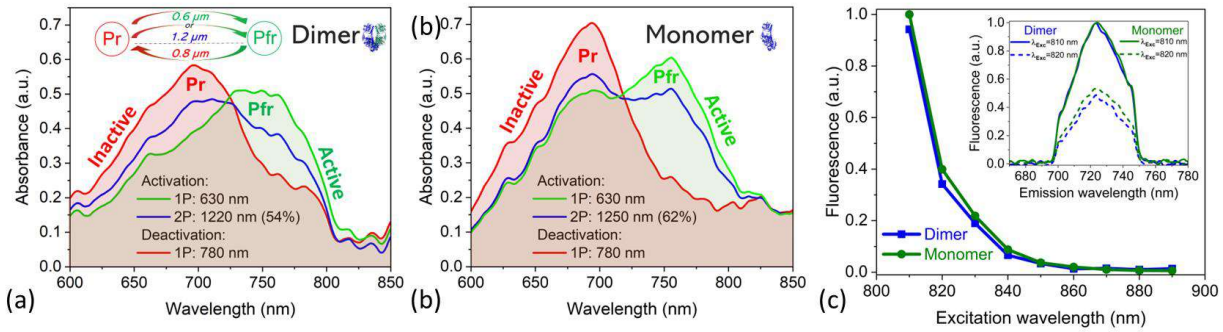

Figure 1: *1P and 2P Pr→Pfr conversion of (a) dimeric and (b) monomeric bacterial phytochromes; (c) 2P fluorescence at a wavelength of 720 nm depending on excitation wavelength.*

ACKNOWLEDGEMENTS

This work was supported by the European Union's Horizon 2020 Research and Innovation Programme under Grant Agreement No. 863214 and the Return to Research grant, Rank Prize.

REFERENCES

[2] D. Galiakhmetova et al., IEEE J. Sel. Top. in Quantum Electronics 29.4: Biophotonics (2022): 1-11.
[2] D. Galiakhmetova et al., Optogenetics and Optical Manipulation 2023. SPIE, 2023.

Changes in the Microcirculation and Metabolism of the Small Intestine after its Sympathetic Denervation

Elena KISELEVA[1], Mikhail BALEEV[2], Anastasia KOMAROVA[1], Evgeniya BEDERINA[3], Artem MOZHEROV[1], Sofia PTUSHKO[1], Marina SHIRMANOVA[1], Vladislav SHCHESLAVSKIY[1] and Maxim RYABKOV[1]

[1]*Institute of Experimental Oncology and Biomedical Technologies, Privolzhsky Research Medical University, Russia*
[2] *City Clinical Hospital No. 30 of Nizhny Novgorod, Russia*
[3] *University Clinic, Privolzsky Research Medical University, Russia*

kiseleva84@gmail.com

ABSTRACT

Growing attention to the profound changes that occur across the entire physiology of individuals with spinal cord injury (SCI) reveals profound knowledge gaps in our understanding of the temporal dimensions and magnitude of organ-specific co-morbidities following SCI [1]. A typical complication of traumatic SCI is digestive tract dysfunction: early enteral insufficiency, neurogenic dysfunction of the small intestine and colon, etc.. Significant changes in bowel function after its sympathetic denervation are manifested by a violation of the absorption, secretory, barrier, evacuation, and immune functions [2,3]. In the future, this triggers a whole cascade of pathological processes that negatively affect both the intestine itself and metabolic processes throughout the body, causing the development of decubitus ulcers [4]. It is essential to understand and identify these broad pathophysiological changes in order to develop appropriate evidence-based strategies for management by clinicians, caregivers and individuals living with SCI [1].

The aim of the study was to assess the dynamics of microcirculation and metabolic changes in the tissues of the small intestine in the acute period of spinal injury in experiment. Wistar rats (n=20) were used to simulate spinal injury by acute complete transection of the spinal cord at the level of Th_5-Th_6 vertebrae. Changes in the vascular network of the intestinal wall, as well as metabolic changes in the cells of the intestinal mucosa were determined 3 and 24 hours after injury. Two animals were included in the control group; intestine samples were taken from them for histological examination without modeling spinal injury. To visualize blood vessels, the optical coherence tomograph with angiography mode (OCTA) was used. Intramural blood circulation was studied from the side of the serous membrane by placing an OCTA probe in contact with the tissue surface and transilluminating the entire wall to the intestinal lumen. The parameters of OCTA images, which were obtained before intestine sympathectomy, were taken as normal. Metabolism was assessed ex vivo immediately after tissue sampling using fluorescence time-resolved microscopy (FLIM) in the spectral channel of the metabolic cofactor NAD(P)H.

The results showed that, after sympathectomy, changes in functioning of intramural blood vessels were observed with a high statistical significance. The occurrence of trauma-induced constriction of the blood vessels led to an especially pronounced decrease in the length of small-caliber (<30 μm) blood vessels 3 hours after injury ($p < 10^{-5}$) and in the length of small (<30 μm) and medium (30-65 μm) blood vessels 24 hours after injury ($p < 10^{-4}$) compared to their initial state. Therefore, the tissues of the intestinal wall are in a state of ischemia, which gradually increases over time. Remarkably, OCTA modality provides the unique ability for real time detection of changes in functional status of the tissues, long before they become visible on histology. The fact is that in the most cases histological examination did not allow assessing the dynamic changes in the vascular network and detected only more pronounced acute discirculatory disorders 24 hours after the spinal injury.

The acute period of spinal cord injury is accompanied by a change in the endogenous autofluorescence of the mucous membrane of the small intestine: in 3 h after injury a statistically significant (p=0.0001) decrease (to 1.05 [1.01; 1.09] ns vs 1.17 [1.12; 1.20] ns before injury) in the mean fluorescence lifetime (τ_m) was recorded, but in 24 h after injury τ_m had a statistically significant (p=0.0001) upward trend (1.23 [1.19; 1.27] ns) relative to the two previous indicators. The percentage contribution of the short component (a_1) in the mucous layer of the intestinal wall 3 hours after the spinal injury increased in comparison with the intact intestine from 73.4 [72.1; 74.8]% to 80.8 [79.6; 81.9]% (p=0.0001) and decreased to 76.1 [75.0; 78.0]% after 24 hours (p=0.0001). The data obtained indicate a change in metabolism in the tissues of the small intestine after spinal cord injury.

The proposed combination of two methods (OCTA and FLIM) can be used in further experiments to clarify the mechanisms of changes in intestinal blood circulation and metabolism in response to trauma of the nervous system.

This research was funded by the Russian Science Foundation, grant number 19-75-10096.

REFERENCES

[1] G.M. Holmes et al, Exp Neurol. 320, 113009, 2019.
[2] E.N. Blanke et al, Neural. Regen. Res. 16, 254-263, 2021.
[3] R. Steensgaard et al, Rehabil. Nurs. 44, 11-19, 2019.
[4] N. Paker et al, Turk. J. Phys. Med. Rehabil. 64, 322-327, 2018.

Diagnostics of peripheral blood flow disorders in various pathologic conditions using wearable laser Doppler flowmetry devices

Elena ZHARKIKH[1] and Andrey DUNAEV[1]

[1]*Research and Development Center of Biomedical Photonics, Orel State University, Russian Federation*

ev.zharkikh@gmail.com

ABSTRACT

Involvement of the blood microcirculation system in many functions of the body leads to the fact that the microcirculatory bed is one of the first links in the pathogenesis of various diseases, such as diabetes mellitus (DM). The aim of the present work was to improve the quality of diagnostics of peripheral blood flow disorders by developing a diagnostic method based on a distributed system of wearable laser Doppler flowmetry (LDF) devices without the use of functional tests.

In the present work, we conducted a study involving patients with diagnosed type 2 DM [1], conditionally healthy volunteers of different age groups [2] and patients undergoing rehabilitation after COVID-19 coronavirus infection [3]. The study consisted of a 10-minute recording of LDF signals simultaneously in the upper and lower limbs without the use of functional tests. Distributed system of wearable analyzers "LAZMA PF" (SPE "LAZMA" Ltd.) was used for registration of LDF signals. The devices were placed on the dorsal surface of wrists, the volar surface of the of fingers and toes and the inner surface of the upper third of the shins. During the measurement. patients were placed in the supine position.

The results of the study revealed an increase in the index of microcirculation (I_m, p.u.) and a decrease in the regulatory activity of blood flow with aging. In patients with DM the decrease in the level of I_m and nutritive blood flow (I_{mn}, p.u.) in the toe area and an increase in these parameters in the wrist area compared to the control group. Also, patients were characterized by decreased myogenic tone in the wrists and decreased contribution of the endothelial oscillations in the total power of the LDF wavelet spectrum in the upper and lower extremities. The contribution of pulse oscillations was elevated in patients in the feet, which may indicate an increase in the vascular wall stiffness. The findings in the wrists may indicate that the body is attempting to compensate for the disturbances in the microcirculation by activating nutritive blood flow and increasing the number of functioning capillaries. Patients with long COVID-19 syndrome were characterized by decreased values of I_m and I_{mn}, as well as increased total oscillatory activity of blood flow in both upper and lower extremities.

Thus, the developed approach to diagnostics of peripheral blood flow disorders, based on the use of wearable LDF analyzers, has been tested in clinical conditions and demonstrated the ability to detect peripheral blood flow disorders in various pathological conditions.

The study was supported by the Russian Science Foundation grant № 23-25-00522.

REFERENCES

[1] E.V. Zharkikh et al, Human Physiology, 48(4), pp. 456-464, 2022.
[2] E.A. Zherebtsov et al, in Biomedical Photonics for Diabetes Research, pp. 107-135.
[3] E.V. Zharkikh et al, Diagnostics 13(5), 920, 2023.

Spatial frequency domain imaging in total blood hemoglobin assessment: comparison to other non-invasive optical techniques

Boris Yakimov[1,2], Kirill Buiankin[1], Georgy Denisenko[2], Ilia Bardadin[1] and Evgeny Shirshin[1,2]

[1]*Faculty of Physics, M.V.Lomonosov Moscow State University*
[2]*Laboratory of Clinical Biophotonics, Biomedical Science and Technology Park, Sechenov First Moscow State Medical University*

bp.jakimov@physics.msu.ru

ABSTRACT

Hemoglobin (Hb) is the main protein in the human blood, responsible for oxygen transport in the body, thus, the assessment of the total Hb concentration in the patient's blood is of high importance. Especially, correct estimation of Hb blood concentration is important to detect the decreased level of total hemoglobin (anemia), as it affects approximately ~30% of woman and children [1], while undiagnosed or improperly treated anemia can lead to adverse outcomes and significant reduction of the life quality [1].
Recently, a large number of works have demonstrated the optical approaches being capable to non-invasively quantitate blood hemoglobin level, including RGB imaging of the conjunctiva [2], analysis of images of the fundus and external eye [3,4], analysis of photographic images of human nails [5], analysis of photoplethysmography data. Despite a large number of similar works, and even start-ups offering non-invasive determination of hemoglobin using smartphone camer, the real accuracy of such approaches is still difficult to determine, since original works are usually overoptimistic in the level of error of the proposed method, which is then not confirmed in independent works. comparing different approaches [6].
One source of error in most optical techniques may be that the detected optical response of the tissues used to determine the hemoglobin level is simultaneously related to the absorption and scattering of light by the tissues. For a more accurate assessment of the absorption coefficient of tissue chromophores, and in particular, hemoglobin, we suggest using the spatial frequency domain imaging method for the subsequent assessment of hemoglobin content in blood. In this report, we will discuss what levels of error can be achieved using this technique, as well as compare it with other optical methods for determining the level of hemoglobin in tissues.

The work was supported by the Russian Science Foundation (grant No. 22-25-00759).

REFERENCES

[1] E. Gayat et al. PloS one 7.1 (2012): e30065.

[2] S. Suner, et al. PloS one 16.7 (2021): e0253495.

[3] A. Mitani Nat Biomed Eng 4, 18–27 (2020).

[4] B. Babenko et al. The Lancet Digital Health 5.5 (2023): e257-e264.

[5] R. G. Mannino,et al.. Nature communications, 9(1) (2018) 4924.

[6] M. F. Young, et al. PLoS One 16.7 (2021): e0254629.

Low-frequency Raman spectroscopy of organic semiconductors and biomolecules

Olga PARASHCHUK[1], Andrey SOSOREV[2], Oleg KHARLANOV[1], Mikhail VENER[3], Artem TRUBITSYN[1] and Dmitry PARASCHUK [1]

1) Faculty of Physics, Lomonosov Moscow State University, Russia

2) Enikolopov Institute of Synthetic Polymeric Materials, Russian Academy of Sciences, Russia

3) Kurnakov Institute of General and Inorganic Chemistry, Russian Academy of Sciences, Russia

olga_par@physics.msu.ru

ABSTRACT

Low-frequency (10–200 cm^{-1}) Raman (LF Raman) spectroscopy provides information on high amplitude molecular motions, motions of parts of molecules and collective motions involving several molecules. Recently, it has been shown that the ratio of integral intensities of the LF Raman spectra to the high-frequency one can be used as an indicator of dynamic disorder and compactization for two classes of materials: π-conjugated organic semiconductors (OSs) - promising for the use in organic electronic devices, and nucleic acids, DNA and RNA, responsible for the vitally important functions of storage, transmission and realization of the genetic information.

The use of OS in high-performance organic electronic devices requires a high mobility of charge carriers, calling for rational design and efficient screening of new high-mobility OS materials. Indeed, high-amplitude intermolecular vibrations in OSs cause dynamic disorder - fluctuations of the charge transfer integrals between the molecules - which disrupts charge delocalization between the molecules and reduces the charge-carrier mobility. It has been established that the Raman intensities of LF modes are related to the contribution of these modes to dynamic disorder [1, 2]. The relative intensity of LF Raman modes shows the lower values in the OSs with a lower dynamic disorder. The corresponding, LF Raman-based approach to probing dynamic disorder has been demonstrated on various OS representatives: four series of oligomeric OSs - polyenes, oligofurans, oligoacenes, and heteroacenes [1]; derivatives of naphthalenediimides [2]; crystalline OSs consisting of π-isoelectronic small molecules (i.e., having the same number of π-electrons) [3]; co-oligomers of thiophene-phenylene CF_3-PTTP-CF_3 and its substituted derivative [4]. As a result, we have formulated a spectroscopic method for a fast and non-contact assessment of the charge-carrier mobility in crystalline OS [5]. We expect that the proposed approach will provide a simple and practical way to rapidly screen among many others OS with high charge mobility prior to their study in electronic devices.

One of the parameters of biomolecules that is important for the integrity of hereditary information and its transmission during cellular processes is the compactization of a biomolecule [6]. It is expected that the relative intensity of the LF Raman spectra of DNA and RNA can be an indicator of their compactization, since in more compact molecules the amplitude of larger-scale molecular motions corresponding to the LF region of the Raman spectra is lower. This is shown for the samples of DNA with different compactization: “cut” and supercoiled DNA and ribosomal and “relaxed” RNA. We also track the changes in the DNA and ribosome spectra with time and find that for the former, a clear decrease of the LF intensity associated with solvent evaporation and denser packing is observed, while for the RNA, the spectrum changes only slightly because of the inherent compactization of the ribosome.

Briefly, we show that LF Raman spectroscopy is a powerful tool for predicting and estimating the most important parameters for OS (carrier mobility) and DNA/RNA (molecular compactization).

REFERENCES

[1] O.G. Kharlanov et al, Adv. Electron. Mater. 7, 2100579, 2021.
[2] M.V. Vener et al, Adv. Electron. Mater. 7, 2001281, 2021.
[3] A.Yu. Sosorev et al, Phys. Chem. Chem. Phys. 23, 15485–15491, 2021.
[4] V.A. Trukhanov et al, RSC Adv. 10, 28128, 2020.
[5] M.K. Nuraliev et al, J. Chem. Phys. 153, 174303, 2022.
[6] A.Yu. Sosorev et al, JETP Lett. 116, 335–341, 2022.

This work was supported by Russian Science Foundation, project #22-72-10056.

Design and optimalization of laser-induced drug release in stroke therapy

Viktória PÉTER[1], László JANOVÁK[2], Mohamed M. ABDELGHAFOUR[2], Béla HOPP[3], Tamás SMAUSZ KOLUMBÁN[3], Eszter FARKAS[4,5], Ferenc BARI[1],

[1]Department of Medical Physics and Informatics, Albert Szent-Györgyi Medical School, University of Szeged
[2]Department of Physical Chemistry and Materials Science, University of Szeged, Hungary
[3]Department of Department of Optics and Quantum Electronics, University of Szeged, Hungary
[4]Hungarian Centre of Excellence for Molecular Medicine, University of Szeged, Cerebral Blood Flow and Metabolism Research Group, Szeged, Hungary
[5]Department of Cell Biology and Molecular Medicine, Albert Szent-Györgyi Medical School, Faculty of Science and Informatics, University of Szeged, Hungary

bari.ferenc@med.u-szeged.hu

Stroke therapy requires precise delivery of potentially neuro-and vasoprotective drugs to the affected area in the brain. Conventional drug administration often results in unintended systemic side effects since the effective concentration in the injured tissue should be high enough. The skull bone is selectively transparent for IR light. Therefore, laser induced drug release allows for localized administration, reduces the systemic distribution of the compound and minimizes the side effects in non-targeted tissues. Nimodipine (NIMO) is an L-type calcium channel blocker specifically used in the treatment of certain types of hemorrhagic stroke. We have shown in various animal models that local application of NIMO accelerates the recovery of blood flow in the injured brain and enhances the reestablishment of neurovascular coupling [1]. Furthermore, it was also presented that the biocompatible poly(ethylene succinate) (PES) polyester is a promising candidate as a drug delivery system (DDS) for the poorly water-soluble NIMO [2]. Its melting temperature (38.4 °C) is close to the human body temperature so minimal local heat treatment which can easily induced by gold nanorods (GNRs) based photothermal therapy [3] allows the release of the encapsulated NIMO.

Materials and methods: The polymeric (PES) component of the DDS was synthetized by direct melt polycondensation method using ethylene glycol and succinic acid monomers [2,5], while the GNRs was prepared according to the well-known wet-chemical synthesis method of Luis M. Liz-Marzán [5]. Encapsulated form of NIMO into the obtained PES polyester was prepared by using precipitation method in the presence of GNRs [2]. Beside the structural (IR, NMR, XRD, etc.) and morphological (TEM, SEM, DLS) characterization of the DDS the thermoanalytical (TG and DSC), colloidal stability and drug release properties of the samples were also investigated.

Results: Laser induced drug release can be performed in non-invasive manner and can reduce the associated risks and complications. In this work the NIMO drug was encapsulated into biocompatible PES polymeric nanoparticles (encapsulation efficiency >90%) loaded with GNRs. The successful polycondensation of the PES polyester with M_w = 5046 g/mol molecular weight (determined by GPC) was confirmed by FTIR and NMR measurements. It was also presented that the GNRs with aspect ratio (AT) of 5,78 ± 0,98 nm have a strong absorption peak at λ= 1140 nm, thus, the rods can be excited with a NIR laser. As a result, a significant increase in temperature (even up to ΔT=20 °C), which can be controlled by the laser intensity, could be induced in the aqueous dispersion. At elevated (T > 38.4 °C) temperature ensured by the laser irradiation of the embedded GNRs the PES polyester was melted, and the spherical structure of the particles were disintegrated. This laser induced heat generation was also manifested in the release properties of the DDS according to the *in vitro* tests.

It is important to note that while laser-induced drug release holds promise in stroke therapy, further research and development are still needed to optimize its efficacy, safety applicability in preclinical settings.

Supported by Laserlab-Europe (ALTIS) and NKFIH124334 (Hungary)

REFERENCES

[1] Menyhart et al., J. Neurochem. 2023 https://doi.org/10.1111/jnc.15792
[2] Abdelghafour et al., Int. J. of Pharma. 618 (2022) 121653, https://doi.org/10.1016/j.ijpharm.2022.121653
[3] Chen et. al., J. Am. Chem. Soc. 2014, 136, 20, 7317−7326, https://doi.org/10.1021/ja412735p
[4] Abdelghafour et al., Polymers 2021, 13, 2725., https://doi.org/10.3390/polym13162725
[5] Liz-Marzán et. al., Coord. Chem. Reviews 249 (2005) 1870–1901, https://doi.org/10.1016/j.ccr.2005.01.030

Comparison of the Fluorescence Spectra of Teeth Samples under UV Excitation

Irina BALAKHNINA, Nikolay BRANDT, Stepan LEBEDENKO, Anna MANKOVA, Samvel VERDIIAN, Igor LEBEDENKO

Faculty of Physics, Lomonosov Moscow State University, Russia

mankova@physics.msu.ru

ABSTRACT

Appearance is important for each person, and, even today, when medicine and cosmetology are well developed, several tasks require specific consideration. In particular, the question arises, can a denture completely replace a natural tooth? In this regard, unresolved problems exist in dental prosthetics. One of them is to mimic the natural fluorescence of the tooth. To imitate natural fluorescence, a zirconia denture is usually coated with special dyes and glazes [1]. The three most commonly used fluorescent materials are Lava Ultimate polymer with ceramic nanofiller, Lava Plus tetragonal zirconia, and Lava Esthetic zirconia. The fluorescence of Lava Ultimate is characterized by two lines peaked at 482 and 435 nm. The other two materials have one fluorescent line peaked at 435 nm. Lava Esthetic material has the highest fluorescence intensity [2]. However, during firing and aging of ceramic prostheses, they start losing their fluorescence properties, which is their significant drawback.

On the other hand, the selection of materials for tooth covering nay involve quantitative comparison of their fluorescent characteristics. This requires the development of a technique for reproducible fluorescence spectroscopy of natural teeth and dentures.

In this work we propose an experimental setup and a method for processing of the fluorescence spectra of teeth, which allows quantitative comparison. Spectra of natural teeth of healthy donors of different ages were measured. The spectra were compared under excitation of similar areas of different teeth and different parts of the same tooth (distal and occlusal surfaces). The excitation of each area was carried out without focusing of radiation on the surface of the tooth.

A DORS 115 lamp with a maximum radiation intensity at a wavelength of 366 nm and a bandwidth of about 16 nm was used as a source of UV excitation. The sample was fixed under a lamp, and scattered and fluorescent light was collected by an optical fiber connected to the input port of the Ocean Insight HR4000 spectrometer. The measurements were performed in a spectral interval of 200–1100 nm with a spectral resolution of about 0.7 nm.

Figure compares two fluorescence spectra of one molar tooth under excitation of its. The spectra are shifted along the vertical axis so that the mean signal in a spectral interval of 200–250 nm is zero. In addition, the spectra are normalized to the intensity of the line at a wavelength of about 360 nm, which results from the Rayleigh scattering of the excitation radiation by the sample. Since the intensity of the Rayleigh scattering is much greater than the fluorescence intensity and weakly depends on a specific sample, the processing makes it possible to quantitatively compare fluorescence intensities of different samples. It can be seen that the fluorescence intensity of the end face of the tooth is approximately 1.3 times higher than the fluorescence intensity of its lateral surface.

The paper discusses the results of measurements of the fluorescence spectra of different parts of the teeth of different donors.

This work was supported in part by the Russian Science Foundation (project no. 21-78-10077).

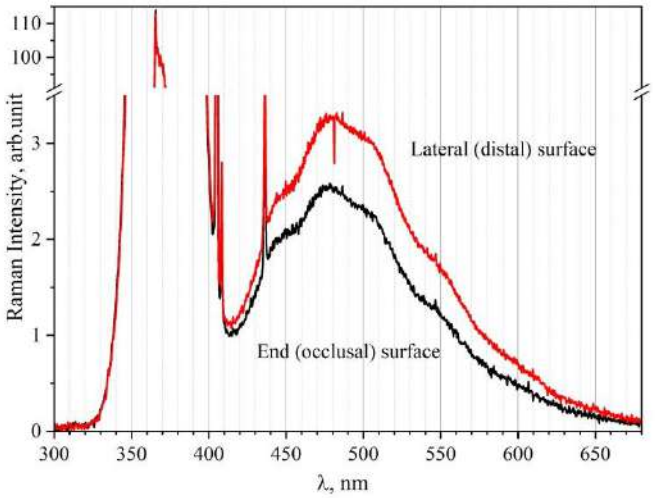

Figure: *Fluorescence spectra of a molar tooth of an adult donor in the occlusal (end) and distal (lateral) areas under excitation with a DORS 115 UV lamp*

REFERENCES

[1] E.E. D'yakonenko, S.A. Verdiyan, D.A. Sakhabieva, and I.Yu. Lebedenko, Stomatologiya 100(3), 109-114, 2021.
[2] A. Kauling, C. Volpato, O. Carvalho, M. Pereira, J. Güth. Dental materials: official publication of the Academy of Dental Materials 34:e127, 2018.

Multivariate analysis and deep learning for recognition of surface-enhanced Raman spectra of human blood in problems of medical physics

Lyudmila Bratchenko[1], Sahar Al-Sammarrae[1], Elena Typikova[1], Peter Lebedev[2], Maria Skuratova[3] and Ivan Bratchenko[1]

1- Samara National Research University, Samara, Russia

2- Samara state medical university, Samara, Russia

3- Samara regional clinical hospital named after NI Pirogov

shamina94@inbox.ru

ABSTRACT

Currently, one of the most accessible methods for the initial assessment of the human body state is a blood test. One of the promising highly selective methods that provide analyzing the component features of biological objects at the molecular level is surface-enhanced Raman spectroscopy (SERS). However, the use of SERS in practical applications is complicated by the risk of insufficient reproducibility associated with the inhomogeneity of the electromagnetic field amplification, the appearance of the blinking effect, and complicated sample preparation. Moreover, in case of multicomponent media, the obtained Raman characteristics are not a linear combination of the spectral contribution of all compounds that make up the tested complex. Therefore, the spectra of body fluids are a combination of the spectral contribution of all analytes, characterized by multicollinearity and nonlinearity. Therefore, the analysis of the spectral characteristics of body fluids is associated with the problem of multiple spectrum overlaps. Current methods for interpreting Raman characteristics are based on multivariate analysis, including chemometric methods [1] and deep learning methods [2]. However, it should be noted that most of the works are focused on the classification of Raman spectra according to a specific attribute, while the selection of the spectral contribution of a particular analyte to the spectrum of the medium and the assessment of its content remains an urgent task in the analysis of the structural and component features of biofluids in medical physics.

In the current study, a database of experimental data was formed based on the registration of the spectral characteristics of the serum and blood plasma of patients with chronic kidney disease, patients with chronic heart failure, conditionally healthy subjects using spectral analysis based on surface-enhanced Raman scattering (more than 600 spectra). A comparative analysis of the multivariate approach (based on the method of projection to latent structures) and the approach involving deep learning (based on a convolutional neural network) for the recognition of SERS spectra of serum and plasma was performed using the example of the problem of sample discrimination by the presence/absence of fibrinogen and the tasks of regression of the content of total protein, urea and creatinine. The interpretation of the constructed classification and regression models is presented to reduce the problem of overfitting and the "black box" of multivariate analysis of the Raman characteristics of multicomponent biological media. The separation of the spectral contribution of creatinine in the bands 630 - 650 cm^{-1}, 720 - 750 cm^{-1}, 1380 - 1415 cm^{-1} and the spectral contribution of urea in the bands 720 - 750 cm^{-1}, 990-1030 cm^{-1} was demonstrated. In general, the proposed method for recognition and interpretation of the Raman spectra of biofluids of the human body can be widely used in biomedical applications, in particular in the field of liquid biopsy.

REFERENCES

[1] Htet T. T. M., et al. PLS-regression-model-assisted raman spectroscopy for vegetable oil classification and non-destructive analysis of alpha-tocopherol contents of vegetable oils, Journal of Food Composition and Analysis, 103, 104119, 2021.

[2] L.A. Bratchenko, et al. Analyzing the serum of hemodialysis patients with end-stage chronic kidney disease by means of the combination of SERS and machine learning, Biomedical Optics Express, 13, 4926-4938, 2022.

Simultaneous detection of fluorescent and hemodynamic signals from deep brain structures in awake mice

Xiaoxi FU[1], Pengcheng LI[1] and Jinling LU[1]

[1]*Britton Chance Center and MoE Key Laboratory for Biomedical Photonics, Wuhan National Laboratory for Optoelectronics, Huazhong University of Science and Technology, China.*

lujinling@hust.edu.cn

ABSTRACT

Brain functional optical imaging plays an important role in neuroscience because of its high spatial and temporal resolution. Multi-mode optical imaging methods is becoming a powerful tool for exploring changes in brain function with its characteristics of multi-parameter simultaneous measurement. In this paper, we present a multi-modal imaging system based on invasive gradient index (GRIN) lens, which combines GCaMP6 fluorescence imaging and laser speckle contrast imaging (LSCI) in deep brain regions through a head-mounted microscopic imaging system. It allows simultaneous detection of the relative changes of neural activity and cerebral blood flow (CBF) in the deep brain region, the electrophysiological signal in the cortex and the body movement information. Using this system, we successfully recorded GCaMP6 fluorescent signals and cerebral blood flow from the ventral posteromedial nucleus (VPM) in thalamus of a head-restrained mouse during cortical spreading depression (CSD).

KEY WORDS: multi-modal optical imaging; micro-endoscope; thalamus; deep brain

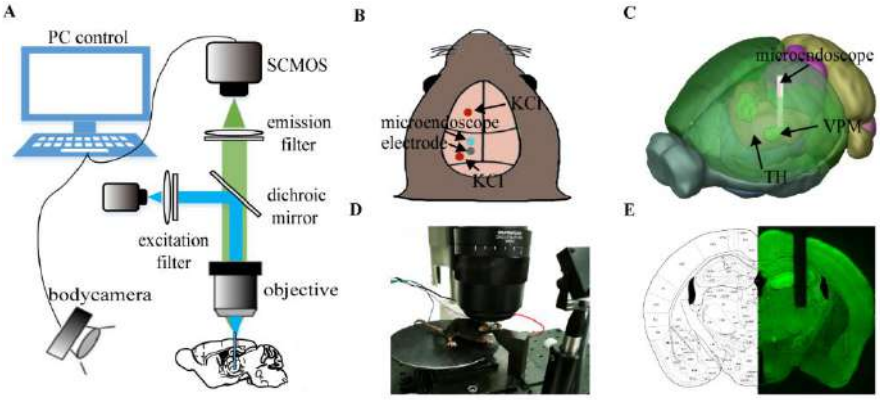

Figure1: *Optical system for VPM fluorescence imaging in awake animals. (A)Schematic of the imaging system. (B-C) Schematic of implantation of the GRIN lens and chronic electrode. The 3D model was obtained from the Allen brain atlas. (D) Head-fixed setup with an infrared camera for motion detection .(E) Brain slices matching the standard mouse brain atlas*

REFERENCES

[1] Misgeld T. et al. Nat. Rev. Neurosci., 7,449-463, 2006.
[2] Ming Chen, et al. Optics Letters 43, 5627-5630, 2018
[3] Fu et al. et al. The Journal of Headache and Pain, 23,15,2022

ACKNOWLEDGEMENTS

This work was supported by National Natural Science Foundation of China (Grant No. 81971659), and Fundamental Research Funds for the Central Universities (HUST: 2019kfyXMBZ009), CAMS Innovation Fund for Medical Sciences (CIFMS, 2019-I2M-5-014) and the director fund of the WNLO.

Fluorescent intravital bioimaging to analyze nanoparticles cytotoxicity and biodistribution using tissue slices

Svetlana Rodimova[1], Artem Mozherov[1], Ilia Shchechkin[1,2], Dmitry Krylov[1,2], Dmitry Kozlov[1,2], Michael Zyuzin[3] and Daria Kuznetsova[1,2]

[1]*Privolzhsky research medical university, Russia*
[2]*Lobachevsky Nizhny Novgorod National Research State University, Russia*
[3] *ITMO University, Russia*

srodimova123@gmail.com

ABSTRACT

Nowaday, an approach based on the use of small bioactives are highly promising [1]. However, there is still a problem of the lack of an effective method for their delivery with a controlled release period, their accumulation and excretion. The use of nanoparticles makes it possible to control the release of bioactive molecules and improve their delivery to liver cells. Modern fluorescence bioimaging. In addition, the use of the model of precision-cut liver slices made it possible to screen several types of nanoparticles, excluding the individual contribution of the animal organism, simplifying the analysis and interpretation of the results.

Precision-cut liver slices were obtained using vibrating microtome 7000 cm3-2 was based on the protocol of Pearen et al. [2], and were placed in 12-well plate with a standard CO2-conditioned form of DMEM supplemented with 0.1 μm of dexamethasone and 10% FBS. Next, cultivation was carried out in DMEM medium with the addition of nanoparticles at a concentration of 50 and 100 mg/ml and incubated for 3, 24, and 48 hours. All obtained tissue explants were preincubated for 1 h in DMEM medium on an orbital shaker (90 rpm). The average size of all nanoparticles was 100 nm. Gold nanoparticles in the form of nanorods were synthesized based on seed mediated mechanism. The synthesis of SiO2 nanoparticles was carried out using the sol-gel method. Polylactide (PLA) nanoparticles were synthesed by single-emulsion solvent extraction. All nanoparticles were modified with a Cy 5 fluorescent label. Liver slices were stained with LysoTracker Yellow HCK-123 and Phalloidin FITC. Using multiphoton microscopy, we assessed the tissue structure of liver slices, and visualized cellular ultrastructures stained with fluorescent dyes. Additionally, X-ray microtomography were used for analyzing the distribution of nanoparticles. Using FLIM, we analyzed the metabolic state of hepatocytes based on fluorescence lifetime contributions of the free and bound forms of NADH and NADPH.

As a result, of those types of nanoparticles (SiO2, gold, and PLA), PLA nanoparticles are the most promising for developing a new approach to stimulating regeneration. PLA nanoparticles accumulated most effectively in liver cells, mainly in the cytoplasm of hepatocytes. Also, using FLIM, we revealed low cytotoxicity of PLA nanoparticles, due to the relative contributions of fluorescence lifetimes of bound form of NADH and NADPH did not differ significantly from control values. The obtained results will became a basis for further development of a strategy to stimulate liver regeneration based on nanoparticles modified with biomolecules.

The work was supported by the Grant from the Russian Science Foundation №23-25-00100.

REFFERENCES

[1] Z. Liu et al, Adv Mat, 30, 1703393, 2018.
[2] M. A. Pearen et al, JoVE, 157, e60992, 2020.

Biomedical label-free method reveals criteria for toxic liver damage in precision-cut liver slices

Maria Karabut[1], Svetlana Rodimova[1], Dmitry Krylov[1,2], Dmitry Kozlov[1,2], Artem Mozherov[1] and Daria Kuznetsova[1,2]

[1] *Privolzhsky research medical university, Russia*
[2] *Lobachevsky Nizhny Novgorod National Research State University, Russia*

maria.karabut@gmail.com

ABSTRACT

Abuse with hepatotoxic agents is a major cause of acute liver failure. The search for new criteria indicating the acute or chronic pathological processes is still a challenging issue that requires the selection of effective tools and a research models. Modern label-free methods of multiphoton microscopy with second harmonic generation (SHG) and fluorescence lifetime imaging microscopy (FLIM) expand the possibilities of studying the structural and functional state of liver tissue at the cellular level [1]. The aim of this work is to identify characteristic changes in the metabolic state of hepatocytes in precision-cut liver slices under toxic damage by the most common toxins - ethanol, carbon tetrachloride (CCl4) and acetaminophen (APAP), commonly known as paracetamol.

Vibrating microtome 7000 cm3-2 was used to obtain liver slices using the protocol of Pearen et al. [2], and were placed in separate wells of a 12-well plate with a standard CO2-conditioned form of DMEM supplemented with 0.1 μm of dexamethasone and 10% FBS, and incubated at 37 °C on orbital shaker (90 rpm). To induce APAP toxic damage, the liver slices were placed for 3 h in a 10 mM solution of APAP diluted in DMEM. To induce ethanol toxic damage, liver slices were placed for 3 h in 25 mM ethanol diluted in DMEM. For the CCl4 model the liver slices were incubated for 3 h with 2 mL standard culture medium, and a piece of filter paper soaked in 10 μL of CCl4 was attached to the lid of the 12-well plates. As a control, we used liver slices cultivated in DMEM without toxins. Monitoring were performed after 3 h, 24 h and 48 h of incubation. Using FLIM, we analyzed the metabolic state of hepatocytes based on fluorescence lifetime contributions of the free and bound forms of NADH and NADPH.

We have determined characteristic optical criteria for toxic liver damage, and these turn out to be specific for each toxic agent, reflecting the underlying pathological mechanisms of toxicity. Multiphoton microscopy revealed damaged liver cells with high and low NAD(P)H autofluorescence intensity. We also showed, that exposure to APAP increases the contribution of the bound form of NAD(P)H, while exposure to ethanol and CCl4 showed a significant decrease in the contribution of the bound form of NAD(P)H, which reflects differences in the mechanisms of damage by each toxic agent. The results obtained are consistent with standard methods of molecular and morphological analysis. Thus, our approach, based on optical biomedical imaging, is effective for intravital monitoring of the state of liver tissue in the case of toxic damage or even in cases of acute liver injury.

The work was supported by the Grant from the Russian Science Foundation №22-25-00098.

REFFERENCES

[1] M. S. Roberts et al, Eur J Pharm Biopharm, 77, 469-488, 2011.
[2] M. A. Pearen et al, JoVE, 157, e60992, 2020.

Evaluation of the safety and biodistribution of nanoparticles in precision-cut liver slices using fluorescent bioimaging

Vadim Elagin[1], Svetlana Rodimova[1], Dmitry Krylov[1,2], Dmitry Kozlov[1,2], Artem Mozherov[1], Michael Zyuzin[3] and Daria Kuznetsova[1,2]

[1]*Privolzhsky research medical university, Russia*
[2]*Lobachevsky Nizhny Novgorod National Research State University, Russia*
[3]*ITMO University, Russia*

elagin.vadim@gmail.com

ABSTRACT

Currently, the development of new methods for delivering bioactive molecules to the liver tissue to stimulate hepatic regeneration remains an urgent task [1]. The most promising approach is the use of nanoparticles as delivery systems. Application of label-free methods of multiphoton microscopy, second harmonic generation (SHG) and time-resolved FLIM microscopy will expand the possibilities of analyzing the metabolic state of hepatocytes. In addition, the use of the model of precision-cut liver slices made it possible to screen several types of nanoparticles, excluding the individual contribution of the animal organism, simplifying the analysis and interpretation of the results. In addition, the model of precision-cut liver slices, will allow simultaneous testing of different types of nanoparticles, excluding the individual contribution of the animal organism.

Vibrating microtome 7000 cm3-2 was used to obtain liver slices using the protocol of Pearen et al. [2], and were placed in separate wells of a 12-well plate with a standard CO2-conditioned form of DMEM supplemented with 0.1 μm of dexamethasone and 10% FBS. Next, cultivation was carried out in DMEM medium with the addition of nanoparticles at a concentration of 50 and 100 mg/ml and incubated for 3, 24, and 48 hours. All obtained tissue explants were preincubated for 1 h in DMEM medium on an orbital shaker (90 rpm). Gold nanoparticles with a size of 100-120 nm in the form of nanorods were synthesized using a standard protocol based on seed mediated mechanism. The synthesis of SiO2 nanoparticles with a size of 20-100 nm was carried out using the sol-gel method. Polylactide (PLA) nanoparticles with a size of 100 nm are tested by single-emulsion solvent extraction. All nanoparticles were modified with a Cy 5 fluorescent label. Liver slices were stained with LysoTracker Yellow HCK-123 and Phalloidin FITC. Using multiphoton microscopy, we assessed the tissue structure of liver slices. Using FLIM, we analyzed the metabolic state of hepatocytes based on fluorescence lifetime contributions of the free and bound forms of NADH and NADPH.

As a result, SiO2 showed low accumulation in the liver cells and, at the same time, low cytotoxicity. Gold nanoparticles showed effective accumulation in liver cells, however, its had strong cytotoxic effect on liver cells. Finally, polylactide nanoparticles showed high accumulation in liver cells, mainly in the cytoplasm of hepatocytes. Using FLIM, we revealed low cytotoxicity of PLA nanoparticles, due to the relative contributions of fluorescence lifetimes of bound form of NADH and NADPH did not differ significantly from control values. Thus, PLA nanoparticles seem to be the most promising for further development of a strategy for stimulating liver regeneration using nanoparticles modified by bioactive molecules. Based on the obtained data, we will select the appropriate miRNAs that stimulate liver regeneration.

The work was supported by the Grant from the Russian Science Foundation №23-15-00421.

REFFERENCES

[1] Z. Liu et al, Adv Mat, 30, 1703393, 2018.
[2] M. A. Pearen et al, JoVE, 157, e60992, 2020.

Photons distribution and propagation in biological tissue

Vanesa LUKINSONE[1], Santa APALKA[1], Uldis RUBINS[1], and Tatiana NOVIKOVA[2]

[1]*University of Latvia, Latvia*
[2] *CNRS, Ecole polytechnique, France*

Vanesa.lukinsone@gmail.com

ABSTRACT

The photon propagation and distribution in biological tissue were measured experimentally utilizing time-resolved spectroscopy. The *exvivo* measurements were done laterally for backscattering and for transmission through tissue. The created method allows measurements for frontal propagation in different thicknesses as well as within different distances, as schematically represented in Fig. 1.

The photon time-of-flight (PTOF) measurement method was utilized in this study. The set-up consisted of a picosecond Fianium white laser, a hybrid detector, processing card SPC-150 from Becker&Hickl, a set of interference filters, and a fiber holding system.
Remitted picosecond laser pulses have been detected at variable input-output fiber distances and tissue thickness in the spectral range 560 - 800 nm, with subsequent analysis of photon path length and light propagation in tissue. The measurements were taken from the skin and brain. Parameters related to the remitted photons, mean path length – will be presented and analyzed for skin, and brain tissue.

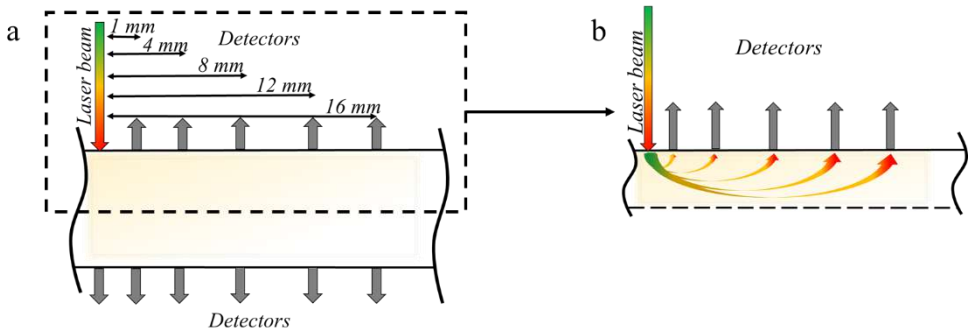

Figure 1: *Schematic of measurement method (a) Lateral backscattering and transmitted photon propagation through tissue, (b) Photon backscattering propagation through tissue for lateral measurements.*

Synthesis of ethosomes with methylene blue for transdermal photocosmetology

Arina VOITOVA[1], Kanamat EFENDIEV[1,2] and Victor LOSCHENOV [1,2]

[1]*BIOSPEC Ltd., Moscow, Russian Federation*
[2]*Prokhorov General Physics Institute of the Russian Academy of Sciences, Moscow, Russian Federation*

arina.voiova@chemistry.msu.ru

ABSTRACT

Transdermal drug delivery by ethosomes through skin barriers is effective method of combating dermatological and cosmetological problems. The ethosomes synthesized by us consist of clinically approved drugs: methylene blue (MB), lecithin, ethanol and water. The MB under light exposure with a wavelength 660 nm is released. On the one hand, MB is a good antioxidant, on the other hand, for the destruction of scar formations and aged skin areas is used. MB ethosomes was synthesized and their delivery method through *stratum corneum* (SC) was tested. The nanocarriers disrupt lipid barrier intercellular interactions and penetrate in the depth. The experiment on pork and human skin confirmed obtained results.

There is a noninvasive drug delivery problem trough protective skin barrier in dermatology and cosmetology. The lipid nanocarriers such as ethosomes in combination with photodynamic therapy (PDT) are offer for the problem solution [1]. The ethosomes with MB through SC are penetrate, further using light exposure with a wavelength 660 nm are disturbed. During aging inflammatory processes, occur in cells. The cells activity leading to the inflammation activation by restoring the mitochondria respiratory chain inhibits by MB [2]. In this case, radiation is either not carried out, or in small doses to cause apoptosis. As is known, apoptosis does not cause an inflammatory reaction. Active cells destruction simultaneously occurring at high doses enhances neoangiogenesis.

The particular aims of the work were MB ethosomes synthesis, obtain nanocarriers with a neutral ζ-potential, investigation their spectral-fluorescent characteristics and penetration depth, anti-aged method development through nanocarriers with PDT.

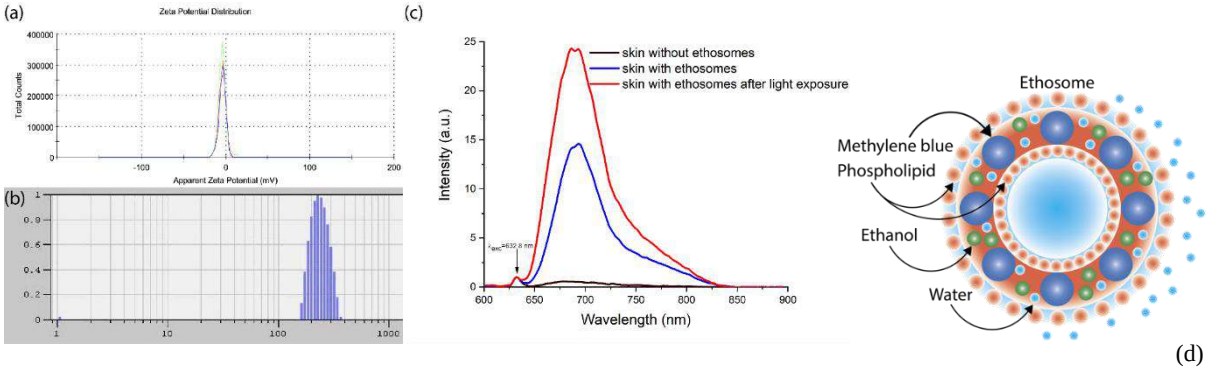

Figures: *(a) ethosomes neutral ζ-potential using a zeta-meter (b) the particle sizes by DLS (c) spectral-fluorescent diagnostics of skin with acne before and after application with ethosomes (d) schematic representation of ethosome.*

The MB ethosomes with neutral ζ-potential was sensitized. The neutral charge allows for deeper penetration trough SC. In addition, their sizes and spectrum-fluorescent characteristics were described. Transdermal delivery MB through nanocarriers and PDT for anti-aged treatment can be perspective.

REFERENCES

[1] Loginova A.G., Nikitenko I.S., Tikhonovsky G.V., Skobeltsin A.S., Voitova A.V., Loschenov V.B. (2022) Development of a method for assessing the depth of penetration of ethosomes with methylene blue into the skin during application and photodynamic exposure. *Biomedical Photonics*, *11*(4), 11-18.

[2] Xue, H., Thaivalappil, A., & Cao, K. (2021). The Potentials of Methylene Blue as an Anti-Aging Drug. *Cells*, *10*(12), 3379.

The study of excited-states relaxation pathways in NADH and FAD by the analysis of fluorescence quantum yield and fluorescence decay times

Ioanna GORBUNOVA[1], Maxim SASIN[1], Marina DANILOVA[1], Victor BELIK[1], and Oleg VASYUTINSKII[1]

[1]*Ioffe Institute, Russian Academy of Sciences, Russia*

i.gorbunova@mail.ioffe.ru

ABSTRACT

Reduced nicotinamide adenine dinucleotide (NADH) and flavin adenine dinucleotide (FAD) are important coenzymes involved in regulation of living cell metabolism and are actively used nowadays for non-invasive monitoring of living cells with FLIM [1]. However, the relationship between fundamental photophysical properties of these coenzymes and biochemical factors is still far from being understood [2, 3]. In this paper, comprehensive studies of fluorescence quantum yield and fluorescence decay times in NADH and FAD under one- and two-photon excitation in water–methanol, water–ethanol and water–propylene glycol solutions have been carried out. The aim of this study was to characterize the processes of nonradiative excited states relaxation in FAD and NADH and analyze the influence of intramolecular and microenvironmental properties on the rate of this processes.

The main results obtained were as follows. The quantum yield of NADH and FAD as a function of alcohols concentrations in solution is shown in (Fig. 1 a)-c)).

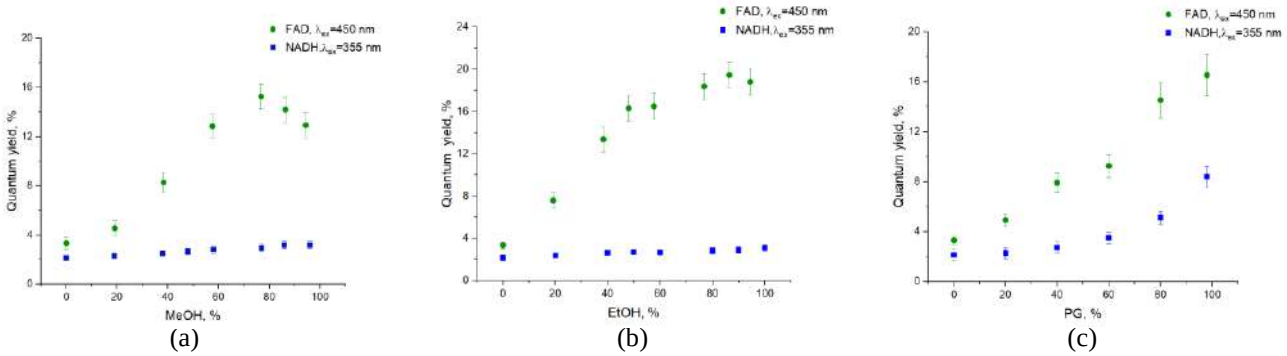

(a) (b) (c)

Figure 1: *Fluorescence quantum yield in NADH (blue squares) and FAD (green circles) as a function of (a) methanol, (b) ethanol, and (c) propylene glycol concentration.*

The quantum yield of both coenzymes increased with ethanol, methanol and propylene glycol concentration. As can be seen in (Fig. 1 a)-c)) a significant difference was observed between the behaviors of NADH and FAD fluorescence quantum yields. Fluorescence decay times τ_1 and τ_2 in NADH increased with alcohol concentrations, while both fluorescence decay times in FAD did not change significantly. The experimental results were analyzed using a novel theoretical model based on the quantum mechanical theory. This model allowed us to separate the contribution of several relaxation pathways in NADH and FAD excited states: relatively slow nanosecond and much faster picosecond processes. It was shown that an increase of fluorescence quantum yield in NADH with methanol and ethanol concentrations was due to change in the rate of relatively slow nanosecond nonradiative relaxation associated with the interaction of NADH with solvent molecules and with change in the NADH conformational composition. At the same time, a decrease in the efficiency of fast picosecond quenching in NADH at high propylene glycol concentrations was found that was explained by a slowdown in the rate of fast intramolecular singlet-triplet conversion and/or nonadiabatic electron transitions in high viscosity solutions. In the case of FAD, the significant increase in the fluorescence quantum yield with alcohols concentration in solution was mainly due to the decrease in efficiency of the rapid picosecond quenching that was caused by an electron transfer in the excited state. These processes in FAD occur due to π-stacking between adenine and isoalloxazine [2]. As a results, a significant difference in the dynamic processes occurring in the excited states of NADH and FAD during photo-excitation was demonstrated.

This research was funded by Russian Science Foundation, grant number 23-22-00230.

REFERENCES

[1] Ung, T.P.L., Lim, S., Solinas, X. et al., Sci Rep, 11, 22171, 2021.

[2] L. Radoszkowicz, et al, J. Phys. Chem. A, 114 (2), 1017–1022, 2010.

[3] I. Gorbunova, et al, J. Phys. Chem. B, 124 (47), 10682 – 10697, 2020.

Night Photostimulation of Clearance of Beta-Amyloid from the Brain of Mice with Alzheimer's Disease

Arina Evsukova[1], Alexander Dubrovskii[1], Inna Blokhina[1], Ivan Fedosov[1], Dariya Zlatogoskaya[1], Viktoria Adushkina[1], Alexander Shirokov[1,2], Andrey Terskov[1], Nikita Navolokin[1,3], Maria Tzoy[1], Ilana Agranovich[1], Valeria Telnova[1], Anna Tsven[1], Jürgen Kurths[1,4,5,6] and Oxana Semyachkina-Glushkovskaya[1,4]

[1]Department of Biology, Saratov State University, Russia.
2Saratov Scientific Centre of the Russian Academy of Sciences (IBPPM RAS), Institute of Biochemistry and Physiology of Plants and Microorganisms, Russia
3Department of Pathological Anatomy, Saratov Medical State University, Russia
4Humboldt University, Institute of Physics, Germany
5Department of Complexity Science, Potsdam Institute for Climate Impact Research, Germany
6Centre for Analysis of Complex Systems, Sechenov First Moscow State Medical University, Russia

arina-evsyukova@mail.ru

ABSTRACT

Alzheimer's disease (AD) is one cause of dementia associated with progressive associated with damages of neurons responsible for memory, language and thinking. With the increase in the aging population worldwide, AD has become a rapidly increasing public health concern. However, pharmacological therapies for AD have failed to show effectiveness and safety. Therefore, the search for non-pharmacological strategies for therapy of AD is an urgent problem in medicine. The meningeal lymphatic vessels (MLVs) plays an important role in resistance to the progression of AD. The development of methods for augmentation of functions of MLVs may contribute to progress in AD therapy. There is evidence that beta-amyloid (Aß) is excreted from brain tissues through the meningeal lymphatic vessels, which are activated during sleep. Photobiomodulation (PBM) is considered to be a non-pharmacological and safe approach for AD therapy. Based on these facts, we assume that PBM-stimulation of lymphatic removal of Aß during sleep may increase resistance to AD in mice.

To test our hypothesis, we studied the therapeutic effects of PBM during wakefulness and sleep in male mice (20-25 g, 3 month age) with the injected model of AD and in healthy animals. A fiber Bragg grating wavelength-locked high-power laser diode (LD-1267-FBG-350, Innolume, Dortmund, Germany) emitting at 1267 nm was used as a source of irradiation. PBM was used as a single laser dose of 9 J/cm^2 (on the skull) and 3 J/cm^2 on the brain surface or the PBM course at 81 J/cm^2 during 9 days. A two-channel cortical EEG/one-channel electromyogram was used for monitoring of wakefulness, non-rapid eye movement (NREM) and rapid eye movement sleep. The ex vivo confocal imaging of the whole brain and the deep cervical lymph nodes (dcLNs) as well as immunohistochemical assay were used for the study of PBM-stimulation of lymphatic removal of Aß from the brain. Additionally, the object recognition test was performed for the study of recognition memory.

In the first step, we analyzed the lymphatic removal of Aβ from the brain in healthy mice and with AD. Our findings revealed significant suppression of removal of fluorescent Aβ (FAβ) from the brain to dcLNs in mice with AD vs. healthy animals. In the second step, we studied the role of sleep in lymphatic removal of FAβ from the brain of healthy and AD mice. The results clearly demonstrate that the intensity of fluorescent signal from FAβ in dcLNs was much higher in mice injected with FAβ prior to sleep vs. awake mice received FAβ in the morning and who were not allowed to sleep during the day. The single PBM significantly increases lymphatic removal of FAβ that is more pronounced if PBM is applied during sleep vs. wakefulness. In the third step, we investigated the therapeutic effects of PBM during wakefulness and sleep under EEG control. The intensity of fluorescent signal from FAβ in dcLNs were higher in mice after PBM during NREM sleep vs. wakefulness. Our findings show also that recognition memory was decreased in AD mice vs. healthy animals that was improved after the PBM-course during NREM sleep better than after the PBM-course during wakefulness. There were no any changes in morphological characteristics of brain tissues after the course of PBM as well as in or in temperature on the skull after single application of PBM suggesting no side effects of PBM.

Our findings clearly demonstrate that the course of PBM during NREM sleep vs. wakefulness has better therapeutic effects for AD providing the best lymphatic removal of Aβ from the brain that is associated with effective recovery of recognition memory in mice with AD. These pioneering data shed light on the restorative mechanism of sleep and are an important informative platform for the development of innovative smart technologies for therapy of AD during sleep.

This study was supported by the RSF grant (23-75-30001) and RF Governmental grant no. 075-15-2022-1094.

Laser-Induced Dielectric Breakdown as a Novel Method for Obtaining Isotopically Enriched Nanoscale Substances

Roman KORNEV[1], Andrey BULANOV[1], Artur ERMAKOV[1] and Igor Gornushkin [2]

[1] *PECVD Department, G.G. Devyatykh Institute of Chemistry of High-Purity Substances of RAS, Russia*
[2]*Instrumental Analytical Department, BAM Federal Institute for Materials Research and Testing, Germany*

romanakornev@gmail.com

ABSTRACT

The possibility of obtaining high-purity, isotopically modified and nanostructured elemental substances ^{29}Si, ^{98}Mo, and ^{100}Mo, as well as ^{98}Mox^{10}By compounds from volatile halides under conditions of laser optical breakdown of a pulsed Nd:YAG laser is shown.

Currently, research in the field of developing new methods for obtaining high-purity, isotopically modified and nanostructured substances is being actively conducted. Interest in Si and Mo combining these forms has noticeably increased.

In nuclear medicine, ^{29}Si-enriched nanoparticles can be used as contrast agents in magnetic resonance imaging (MRI), and ^{98}Mo and ^{100}Mo isotopes can be used to obtain the unstable ^{99m}Tc radioisotope. These applications do not require large amounts of isotopically modified Si and Mo. Their obtaining belongs to the problems of small chemistry. When obtaining isotopically modified Si and Mo, it is expedient to use their volatile fluorides, for which technologies of isotope enrichment and deep purification are well developed. These halides have high chemical and thermal stability; therefore, plasma-chemical methods based on the plasma of a pulsed discharge generated by laser breakdown can be promising for separating ^{29}Si, ^{98}Mo, and ^{100}Mo from them. Laser breakdown in H_2+Ar+SiF_4 and H_2+Ar+MoF_6 mixtures in various stoichiometric ratios in the pressure range 30–760 Torr was carried out using a pulsed Nd:YAG laser. The pulse duration at a wavelength of 1064 nm was 15 ns, the repetition rate was 5 Hz. A pulse energy of 800 mJ was focused by a lens with a focal length of 5 cm. The energy density at the focus was 26 J/cm^3. It has been shown that when using a mixture based on 29SiF4, the sample contains a ^{29}Si crystalline phase with an average grain size of 30–50 nm (Fig. 1a). When using a mixture based on ^{98}MoF6, the sample contains a ^{98}Mo crystalline phase with an average grain size of 70–100 nm (Fig. 1b).

In this type of gas discharge, the possibility of forming superhard materials, isotopically modified molybdenum borides, was also studied. These substances in the form of nanosized particles have improved tribological properties. After ablation of metallic Mo in the H_2 + BF_3 mixture, the main phase was MoB_2 in the form of a nanodispersed powder with an average grain size of 100 nm (Fig. 1c) [1].

A technique for modeling gas-dynamic and thermal conditions in a low-temperature chemically active plasma induced by laser breakdown is proposed.

Using computational experiments, the features of gas mixture heating and the formation of nanoparticles in the LIBS reactor were studied.

The work was supported by the state task of the Ministry of Science and Higher Education of the Russian Federation, topic No. 0095-2019-0008.

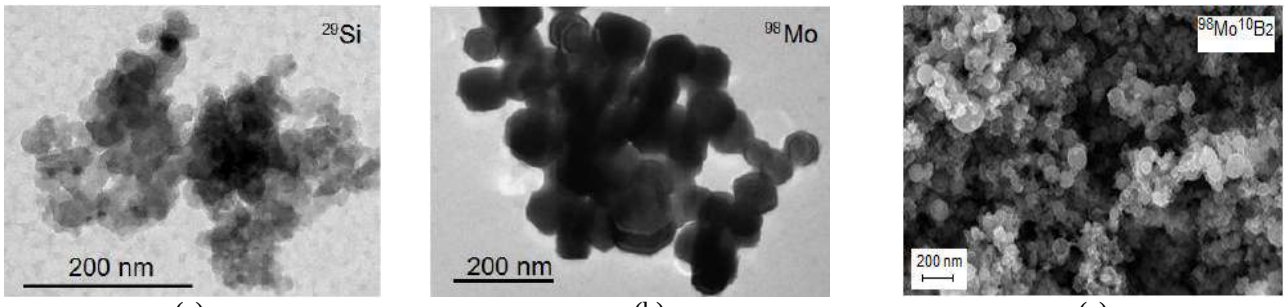

(a) (b) (c)

Figure 1. *(a) Microstructure of ^{29}Si (b) Microstructure of ^{98}Mo (c) Microstructure of $^{98}Mo^{10}B$.*

REFERENCES

[1] R. Kornev et al, Plasma Chemistry and Plasma Processing 42, 395–412, 2022

Table of contents

List of participants

- Bari Ferenc
- Bartels Randy
- Bizheva Kostadinka
- Blondel Walter
- Bowden Audrey
- Bratchenko Ivan
- Bratchenko Lyudmila
- Brinkmann Ralf
- Bryanskaya Ekaterina
- Cherkasova Olga
- Conde Olga M.
- Darvin Maxim
- Dremin Viktor
- Drexler Wolfgang
- Dubrovsky Alexander
- Dunaev Andrey
- Elagin Vadim
- Ermakova Polina
- Evsukova Arina
- Gelikonov Grigory
- Genina Elina
- Huber Robert
- Kienle Alwin
- Kiseleva Elena
- Kistenev Yury

- Kornev Roman
- Kuznetsova Daria
- Larin Kirill
- Larina Irina
- Leitgeb Rainer
- Li Pengcheng
- Lu Jinling
- Lugovtsov Andrei
- Lukinsone Vanesa
- Mankova Anna
- Merdalimova Anastasiia
- Nadkarni Seemantini
- Novikova Tatiana
- Oliveira Luís
- Parashchuk Olga
- Popov Alexey
- Potapova Elena
- Priezzhev Alexander
- Razansky Daniel
- Rodimova Svetlana
- Rollins Andrew
- Schneckenburger Herbert
- Semenova Irina
- Shimolina Liubov
- Shirshin Evgeny
- Shkurinov Alexander
- Singh Manmohan
- So Peter
- Turchin Ilya
- Tplv Valery
- Vilches Clara
- Voitova Arina

- Yakimov Boris
- Yanina Irina
- Yesilkoy Filiz
- Yuzhakova Diana
- Zawadzki Robert
- Zharkikh Elena

Author Index